NASA TECHNICAL MEMORANDUM

NASA TM X-1616

NASA TM X-1616

ATLAS-CENTAUR FLIGHT PERFORMANCE FOR SURVEYOR MISSION B

by NASA Lewis Staff

Lewis Research Center

Cleveland, Ohio

NATIONAL AERONAUTICS AND SPACE ADMINISTRATION • WASHINGTON, D. C. • SEPTEMBER 1968

NASA TM X-1616

ATLAS-CENTAUR FLIGHT PERFORMANCE FOR SURVEYOR MISSION B

By NASA Lewis Staff

Lewis Research Center
Cleveland, Ohio

NATIONAL AERONAUTICS AND SPACE ADMINISTRATION

For sale by the Clearinghouse for Federal Scientific and Technical Information
Springfield, Virginia 22151 – CFSTI price $3.00

ABSTRACT

The second operational Atlas-Centaur launch vehicle AC-7, with Surveyor SC-2, was launched on September 20, 1966. The flight profile was a direct-ascent mission to inject the Surveyor into a lunar intercept trajectory. Subsequent to injection, a vernier engine on the Surveyor failed to fire. The spacecraft tumbled out of control and failed to complete the mission. This report includes a flight performance evaluation of the Atlas-Centaur launch vehicle systems from lift-off through spacecraft separation and Centaur retromaneuver.

CONTENTS

I. SUMMARY

The second operational Atlas-Centaur vehicle AC-7, with Surveyor spacecraft SC-2, was successfully launched from Eastern Test Range Complex 36A on September 20, 1966, at 0731:59.8 hours eastern standard time. The vehicle was launched near the closing of the launch window on a flight azimuth of 114°. The boost phase pitchover program was started at T + 15 seconds. All Atlas and Centaur systems performed properly and the spacecraft was successfully injected into a lunar intercept trajectory. The flight profile was a single-burn (direct-ascent) mission. Orbit injection of the spacecraft was very accurate and a midcourse correction of only 1.20 meters per second (miss plus time of flight) would have been required to place the Surveyor on its intended target. The planned midcourse maneuver by the Surveyor, however, was unsuccessful as one of the three Surveyor vernier motors failed to fire. The spacecraft tumbled out of control and failed to complete the mission.

This report includes an evaluation of the flight performance of the Atlas-Centaur launch vehicle systems from lift-off through spacecraft separation and Centaur retro-maneuver.

II. INTRODUCTION

by John J. Nieberding

Atlas-Centaur launch vehicle AC-7 boosted Surveyor SC-2 into a direct-ascent lunar intercept trajectory. This was the second operational flight, Mission B, in a series of seven planned for 1966-68.

Centaur was developed as a second stage for a modified Atlas D missile. The research and development flight program began in 1962 and was successfully completed on August 11, 1965 with the flight of AC-6. This flight demonstrated the ability of Atlas-Centaur to support the Surveyor mission by using a direct-ascent flight profile.

The first operational direct-ascent flight, AC-10, flew on May 30, 1966 (see ref. 1). It successfully injected SC-1 on a lunar trajectory which terminated when the spacecraft executed the first controlled soft landing of a space vehicle on the lunar surface. Surveyor SC-1 transmitted more than 15 000 pictures from its landing site at 2.58° South latitude, 43.35° West longitude.

The mission of SC-2 was designed to be essentially the same as that for SC-1 except that the landing site was changed to 0.05° South latitude, 5.32° West longitude to provide photographs of a different lunar region. This second Surveyor was launched on September 20, 1966 by AC-7. The Atlas-Centaur launch vehicle was required to inject Surveyor on a lunar trajectory with sufficient accuracy that the midcourse correction required at 20 hours after injection would not exceed 50 meters per second. The Centaur was also required to perform a retromaneuver after spacecraft separation to prevent impact of the Centaur on the Moon and to minimize the probability that the Surveyor star sensor would respond to light reflected from Centaur rather than from the star Canopus.

This report presents an evaluation of the Atlas-Centaur flight AC-7 and its support of Mission B objectives. The performance of both Atlas and Centaur Systems is described and evaluated.

III. LAUNCH VEHICLE DESCRIPTION

by Eugene E. Coffey

The Atlas-Centaur AC-7 was a two-stage launch vehicle consisting of an Atlas first stage and a Centaur second stage. Figure III-1 shows the Atlas-Centaur lifting off with Surveyor. Both stages were 10 feet (3.05 m) in diameter and were connected by an interstage adapter. The composite vehicle was 113 feet (34.44 m) in length and weighed 302 806 pounds (137 351 kg) at lift-off. The Atlas and the Centaur stage utilized thin-wall, pressurized, main propellant tank sections of monocoque construction to provide primary structural support for all vehicle systems.

The first stage Atlas vehicle was 65 feet (19.81 m) long. It was powered by a standard Rocketdyne MA-5 propulsion system consisting of two booster engines with 330 000 pounds (1467.9×10^3 N) thrust total, a single sustainer engine of 57 000 pounds (253.55×10^3 N) thrust and two small vernier engines of 1000 pounds (4.448×10^3 N) thrust each. These engines, which burned liquid oxygen and kerosene, were ignited simultaneously on the ground. The booster engines were gimbaled for roll and directional control during the booster phase of the flight. This phase was completed when the vehicle acceleration equaled 5.7 g's and the booster engines were cut off. The booster engines were jettisoned 3.1 seconds after booster engine cutoff. The sustainer engine and the vernier engines continued to burn after booster engine cutoff for the Atlas sustainer phase of the flight. During this phase, the sustainer engine gimbaled for directional control, while the vernier engines gimbaled for roll control. The sustainer and vernier engines fired until propellant depletion. The Atlas was separated from the Centaur, after sustainer engine cutoff, by the firing of a shaped-charge severance system. The firing of a retrorocket system, required to back the Atlas and the interstage adapter away from the Centaur, completed the separation of these stages. The Atlas stage with the interstage adapter is shown in figure III-2. Other major systems of the Atlas first stage included flight control, structures, separation, propellant utilization, telemetry and instrumentation, flight termination (destruct), and electrical.

The second-stage Centaur vehicle, including the nose fairing, was 48 feet (14.63 m) long. Centaur, a high-specific impulse (433 sec) vehicle was powered by two Pratt & Whitney RL10A3-1 engines which generated 30 000 pounds (133.45×10^3 N) thrust total. These engines burned liquid hydrogen and liquid oxygen. The Centaur main engines gimbaled to provide directional and roll control during Centaur powered flight. Hydrogen peroxide engines (3.5, 6, and 50 lb (16, 27, and 222 N) thrust) mounted on the aft periphery of the tank, provided attitude control and additional thrust for vehicle reorientation after Centaur main engine cutoff. The Centaur was equipped with four insulation panels (1-in. - (2.54-cm-) thick glass fabric sandwich construction with a polyurethane foam core) for insulating the hydrogen tank. The insulation panels and nose fairing were jettisoned during the Atlas sustainer phase. The fiberglass nose fairing was used to provide an aerodynamic shield for the Surveyor spacecraft, guidance equipment, and electronic packages during ascent. The Centaur used an inertial guidance system. The Centaur stage is shown in figure III-3. Additional major systems of the Centaur include flight control, structures, separation, propellant utilization, telemetry and instrumentation, flight termination (destruct), C-band radar tracking beacon, guidance, and electrical.

The Atlas-Centaur launch vehicle AC-7, which injected Surveyor SC-2 into a lunar intercept trajectory, was substantially similar to AC-10, the first fully operational launch vehicle which successfully injected Surveyor SC-1 into a lunar intercept trajectory (see ref. 1).

The major systems as they were configured for the Atlas-Centaur launch vehicle AC-7 are delineated in the subsequent sections of this report.

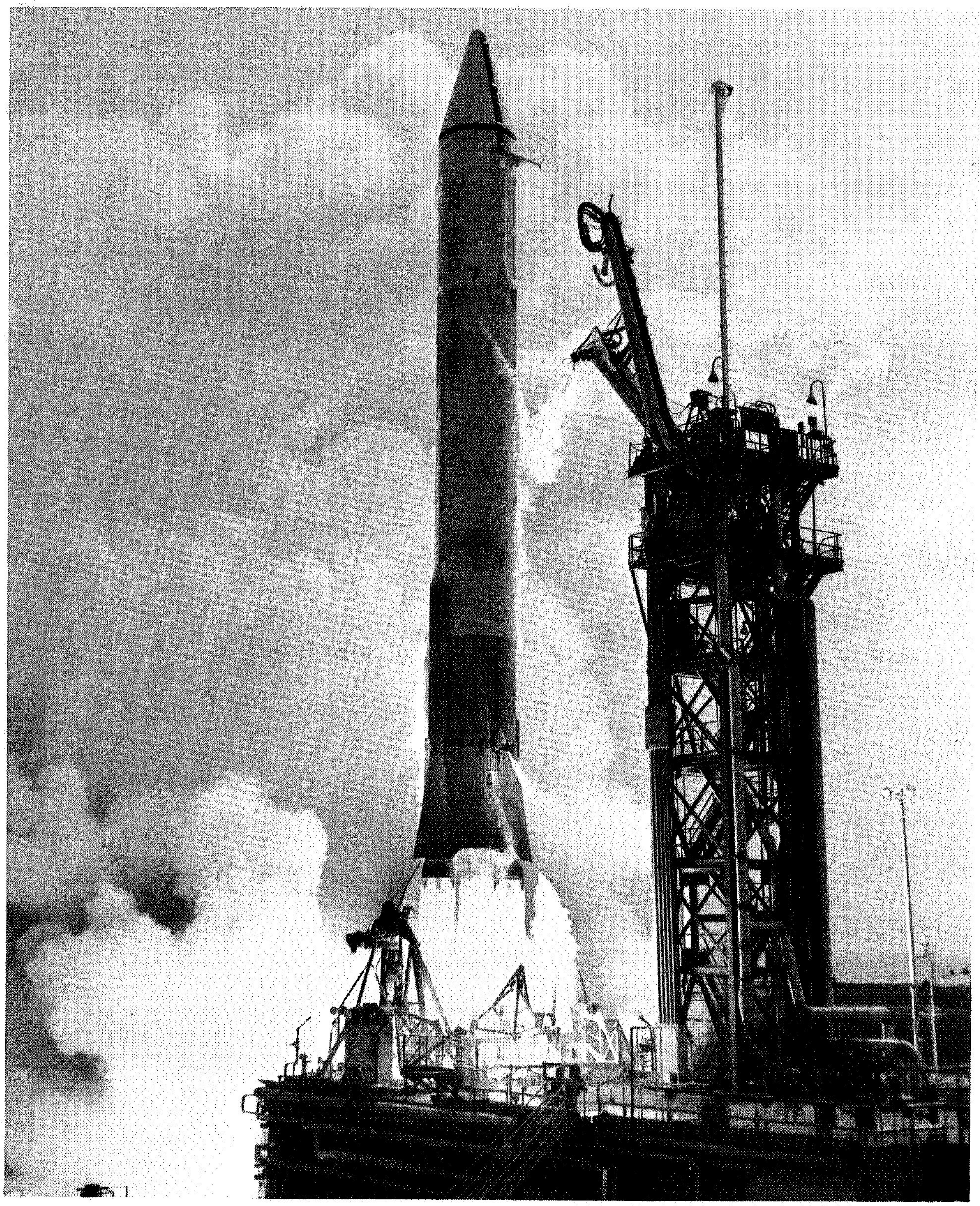

Figure III-1. - Atlas-Centaur lifting off with Surveyor, AC-7.

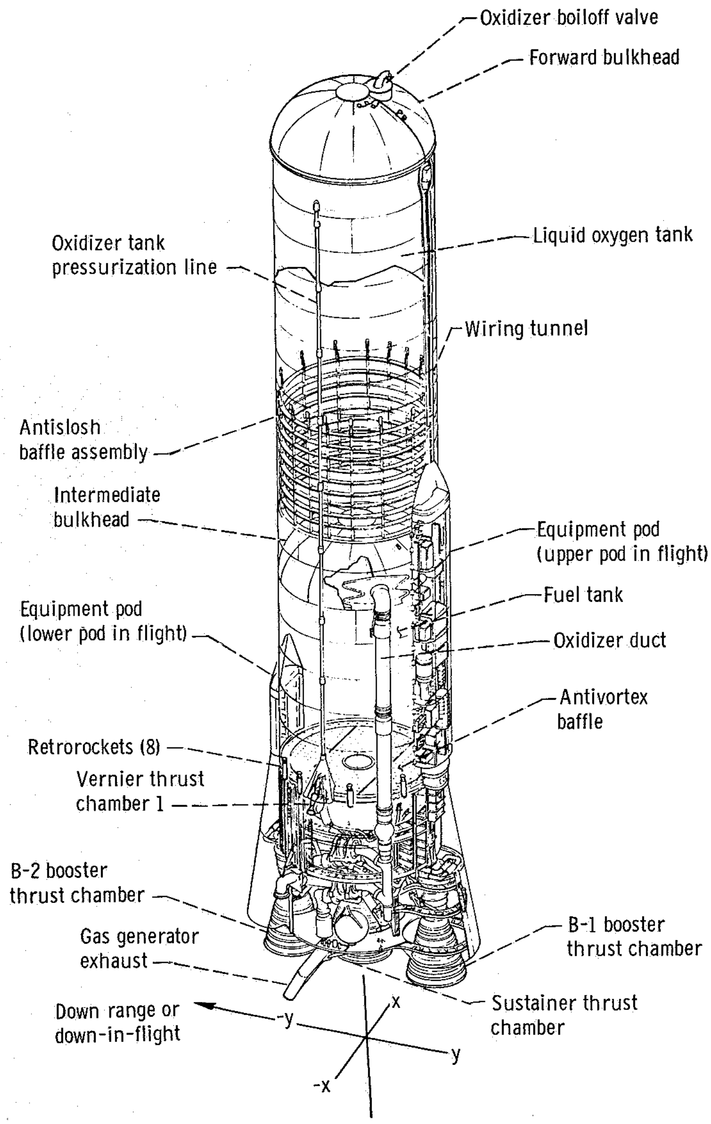

Figure III-2. - Atlas launch vehicle, AC-7.

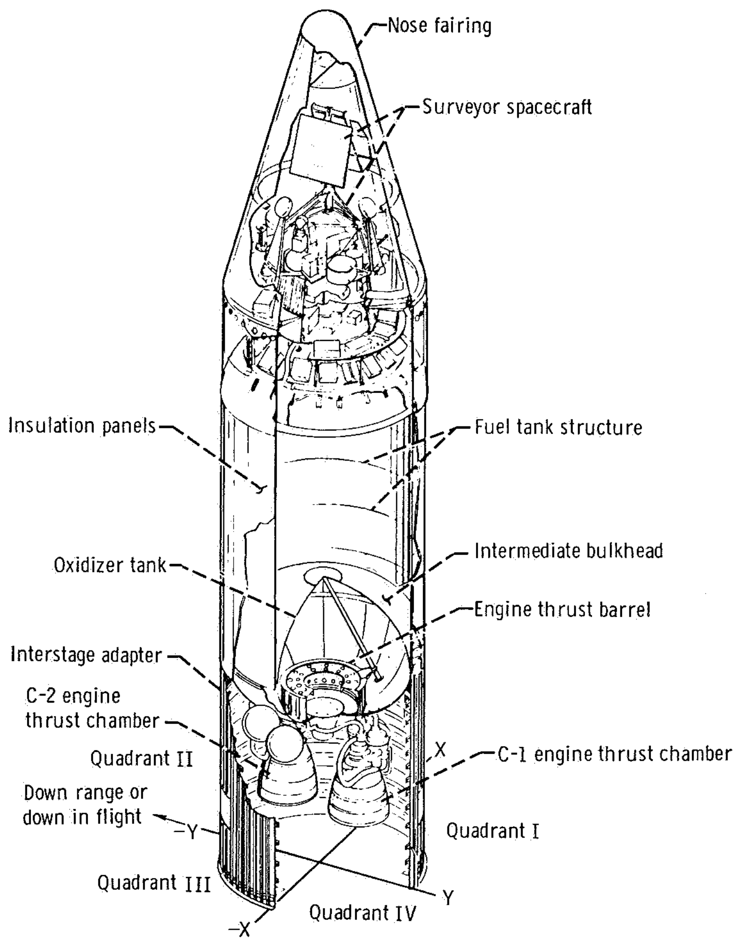

Figure III-3. - Centaur launch vehicle, AC-7.

IV. MISSION PERFORMANCE

by William A Groesbeck

The second operational Atlas-Centaur launch vehicle AC-7, with Surveyor spacecraft SC-2, was launched from Eastern Test Range Complex 36A on September 20, 1966, at 0731:59.8 hours eastern standard time. The launching was successful with the vehicle lift-off occurring near the close of the available launch window. AC-7 was programmed to fly a single-burn direct-ascent lunar intercept trajectory from which the operational Surveyor spacecraft would attempt a controlled soft landing on the lunar surface. Weight of the combined vehicle at lift-off was 302 806 pounds (137 351 kg), giving a thrust to weight ratio of 1.29. A compendium of the AC-7 mission profile and the Surveyor-Earth-Moon trajectory is shown in figures IV-1 and IV-2. For reference also, a listing of the postflight vehicle weights summary, atmospheric sounding data, trajectory data, Surveyor launch windows, and flight events record, are given in appendix A.

ATLAS FLIGHT PHASE

Vehicle lift-off was normal. The guidance system inertial reference was locked in at T - 8.5 seconds, but guidance steering commands were not issued for vehicle steering until after Atlas booster staging. During this time from lift-off (T - 0) to booster staging, the vehicle was flown on a preprogrammed trajectory. The Atlas flight control system initiated the preset roll program at T + 2 seconds in order to realine the vehicle from the launch azimuth of 105° to a flight azimuth of 114.36°. After the roll attitude stabilized on the flight azimuth, the flight programmer initiated the booster pitchover program at T + 15.45 seconds. Winds aloft and maneuvering requirements were not severe, and the maximum booster engine gimbal deflections during the ascent did not exceed 1.7°.

The programmed Centaur hydrogen tank nonventing period following lift-off was interrupted at T + 47.5 seconds as tank pressure reached the relief pressure of the high range secondary vent valve. The valve cycled three times emitting momentary puffs of hydrogen. Seconds later at T + 68 seconds, the primary vent valve was programmed to the relief mode allowing tank pressure to blow down. The ullage pressure was then controlled at a lower pressure within the regulating range of the primary vent valve.

Thrust buildup and vehicle acceleration during boost phase proceeded according to the mission plan, and at an acceleration of 5.65 g's, which occurred at T + 142.6 seconds, the Centaur guidance issued the booster engine cutoff signal. Three seconds later at T + 145.6 seconds, the staging command was given by the Atlas programmer, and the booster engines separated from the vehicle. Staging transients were mild and momentary vehicle rate excitation in pitch, yaw, or roll did not exceed 3.96 degrees per second. Low amplitude slosh was excited in the Atlas liquid oxygen tank but it was almost completely damped out within a few seconds. Guidance steering commands were first admitted to the Atlas flight control system 8 seconds after booster engine cutoff. Slight steering errors, due to differences in vehicle attitude and the desired steering vector, were corrected in less than 3 seconds, and the guidance system issued commands to continue a pitchover during the Atlas sustainer phase.

Insulation panels were jettisoned during the sustainer phase at T + 176.6 seconds. All panels were completely severed by the shaped charge and fell clear of the vehicle. Similarly, the nose fairing unlatch command was given at T + 202.4 seconds and the thrustor bottles, firing 0.5 second later, rotated the fairing halves away from the vehicle. Vehicle angular rates due to the jettisoning of the insulation panels and nose fairing were low and did not exceed 3.76 degrees per second in pitch or yaw or 1.68 degrees per second in roll.

Sustainer and vernier engine systems performed satisfactorily, building up from a rated sea level thrust of 58 340 pounds (259 508 N) to a total vacuum thrust of 81 000 pounds (360 304 N) at engine cutoff. This thrust boosted the vehicle to an Earth referenced velocity of 11 428 feet per second (3490 m/sec) (inertial velocity of 12 658 feet per second) (3860 m/sec) and an acceleration of 1.8 g's at engine shutdown. The propellant utilization system operated satisfactorily and controlled the propellant consumption to a near simultaneous fuel and liquid-oxygen depletion. The depletion of the usable propellants caused sustainer and vernier engine cutoff at T + 235.1 seconds.

Coincident with sustainer engine cutoff, the guidance steering commands to flight control were discontinued allowing the vehicle to coast in a noncontrolled flight mode. This guidance mode prevented gimbaling the Centaur engines under nonthrusting conditions and helped maintain required clearances between the engines and the interstage adapter during staging.

Atlas staging command from the flight programmer was given at T + 237.1 seconds, and the shaped-charge fired severing the two vehicles. Eight retrorockets on the Atlas then fired and pushed the Atlas stage away from the Centaur. The Centaur stage, however, did experience some slight disturbances during the Atlas sustainer engine shutdown and vehicle staging sequence. These disturbances caused the vehicle to drift only slightly off the steering vector. The angular rates did not exceed 0.16 degree per second and the drift error was corrected within 5.1 seconds, after start of Centaur main engines when guidance steering commands were again issued to the flight control system.

CENTAUR FLIGHT PHASE

Centaur stage boost pumps were started prior to sustainer engine cutoff and were deadheaded through staging until main engine start. Required net positive suction pressure during the near-zero-gravity period from sustainer engine cutoff until main engine start at T + 246.6 seconds was provided by pressure pulsing the propellant tanks with helium. Ullage pressures were increased from 30.4 to 39.7 psia (20.9 to 27.3 N/cm^2 abs) in the oxygen tank and from 19.7 to 20.4 psia (13.6 to 14.1 N/cm^2 abs) in the hydrogen tank. Eight seconds prior to main engine start, the Centaur programmer issued preparatory commands for main engine firing. Main engines were gimbaled to the zero position. Cooldown valves were opened to flow liquid propellants through the lines and chill down the engine turbopumps. Chilldown of the lines ensured liquid at the pump inlets as required for a uniform and rapid thrust buildup at engine ignition. At T + 246.6 seconds, the ignition command was given by the flight control programmer, and the engine thrust increased to full flight levels.

Guidance steering for the Centaur stage was started at T + 250.6 seconds, after the engine thrust was fully established. Guidance steering commands had been discontinued during the main engine start sequence to allow the engines to be centered and prevent excessive vehicle angular motion. During this interval without guidance steering, residual angular rates and disturbing torques induced by staging transients resulted in only a slight vehicle drift off the steering vector. This attitude drift was corrected within 4 seconds, and the steering commands again provided the required pitch down rate to home in on the injection velocity vector.

The propellant utilization system controlled the mixture ratio during main engine firing to an average value of 4.98.

About 60 seconds prior to the end of Centaur powered flight, the pitchover rate decreased as the vehicle homed in on the desired orbital injection conditions for the Surveyor lunar transfer intercept. At T + 686.2 seconds, the guidance computed velocity-to-be-gained was zero and the main engines were cutoff. Orbit insertion occurred approximately 1700 nautical miles (3150 km) southeast of Cape Kennedy at an injection velocity of 34 549 feet per second (10 530 m/sec). Engine cutoff occurred with 261 pounds (118 kg) of burnable propellants remaining, or enough for 3.6 more seconds of engine firing.

SPACECRAFT SEPARATION

Coincident with main engine cutoff, the guidance steering commands were temporarily discontinued, and the coast phase hydrogen peroxide attitude control system was activated. Rates imparted to the vehicle at main engine cutoff were mild and were quickly damped by the attitude control system to rates less than 0.2 degree per second. The residual motion below this threshold allowed only a negligible drift in vehicle attitude. This drift did not interfere with the subsequent spacecraft separation.

The Centaur with the Surveyor spacecraft then coasted in a near-zero-gravity field for about 68 seconds. This coast period allowed for canceling the residual vehicle rates and preparing the spacecraft for separation. Signals from the Centaur programmer were given to the spacecraft to extend landing gear and omniantennas, to turn on spacecraft transmitter high power, and to arm the spacecraft for separation. All commands were received and executed by the spacecraft.

Separation of the spacecraft was commanded at T + 752.6 seconds. The attitude control system was disabled, pyrotechnically operated latches were fired, and the spring-loaded mechanism pushed the Surveyor to impart an approximate 0.75 feet per second (0.228 m/sec) separation velocity. Full extension of all three springs occurred within 1 millisecond of each other. Turning rates of the spacecraft after separation did not exceed 0.34 degree per second. These rates were well below the maximum allowable of 3.0 degrees per second.

CENTAUR RETROMANEUVER

The Centaur vehicle was required to execute a turnaround and retrothrust maneuver after spacecraft separation. This maneuver was necessary to eliminate the possibility of the Surveyor star sensor acquiring the reflected light of Centaur rather than the star Canopus. A second objective of the retromaneuver was to prevent impact of Centaur on the Moon. A guidance vector for the turnaround was selected which was the reciprocal of the velocity vector at main engine cutoff. Execution of the turnaround was commanded at T + 757.7 seconds, 5 seconds after spacecraft separation. Guidance system logic accounted for any vehicle drift since main engine cutoff and steering commands were given which rotated the Centaur in the shortest arc from its actual position to the new retrovector. Turning rate during the reorientation was limited, for structural considerations, to a maximum of 1.6 degrees per second.

About half way through the turnaround at T + 797.7 seconds, two 50-pound (222.4-N) thrust hydrogen peroxide engines were fired for 20 seconds to impart lateral as well as additional longitudinal separation from the spacecraft. The lateral separation was necessary to minimize the impingement of frozen particles on the spacecraft during the subsequent blowdown of residual Centaur propellants through the main engines. During this lateral thrust maneuver, the impingement forces on the vehicle from the hydrogen peroxide engine exhaust plumes were unexpectedly high and produced a clockwise roll disturbing torque. These impingement forces required the 3.5- and 6.0-pound (15.55- and 26.6-N) thrust attitude control engines to operate 50 percent of the time to maintain vehicle orientation.

The turnaround maneuver was completed at T + 839 seconds after rotating the vehicle through 157°. Once the retrovector was acquired, the attitude control maintained the vehicle position on the vector within 1.5°.

The retrothrust maneuver was initiated by programmer command at T + 992.6 seconds. The main engines were gimbaled to aline the thrust vector with the vehicle center of gravity and the engine prestart valves were opened, allowing the residual propellants to flow down through the engines. Expelling the propellants provided sufficient thrust to alter the Centaur orbit, and the relative separation distance from the spacecraft at the end of 5 hours was 730 kilometers. This distance was more than two times the required minimum. Alteration of Centaur's orbit was also sufficient to prevent it from impacting the Moon. At completion of the retromaneuver at T + 1242.6 seconds, all vent valves were enabled to the relief or normal regulating mode. Flight control and all other systems were deenergized, allowing the spent vehicle to continue its orbit in a non-stabilized flight mode.

SURVEYOR TRANSIT PHASE

The Surveyor spacecraft was injected into its lunar intercept trajectory with such accuracy that lunar impact would have occurred without any midcourse correction. To impact on its preselected target, a slight midcourse velocity correction of only 1.16 meters per second for miss distance only, or 1.20 meters per second for miss plus time of flight, would have been required. However, when this midcourse maneuver was attempted at T + 16 hours 4 minutes from lift-off, one of the three vernier thrust engines failed to fire, and the spacecraft tumbled out of control. Repeated attempts to fire the engines and regain control of the spacecraft were unsuccessful, and the mission was terminated.

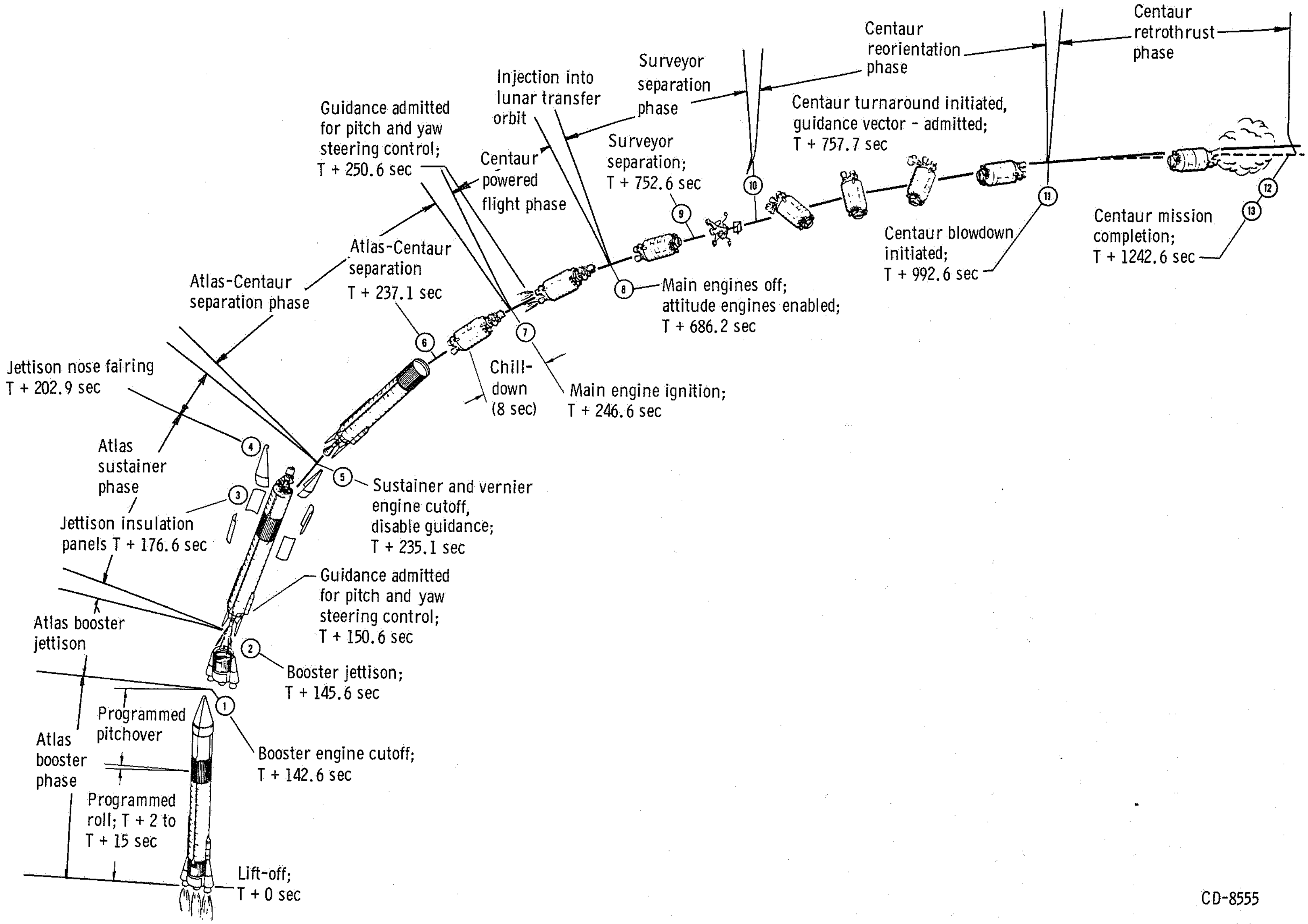

Figure IV-1.–AC-7 flight sequence compendium.

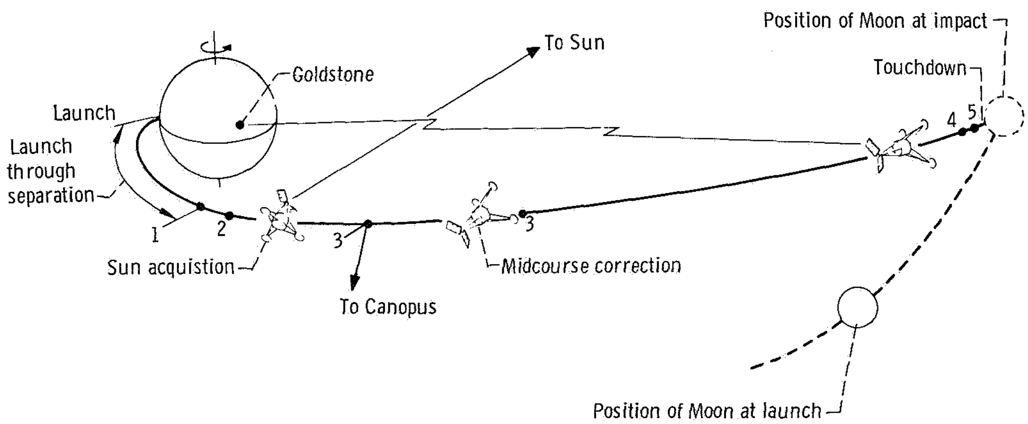

Figure IV-2. - Planned Surveyor-Earth-Moon trajectory, AC-7. 1, injection and separation; 2, initial deep space instrumentation facility; 3, star acquisition and verification; 4, retrophase (planned for about 96 km from Moon); 5, vernier descent (planned for 35 000 feet (10 668 km) above Moon's surface).

PRECEDING PAGE BLANK NOT FILMED.

V. LAUNCH VEHICLE SYSTEM ANALYSIS

PROPULSION

by Steven V. Szabo, Jr., Ronald W. Ruedele, Kenneth W. Baud, and Donald B. Zelten

Atlas

System description. - The Rocketdyne MA-5 engine system utilized by the Atlas consisted of two booster engines, a sustainer engine, two vernier engines, an engine start system, a logic control package, and an associated electrical system. The systems are shown schematically in figure V-1.

All engines were the single-start type and used liquid oxygen (oxidizer) and kerosene (RP-1 (fuel)) as propellants. The engines were hypergolically ignited by using pyrophoric fuel cartridges. The pyrophoric fuel preceeded the RP-1 into the thrust chamber and initiated ignition with the liquid oxygen. Combustion was then sustained by the RP-1 and liquid oxygen. All thrust chambers were regeneratively cooled by using fuel as the coolant.

The acceptance test thrust values of the engines at sea level were as follows:

Engine	Weight	
	lb force	N
Booster (2)	328 600	1.4616×10^{6}
Sustainer (1)	57 000	2.535×10^{5}
Vernier (2)	2 000	8.896×10^{3}

The booster engine system consisted of two gimbaled thrust chamber assemblies and a common power package consisting of a gas generator, two turbopumps, and a supporting control system. The sustainer engine was a gimbaled engine assembly consisting of a thrust chamber, gas generator, turbopump, and supporting control system. The two vernier engines consisted of thrust chamber assemblies, propellant valves, gimbal bodies, and mounts. The self-contained engine start system consisted of an oxidizer start tank, a fuel start tank, and the associated control system.

TABLE V-I. - ATLAS ENGINE SYSTEM REQUIREMENTS AT

ENGINE START, AC-7

(a) U. S. Customary Units

Parameter	Requirement at engine start	Value at engine start
Booster liquid oxygen regulator reference pressure, psia	593 to 613	604
Sustainer liquid oxygen regulator reference pressure, psia	801 to 841	817
Booster 2 turbine inlet temperature, ^{o}F	> 0	80
Sustainer engine turbine inlet temperature, ^{o}F	> 0	69
Liquid oxygen temperature at breakaway valve (fill and drain valve), ^{o}F	> -283	-285

(b) SI Units

Booster liquid oxygen regulator reference pressure, N/cm^2 abs	409 to 423	416
Sustainer liquid oxygen regulator reference pressure, N/cm^2 abs	552 to 580	563
Booster 2 turbine inlet temperature, ^{o}K	> 255.5	300
Sustainer engine turbine inlet temperature, ^{o}K	> 255.5	294
Liquid oxygen temperature at breakaway valve (fill and drain valve), ^{o}K	< 98.3	97

System performance. - Engine start and thrust buildup transients were normal. Propulsion system parameter requirements at engine start and the actual measured value are given in table V-I. The total calculated thrust of the engines at lift-off was 391 000 pounds (17.39×10^5 N), well within the limits of allowable engine performance. Comparable thrust from acceptance tests was 387 600 pounds (17.24×10^5 N).

In-flight engine system operation was satisfactory. A summary of the engine system data is given in table V-II. Booster engine cutoff command was generated by the guidance system when the vehicle attained an acceleration of 5.56 g's. Sustainer engine cutoff command was initiated by the fuel (RP-1) depletion sensors. The depletion of usable liquid oxygen was also imminent at this time, as indicated by the sustainer liquid oxygen pump inlet pressure (see section on Atlas Propellant Utilization System).

TABLE V-II. - ATLAS ENGINE SYSTEM PERFORMANCE DATA, AC-7

(a) U. S. Customary Units

Engine parameter	Flight time, sec		
	T + 10	Booster engine cutoff T + 142.6	Sustainer engine cutoff T + 235.1
Booster engine 1:			
Chamber pressure, psia	583	591	------
Pump speed, rpm	6 378	6 310	------
Pressure at oxidizer pump inlet, psia	59	79	------
Pressure at fuel pump inlet, psia	69	54	------
Booster engine 2:			
Chamber pressure, psia	581	589	------
Pump speed, rpm	6 300	6 300	------
Pressure at oxidizer pump inlet, psia	60	84	------
Pressure at fuel pump inlet, psia	69	56	------
Booster gas generator combustion chamber pressure, psia	524	524	------
Booster liquid oxygen regulator reference pressure, psia	638	628	------
Sustainer chamber pressure, psia	702	702	692
Sustainer pump speed, rpm	10 140	10 110	10 216
Pressure at sustainer oxidizer injector manifold, psia	840	851	831
Sustainer fuel pump discharge pressure, psia	942	958	958
Sustainer oxidizer regulator reference pressure, psia	831	831	831
Sustainer gas generator discharge pressure, psia	576	584	584
Pressure at sustainer fuel pump inlet, psia	72	63	43
Pressure at sustainer pump inlet, psia	64	89	34
Temperature at sustainer oxidizer pump inlet, ^{o}F	-285	-280	-281
Vernier 1 chamber pressure, psia	363	363	367
Vernier 2 chamber pressure, psia	355	350	367

(b) SI Units

Booster engine 1:			
Chamber pressure, N/cm^2 abs	402	407.5	------
Pressure at oxidizer pump inlet, N/cm^2 abs	40.7	54.5	------
Pressure at fuel pump inlet, N/cm^2 abs	47.6	37.2	------
Booster engine 2:			
Chamber pressure, N/cm^2 abs	400.6	406.1	------
Pressure at oxidizer pump inlet, N/cm^2 abs	41.4	57.9	------
Pressure at fuel pump inlet, N/cm^2 abs	47.6	38.6	------
Booster gas generator combustion chamber pressure, N/cm^2 abs	361.3	361.3	------
Booster liquid oxygen regulator reference pressure, N/cm^2 abs	440	434	------
Sustainer chamber pressure, N/cm^2 abs	484	484	477
Pressure at sustainer oxidizer injector manifold, N/cm^2 abs	579	586.7	572.9
Sustainer fuel pump discharge pressure, N/cm^2 abs	649.5	660.5	660.5
Sustainer oxidizer regulator reference pressure, N/cm^2 abs	572.9	572.9	572.9
Sustainer gas generator discharge pressure, N/cm^2 abs	397	403	403
Pressure at sustainer fuel pump inlet, N/cm^2 abs	49.6	43.4	29.6
Pressure at sustainer oxidizer pump inlet, N/cm^2 abs	44.1	61.4	23.4
Temperature at sustainer oxidizer pump inlet, ^{o}K	97.2	99.9	99.4
Vernier 1 chamber pressure, N/cm^2 abs	250.3	250.3	253
Vernier 2 chamber pressure, N/cm^2 abs	244.7	241.3	250.3

Centaur Main Engines

System description. - Two Pratt & Whitney RL10A3-1 engines were used to provide thrust for the Centaur stage. These were high-energy hydrogen-oxygen engines with a nozzle expansion ratio of 40. Rated vacuum thrust of each engine was 15 000 pounds (66 700 N) at a design thrust chamber pressure of 300 psia (206.5 N/cm^2 abs) and an oxidizer to fuel mixture ratio of 5.0. The specific impulse rating was 433 seconds.

The engine system, shown schematically in figure V-2, utilized a regeneratively cooled thrust chamber and a turbopump fed propellant flow system. Pumped fuel, after cooling the thrust chamber, was expanded through a turbine, which drove the propellant pumps. By regulating the amount of fuel bypassed around the turbine as a function of combustion chamber pressure, it was possible to vary turbopump speed and thereby control engine thrust. The oxidizer was pumped directly to the propellant injector through the propellant utilization (mixture ratio control) valve. Ignition was accomplished by a spark igniter recessed in the propellant injector face. Engine start and stop sequences were controlled by pneumatically operated valves actuated by electrical signals from the vehicle. At engine shutdown, the main fuel valve as well as the oxidizer and fuel inlet valves were commanded closed simultaneously to effect a rapid thrust tail off. The engines were gimbal mounted to permit thrust vector control for steering the vehicle.

System performance. - Main engine performance appeared normal throughout the flight. Eight seconds prior to main engine start, the engine inlet valves were opened to flow liquid propellants through the lines and chill down the engine pumps. Command for engine ignition was given by the flight control programmer at T + 246.6 seconds and thrust increased normally to full flight levels. Thrust chamber pressure rise for the engine start transient is presented in figure V-3. Start transient oxidizer pump speed is plotted as a function of chamber pressure in figure V-4. The trace of the AC-6 flight, having a high start transient overshoot, has been introduced for purposes of comparison. Start total impulse to 95 percent of rated thrust was calculated to be 3172 and 2746 pound-seconds (14 100 and 12 210 N-sec) for the C-1 and C-2 engines, respectively. Corresponding engine acceleration times were 1.26 and 1.28 seconds, respectively. Start total impulse from main engine start through 2 seconds was 14 210 and 13 776 pound-seconds (63 200 and 61 100 N-sec), respectively. This 434 pound-second (2100 N-sec) difference in start total impulse was not significant.

Liquid hydrogen and liquid oxygen pump inlet temperature and pressure data are presented in figures V-5 and V-6, respectively. For any fluid inlet temperature, the pressure remained above saturation. The margin between the steady-state operating limit and the actual inlet conditions ensured satisfactory values of net positive suction pressure.

TABLE V-III. - CENTAUR ENGINE SYSTEM DATA SUMMARY, AC-7

(a) U.S. Customary Units

Parameter	Expected value	Time from main engine start, sec					
		90		200		435	
		Engine					
		C-1	C-2	C-1	C-2	C-1	C-2
Total pressure at hydrogen pump inlet, psia	22.0 to 43.3	34.9	34.9	35.3	35.0	31.8	31.2
Temperature at hydrogen pump inlet, ^{o}R	33.0 to 39.8	38.7	38.6	38.2	38.1	36.8	36.6
Total pressure at oxidizer pump inlet, psia	45.8 to 77.0	65.4	66.8	71.4	71.4	64.1	67.1
Temperature at oxidizer pump inlet, ^{o}R	171.2 to 183.0	177.4	177.4	176.9	176.9	173.3	173.3
Oxidizer pump speed[a], rpm	11 113 to 11 701	11 101	11 489	11 154	11 646	11 093	11 421
Venturi upstream pressure[a], psia	628 to 686	665.6	682.1	673.1	684.9	663.5	675.0
Temperature at turbine inlet, ^{o}R	294 to 358	327.5	348.4	309.2	328.1	319.5	342.0
Differential pressure across oxidizer injector, psid	39 to 55	47.1	46.8	44.0	44.6	44.3	45.0
Engine chamber pressure[a], psia	293 to 299	293.9	297.8	291.2	293.7	293.8	292.0

(b) SI Units

Total pressure at hydrogen pump inlet, N/cm^2 abs	15.0 to 29.8	24.1	24.1	24.3	24.1	21.9	21.5
Temperature at hydrogen pump inlet, ^{o}K	18.3 to 22.1	21.5	21.4	21.2	21.2	20.4	20.3
Total pressure at oxidizer pump inlet, N/cm^2 abs	31.6 to 52.9	45.1	46.1	49.2	49.2	44.2	46.3
Temperature at oxidizer pump inlet, ^{o}K	95.2 to 101.8	98.6	98.6	98.3	98.3	96.3	96.3
Venturi upstream pressure[a], N/cm^2 abs	433 to 473	458.9	470.3	464.1	472.2	457.5	465.4
Temperature at turbine inlet, ^{o}K	163.3 to 198.9	181.9	193.6	171.8	182.3	177.5	190.0
Differential pressure across oxidizer injector, N/cm^2	26.9 to 37.9	32.5	32.3	30.3	30.8	30.5	31.0
Engine chamber pressure[a], N/cm^2 abs	202.0 to 206.1	202.6	205.3	200.8	202.5	202.6	201.3

[a]Expected values are for zero propellant utilization valve angle.

Steady-state engine operating conditions are summarized and compared with corresponding predicted values in table V-III. All actual flight values were within the allowable tolerances.

Engine performance values of thrust, specific impulse, and mixture ratio determined from the Pratt & Whitney C* iteration technique at main engine start plus 90 seconds are compared with expected values in table V-IV. Thrust, specific impulse, and mixture ratio for the entire flight using the Pratt & Whitney Aircraft C* iteration technique and the Pratt & Whitney Aircraft regression technique are presented in figure V-7. The change of values following main engine start plus 90 seconds is a result of enabling the propellant utilization system. An average value of 432.5 seconds for vehicle specific impulse over the time interval from T + 420 to T + 645 seconds was determined from a calculation based on guidance thrust velocity data. This value agrees favorably with the instantaneous engine system data obtained by the Pratt & Whitney C* calculation. A discussion of these performance techniques is given in appendix B.

Engine shutdown appeared normal. Chamber pressure began to decay 0.08 and 0.10 second following the main engine cutoff signal for the C-1 and C-2 engines, respectively. These values compared favorably with those obtained on previous vehicles. Vehicle shutdown impulse was calculated to be 3283 pound-seconds (14 600 N-sec) which was 109 pound-seconds (485 N-sec) higher than the predicted level of 3174±175 pound-seconds (14 100±778 N-sec). However, the spacecraft midcourse correction, which must correct for any shutdown impulse deviation from normal, was only 1.20 meters per second (miss plus time of flight). This value is low when compared with the spacecraft capability of 50 meters per second and when compared with the correction of 3.8 meters per second required on AC-10. (See GUIDANCE AND FLIGHT CONTROL SYSTEMS section for a more detailed explanation of the guidance system midcourse correction requirements.)

TABLE V-IV. - CENTAUR ENGINE PERFORMANCE AT ENGINE START PLUS 90 SECONDS, AC-7

Parameter	Engine performance values		
	Expected values[a]	C-1 engine	C-2 engine
Thrust, lb; N:			
Acceptance test	------------------------------	15 028; 66 750	15 070; 66 800
Flight	14 700 to 15 226; 65 331 to 67 669	14 870; 66 000	15 170; 67 400
Specific impulse, sec	429.8 to 438.4	435.5	435.7
Oxidizer to fuel mixture ratio	4.935 to 5.093	5.02	5.09

[a]Based on zero propellant utilization valve angle and standard inlet conditions.

Centaur Boost Pumps

System description. - Boost pumps were used in the liquid oxygen and liquid hydrogen tanks on Centaur to supply propellants to the main engine pumps at required inlet pressures. Both pumps were a mixed-flow type and were powered by gas-driven turbines, as shown in figures V-8 to V-11. Superheated steam and oxygen from the catalytically decomposed products of hydrogen peroxide were supplied to drive the turbines. A constant turbine power on each unit was maintained by metering the hydrogen peroxide through fixed orifices upstream of the catalyst bed.

Boost pump performance. - Performance of the boost pumps was satisfactory during the entire flight. Boost pump start command was initiated at lift-off plus 204.2 seconds and was terminated simultaneously with main engine cutoff at lift-off plus 686.2 seconds. First indications of turbine inlet pressures were evident at 1.8 and 2.8 seconds after boost pump start for fuel and oxidizer boost pumps, respectively.

Steady-state turbine inlet pressures are shown in table V-V. Average values were within 5 psi (3.45 N/cm^2) of the expected values with up to 55 psi (37.9 N/cm^2) peak-to-peak pressure oscillations superimposed. Oscillations of 100 psi (68.9 N/cm^2) peak to peak have been experienced on previous flights and in ground tests with no apparent effect on turbine performance.

Oxidizer and fuel turbine steady-state speed data (as shown in fig. V-12) were higher than the expected values calculated from ground acceptance test data. These differences were attributed to the inability of the ground tests to simulate correctly the actual flight conditions.

TABLE V-V. - CENTAUR BOOST PUMP TURBINE INLET PRESSURES, AC-7

Parameter	Expected steady-state value[a]	Time from boost pump start command, sec					
		40	100	200	300	400	480
Oxidizer[b] turbine inlet pressure, psia; N/cm^2 abs	103.4±10; 71.4±6.9	101; 69.7	102.3; 70.6	104.5; 72.0	103.5; 71.4	103.5; 71.4	104.5; 72.0
Fuel[c] turbine inlet pressure, psia; N/cm^2 abs	143.5±10; 99.0±6.9	145.9; 100.5	146.9; 101.2	147.3; 101.7	147.9; 102.0	147.9; 102.0	147.9; 102.0

[a]Expected value is calculated based on last vendor acceptance test values corrected for the flight hydrogen peroxide bottle pressure.

[b]Flight values are average values with superimposed oscillations increasing to 10 psi (6.89 N/cm^2) maximum peak to peak near the end of boost pump operation.

[c]Flight values are average values with superimposed oscillations increasing to 55 psi (37.9 N/cm^2) maximum peak to peak near the end of boost pump operation.

An unexpected decrease in oxidizer boost pump turbine speed occurred 18 seconds after boost pump start command. Three seconds later, the speed had dropped by 1100 rpm. The boost pump turbine then recovered and attained its original speed by boost pump start plus 26 seconds. This drop in turbine speed was momentary and did not affect the engine start. No firm conclusions have been reached for the cause of the speed drop.

Turbine bearing temperature data are shown in figure V-13. Temperatures prior to lift-off were well above the lower limit of 435° R (242° K). The rate of temperature rise on both units during boost pump operation is comparable to previous flights. No sudden changes in temperature rise rate occurred, which would be indicative of gearbox problems.

Centaur Hydrogen Peroxide Attitude Control Engines

System description. - Attitude control of the Centaur vehicle during the coast phase after main engine cutoff and during the Centaur reorientation and retromaneuver was provided by a combination of fixed-axis constant-thrust hydrogen peroxide engines. The system is shown in figure V-14. Hydrogen peroxide was fed to the engines from a positive-expulsion, bladder-type storage bottle which was pressurized to about 300 psia (206.8 N/cm^2 abs) by the pneumatic system. Firing commands to the engines were given by the Centaur flight control system in response to guidance steering information.

On AC-7, the attitude control system was composed of four engines, 50 pounds (222.4 N) thrust each, and two clusters of three engines each. Each cluster contained one 6-pound (26.7-N) and two 3.5-pound (15.6-N) thrust engines. These engines were used for attitude control and vehicle reorientation after main engine cutoff. The 50-pound (222.4-N) engines provided thrust midway through the Centaur reorientation to provide lateral as well as increased axial separation distance from the spacecraft. These 50-pound (222.4-N) thrust engines were also called on by control logic if disturbances on the vehicle exceeded the control capability of the 3.5- and 6.0-pound (15.6- and 26.7-N) thrust engines.

Engine performance. - All engines operated satisfactorily during the flight. The 3.5- and 6.0-pound (15.6- and 26.7-N) thrust attitude control engines were instrumented to record thrust chamber temperatures. All temperature measurements appeared normal, and firing commands corresponded with vehicle angular rate data to indicate normal engine firing. At lift-off, 133.4 pounds (60.5 kg) of hydrogen peroxide were tanked. Approximately 70 pounds (31.7 kg) were consumed by the engines and boost pumps during the flight.

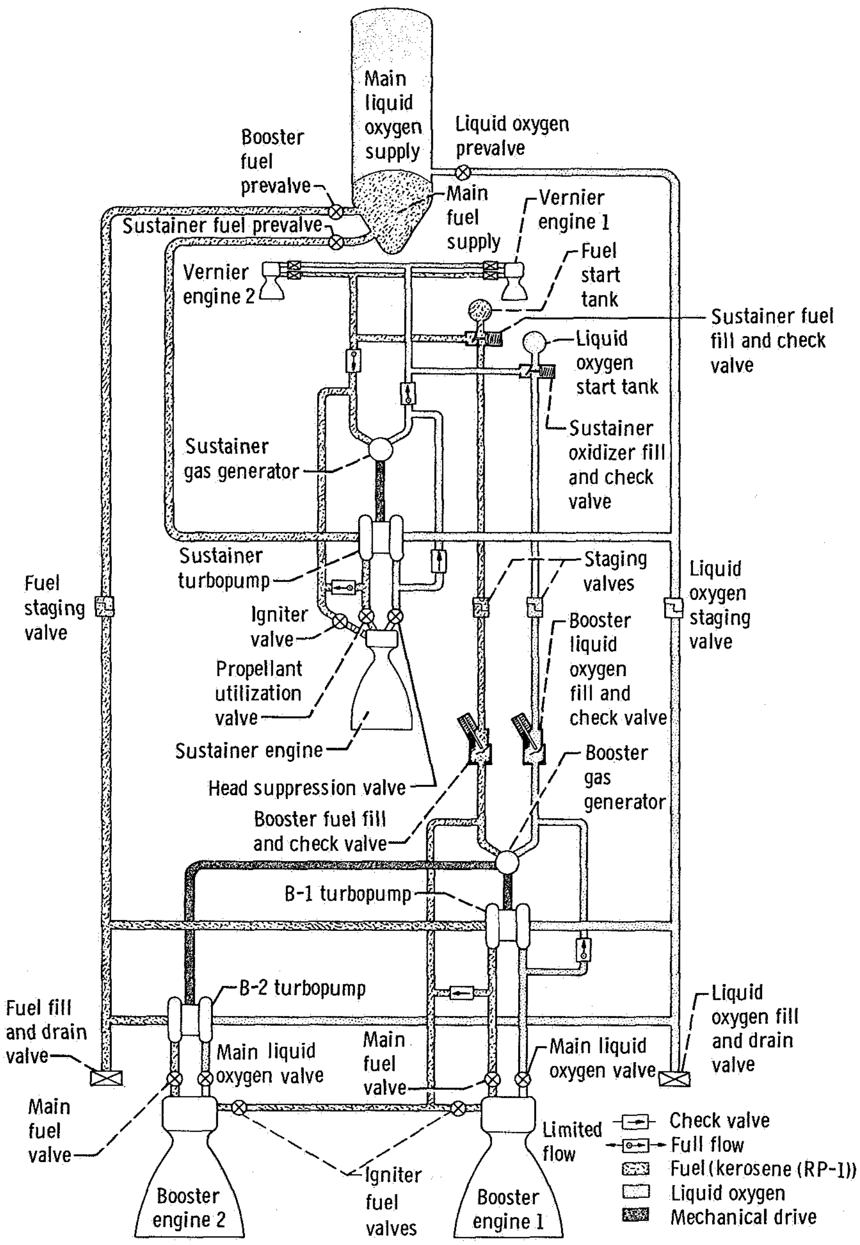

Figure V-1. - Atlas propulsion system schematic drawing, AC-7.

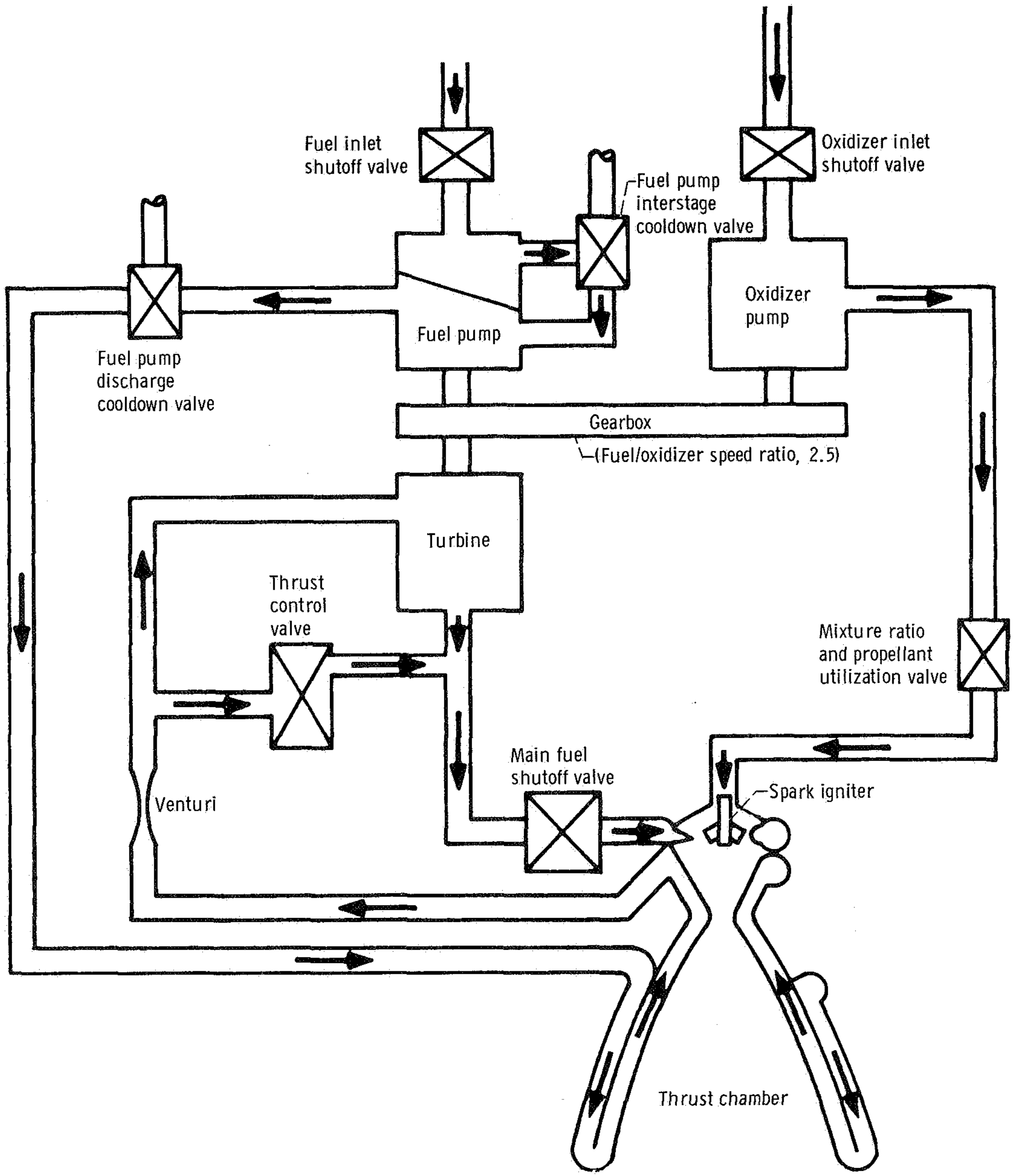

Figure V-2. - Centaur propulsion system schematic drawing, AC-7.

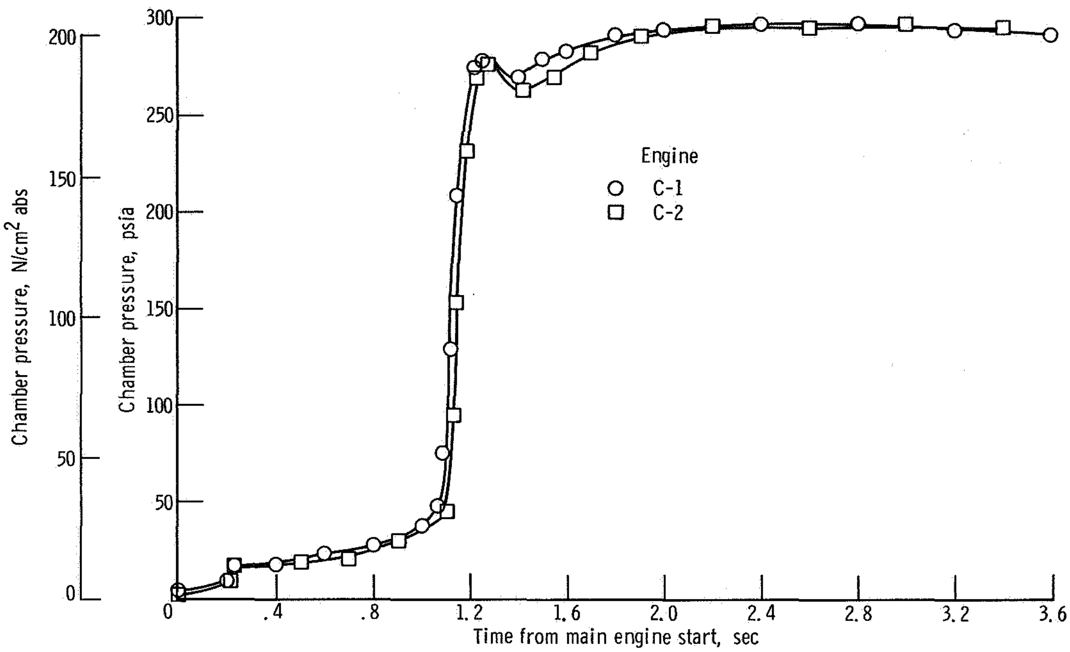

Figure V-3. - Engine chamber pressure start transient, AC-7.

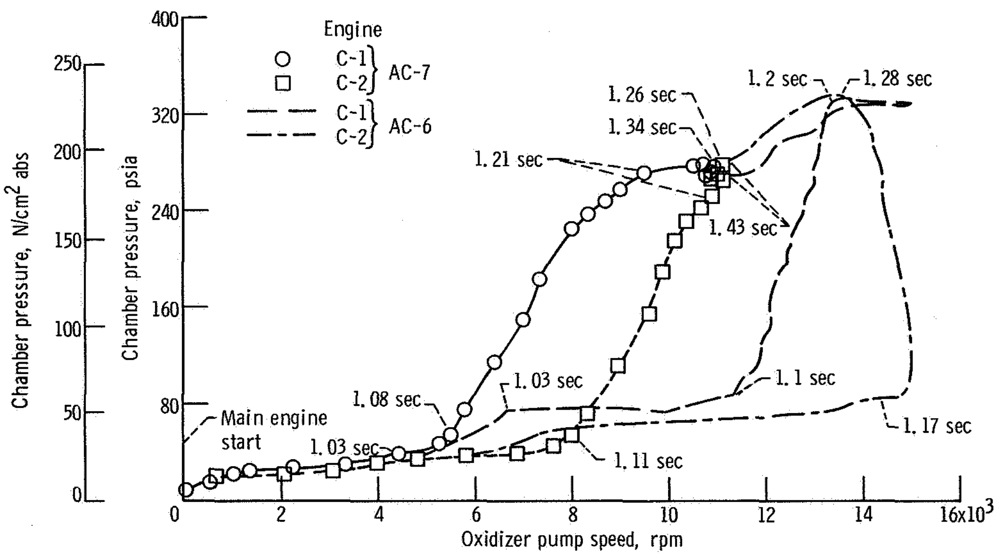

Figure V-4. - Comparison of engine start transient characteristics, AC-7. All times are from main engine start.

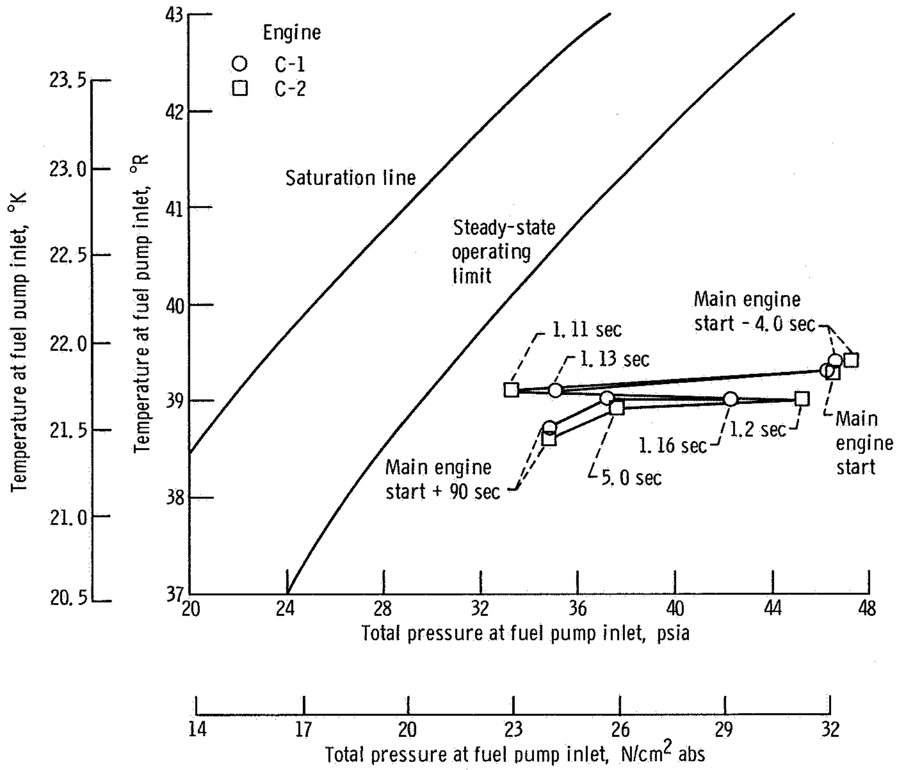

Figure V-5. - Fuel pump inlet conditions near engine start, AC-7.

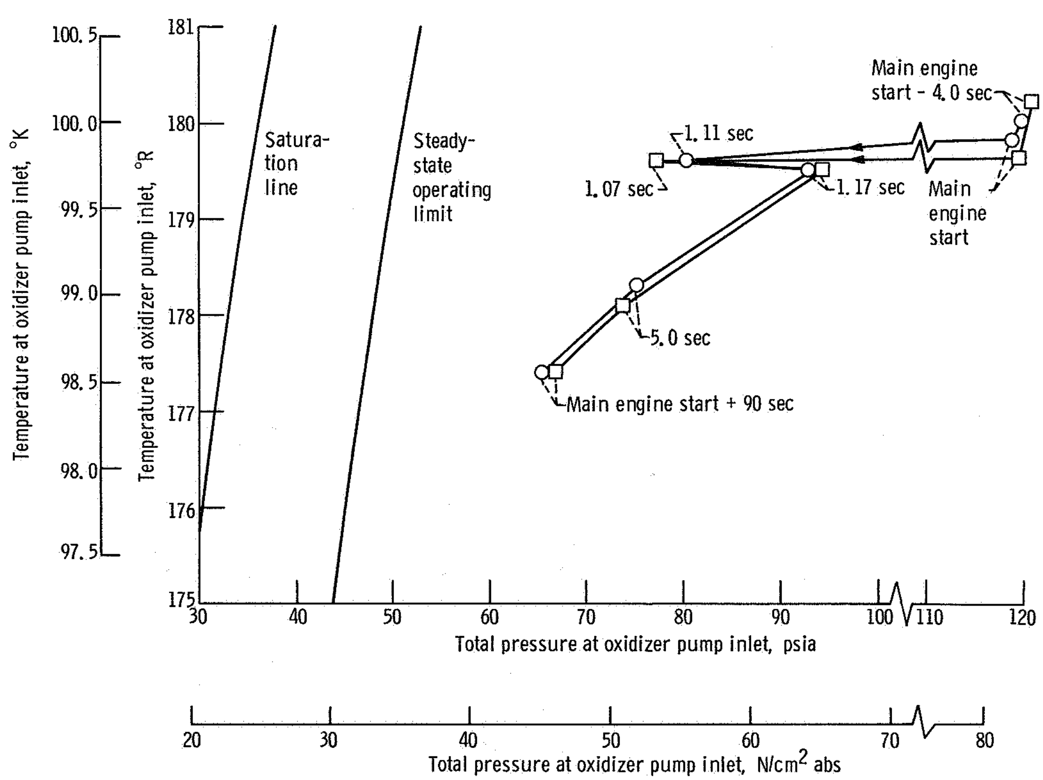

Figure V-6. - Oxidizer pump inlet conditions near engine start, AC-7.

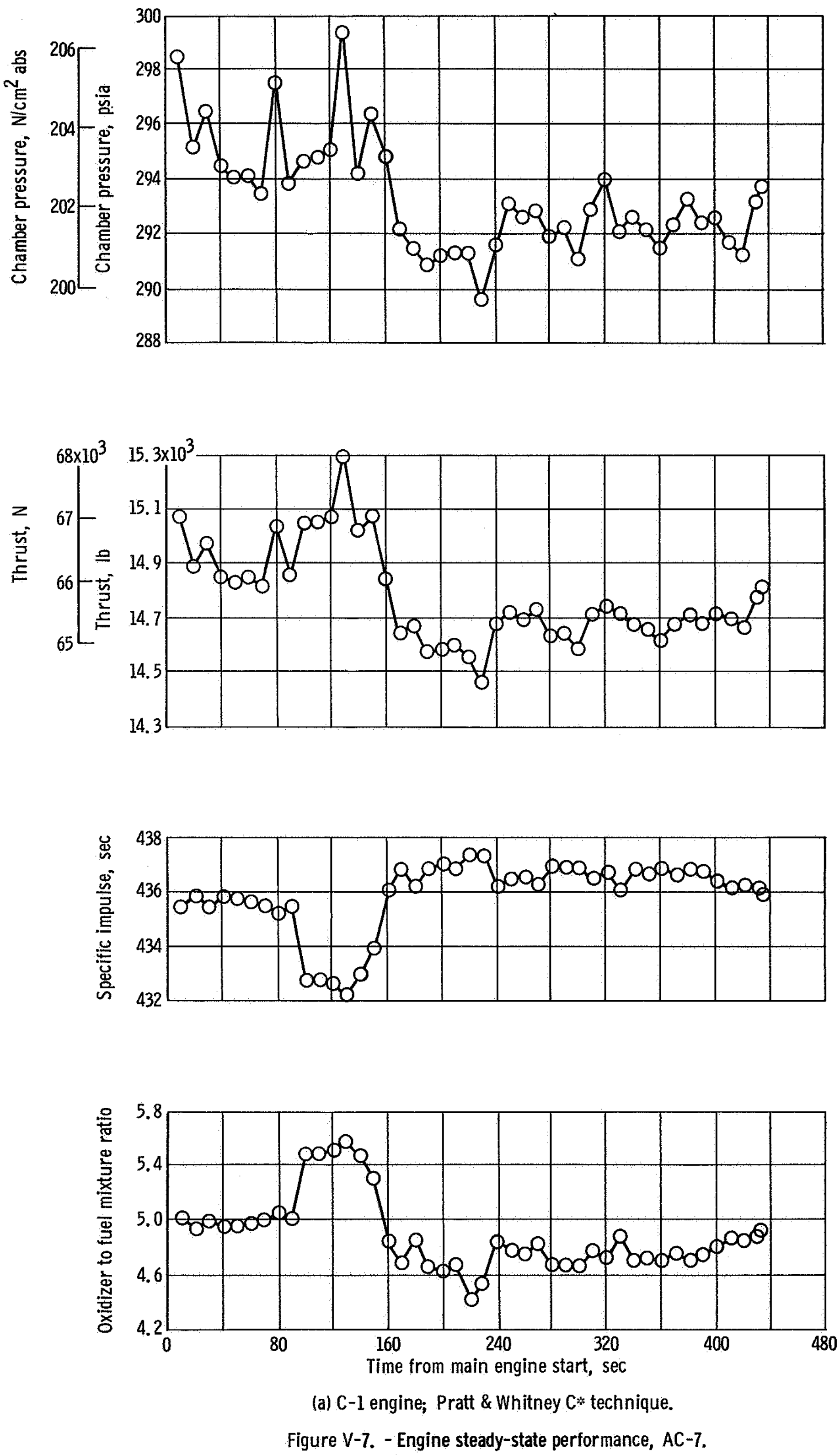

(a) C-1 engine; Pratt & Whitney C* technique.

Figure V-7. - Engine steady-state performance, AC-7.

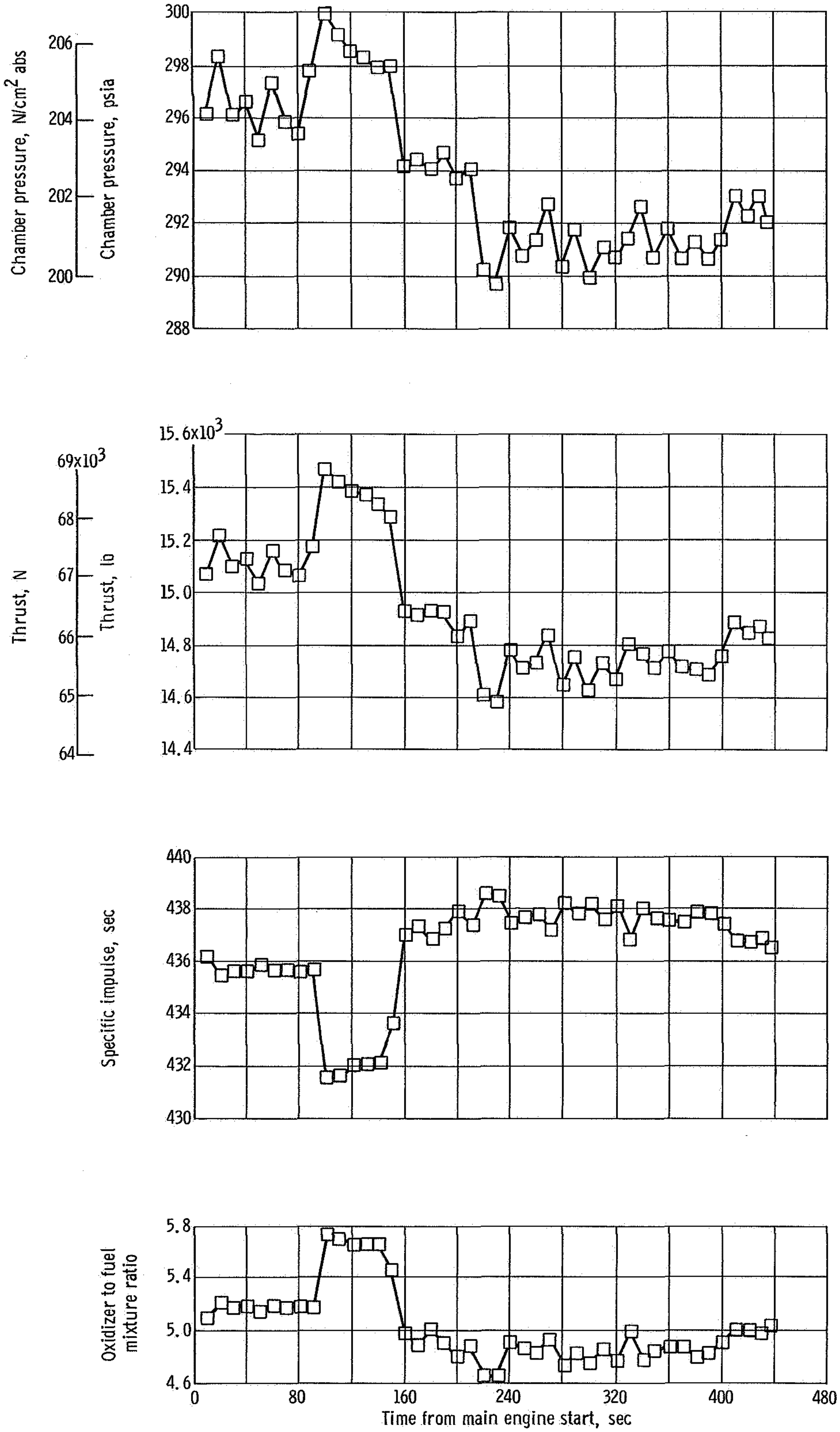

(b) C-2 engine; Pratt & Whitney C* technique.

Figure V-7. - Continued.

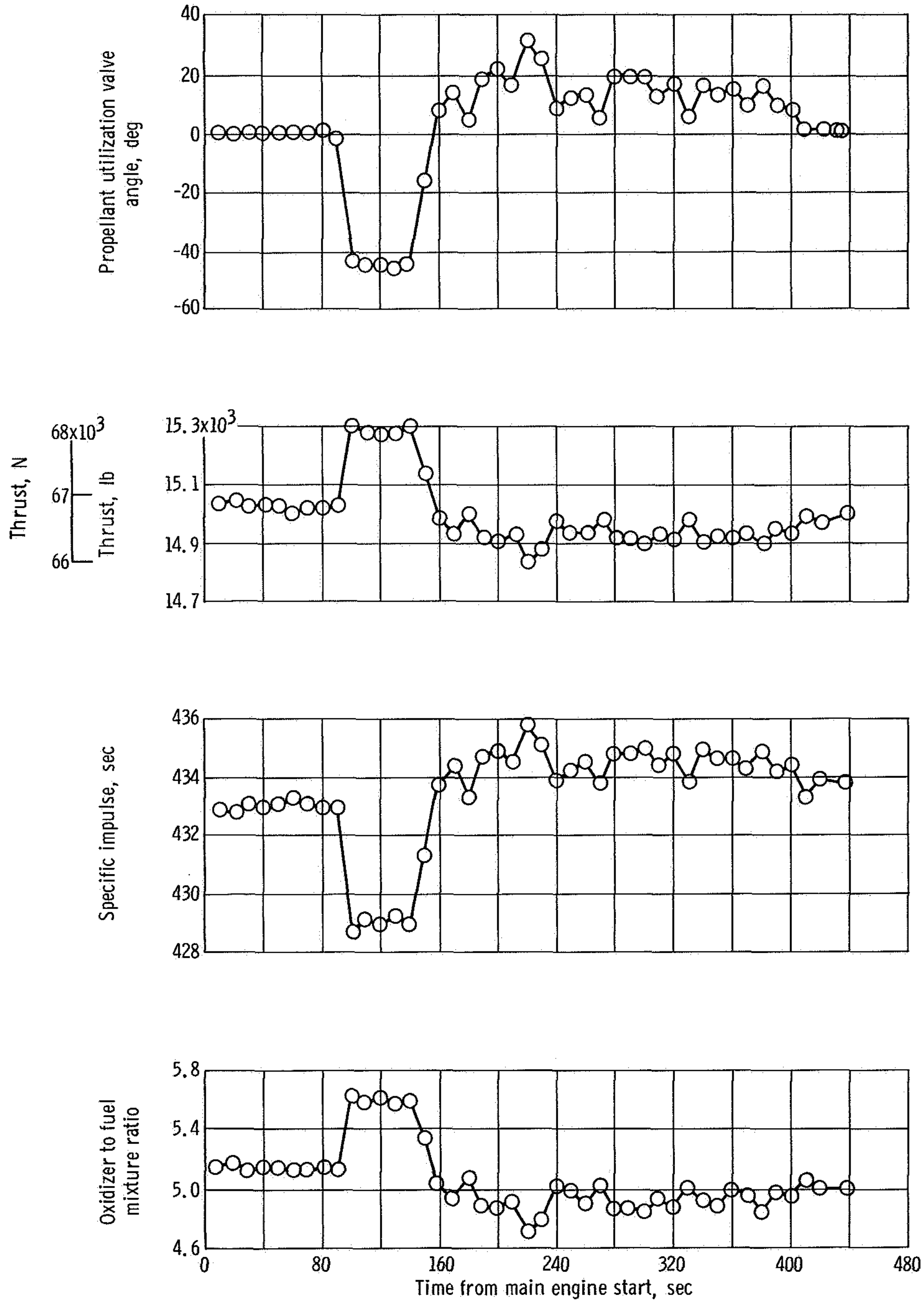

(c) C-1 engine; Pratt & Whitney regression technique.

Figure V-7. - Continued.

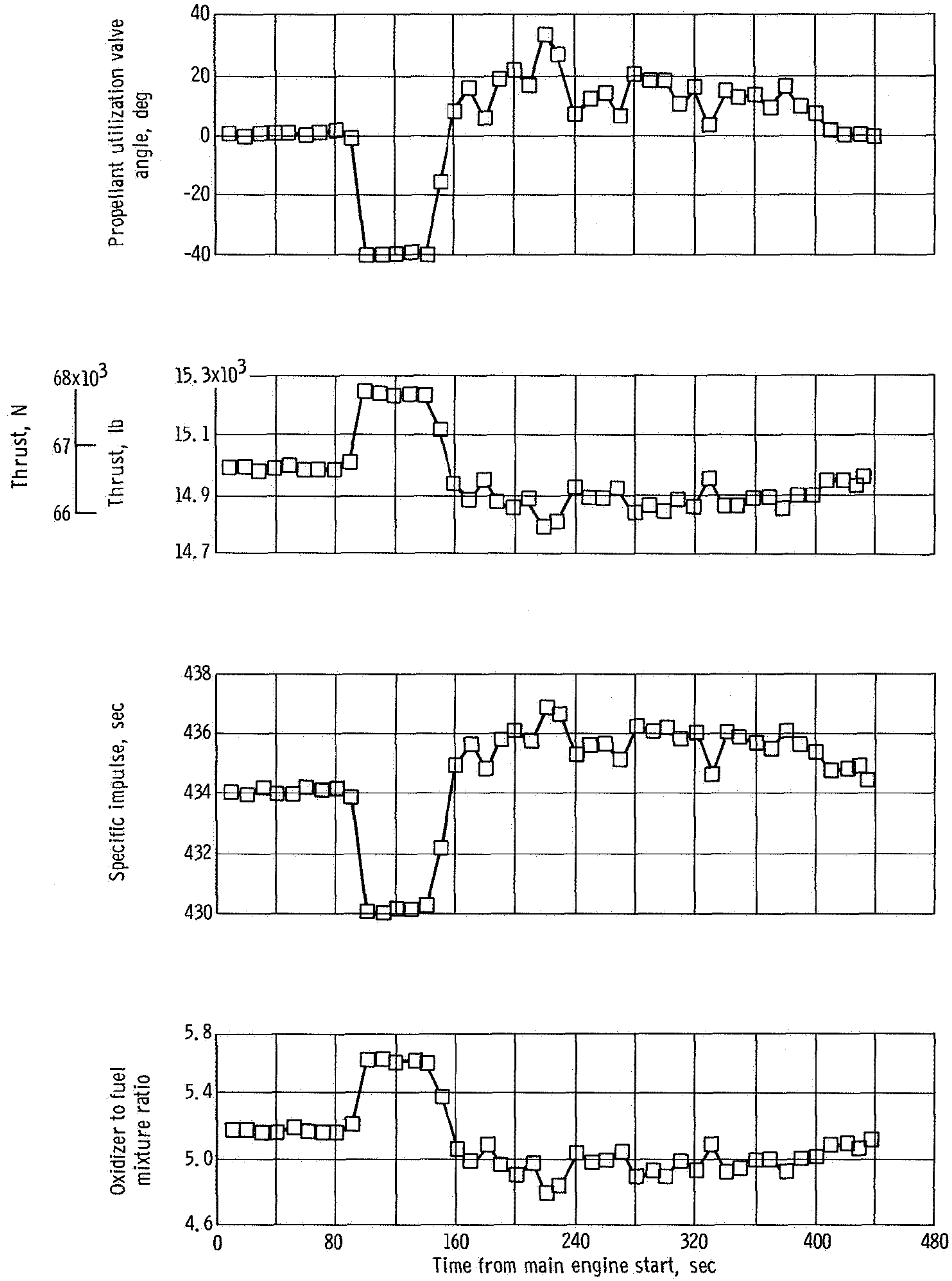

(d) C-2 engine; Pratt & Whitney regression technique.

Figure V-7. - Concluded.

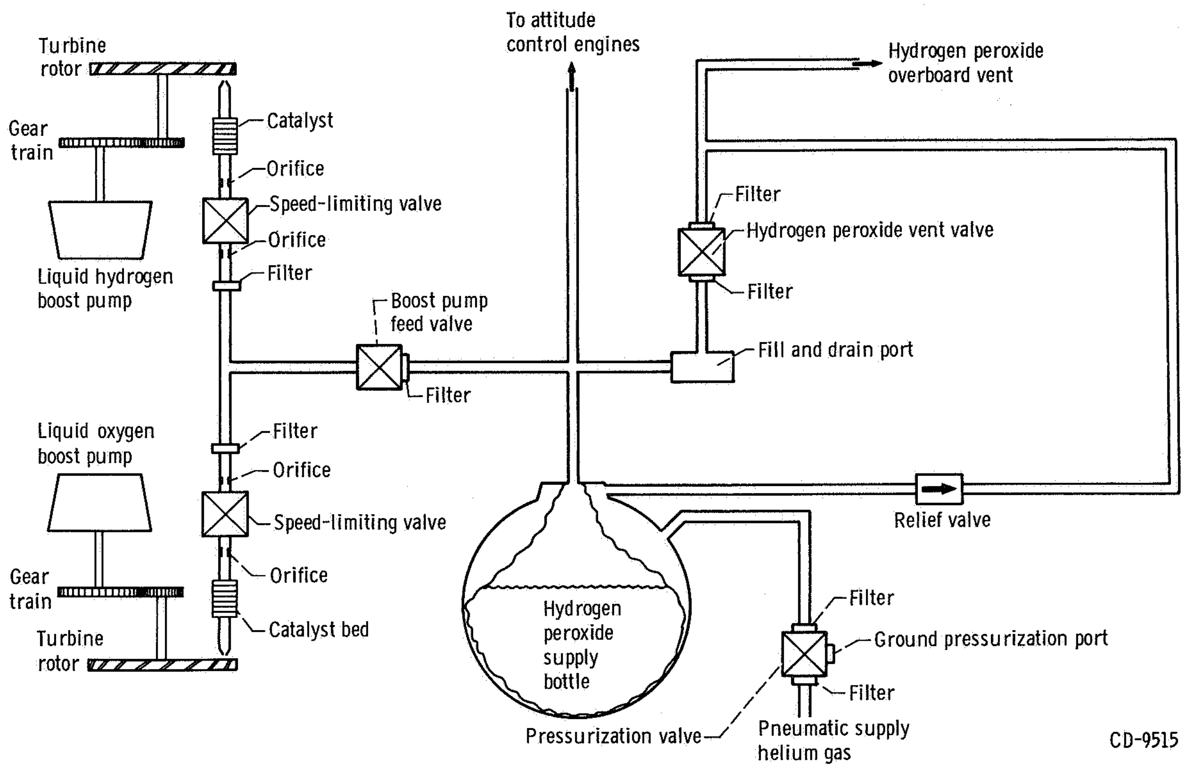

Figure V-8. - Schematic drawing of Centaur boost pump hydrogen peroxide supply, AC-7.

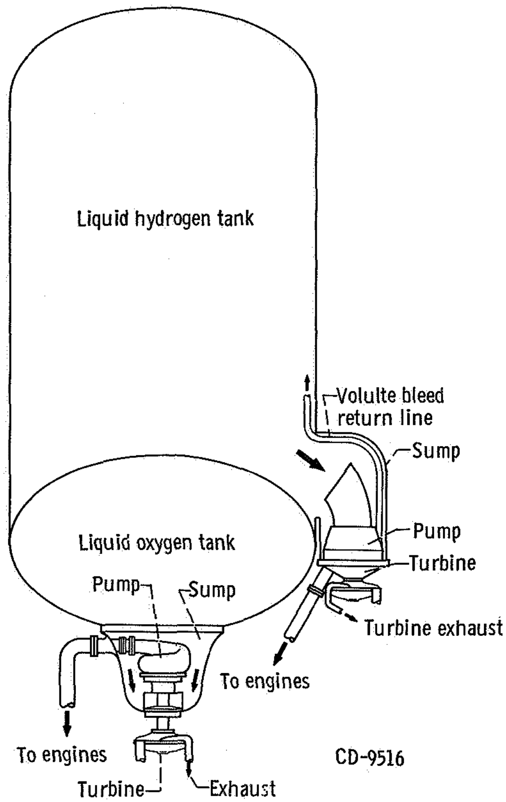

Figure V-9. - Centaur fuel and oxidizer boost pump arrangement, AC-7.

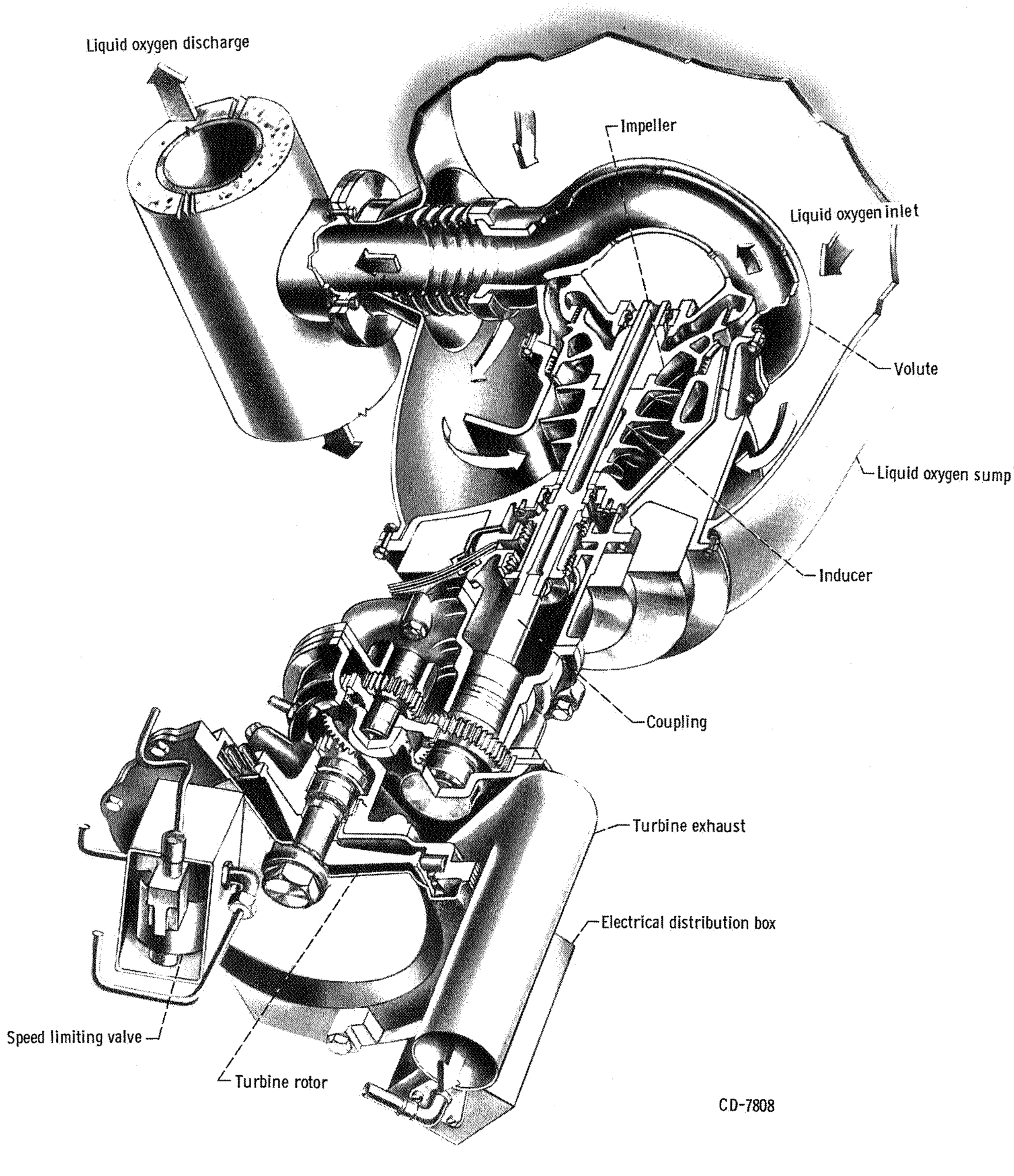

Figure V-10. - Centaur liquid oxygen boost pump and turbine cutaway, AC-7.

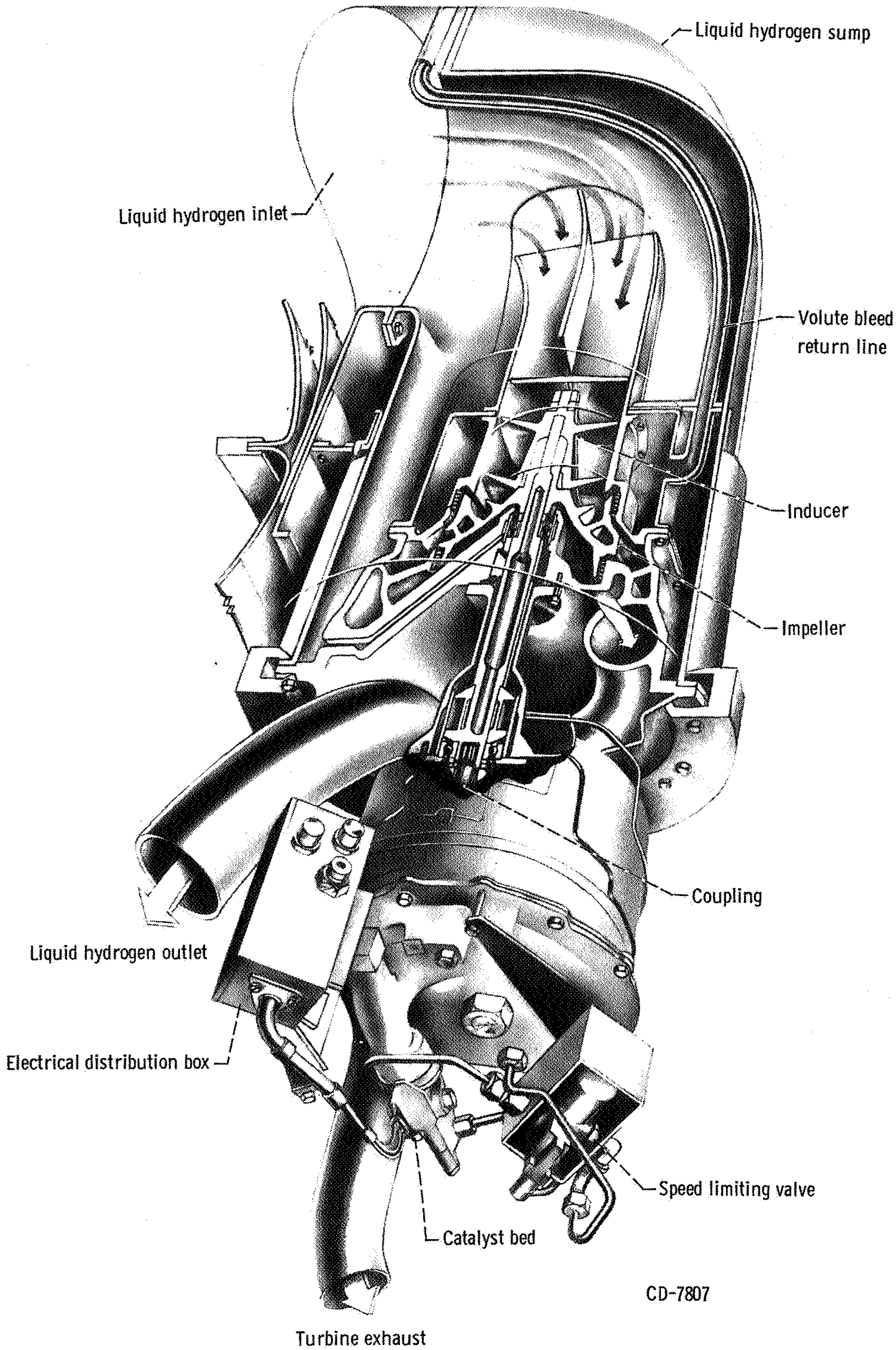

Figure V-11. - Centaur liquid hydrogen boost pump and turbine cutaway, AC-7.

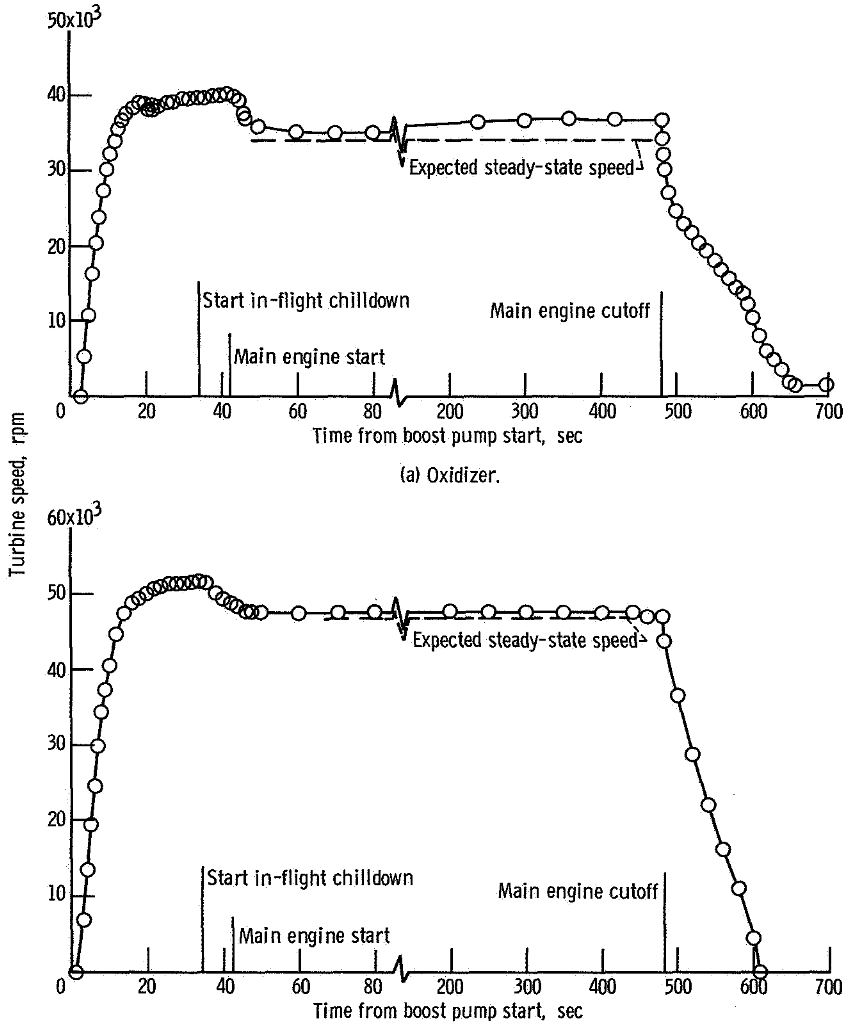

Figure V-12. - Centaur boost pump turbine speed, AC-7.

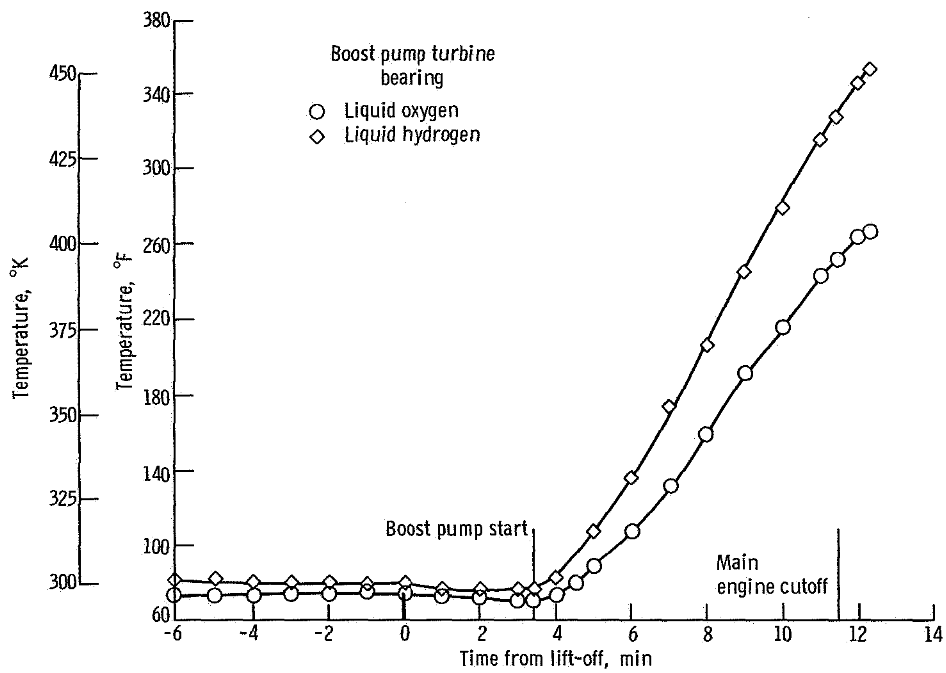

Figure V-13. - Centaur boost pump turbine bearing temperature, AC-7.

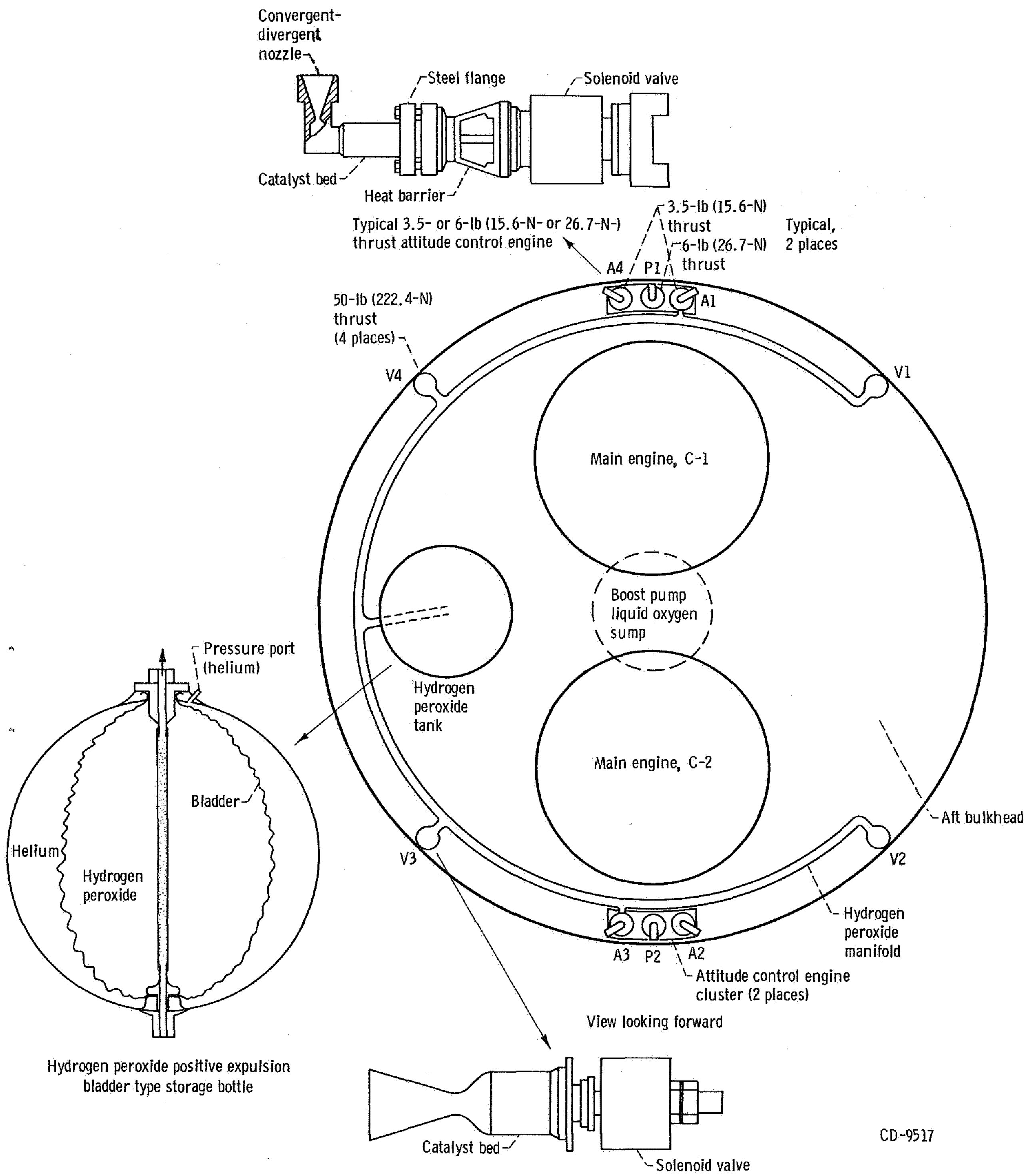

Figure V-14. - Centaur hydrogen peroxide engine system, AC-7. (The 3.5-lb (15.6-N) engines are canted approximately 25° outboard.)

PROPELLANT LOADING AND PROPELLANT UTILIZATION

by Steven V. Szabo, Jr.

Level Indicating System for Propellant Loading

System description. - Atlas propellant levels in the tanks for flight were determined by using liquid level sensors located at discrete points in the fuel and oxidizer tanks, as shown in figure V-15. The sensors located in the liquid oxygen tank were the platinum hot-wire type.

The associated control circuitry for the fuel level sensors was an oscillator circuit that used the resonant characteristics of the piezoelectric crystal to maintain oscillations. When the sensor was immersed in liquid, the vibratory oscillations of the crystal were damped causing the control circuit to stop oscillating. This cessation of oscillations deenergized a control relay and provided a signal to the propellant loading operator.

The control unit for the platinum hot-wire liquid oxygen sensors was an amplifier that detected a change in voltage level (similar to a Schmidt trigger circuit). The liquid oxygen sensors were supplied with a near constant current source (approximately 200 mA). The voltage drop across a sensor reflected the resistance value of the sensor. The sensing element was a 1-mil platinum wire which had a linear resistance temperature coefficient. When dry (warm), the wire had a high resistance and therefore a high voltage drop. When immersed in a cryogenic (cold), it had a low resistance and a low voltage drop. When the sensor was wetted, a control relay was deenergized and a signal was sent to the propellant loading operator.

The Centaur propellant level indicating system is shown in figure V-16. It utilized hot-wire level sensors in both the liquid oxygen and liquid hydrogen tanks. The sensors were similar in operation to the ones in the Atlas liquid oxygen tank.

Propellant weights. - Atlas fuel weight was 76 294 pounds (34 606 kg) at lift-off at a density of 49.58 pounds per cubic foot (793.3 kg/m^3). Atlas liquid oxygen weight at engine ignition was 175 271 pounds (79 500 kg) at a density of 69.36 pounds per cubic foot (1110 kg/m^3).

Centaur propellant loading was satisfactorily accomplished with 5277 pounds (2393.6 kg) of liquid oxygen and 25 520 pounds (11 572.2 kg) of liquid oxygen on board at lift-off. Data used to determine propellant weights at lift-off are given in table V-VI.

TABLE V-VI. - CENTAUR PROPELLANT LOADING DATA, AC-7

(a) U.S. Customary Units

Quantity or event	Propellant tank	
	Hydrogen	Oxygen
Sensor required to be wet at T - 90 sec, percent	99.80	---------
Sensor required to be wet at T - 75 sec, percent	-------	100.20
Sensor vehicle station number	174.99	373.16
Tank volume at sensor[a], ft^3	1256.69	370.94
Ullage volume at sensor, ft^3	11.22	6.58
Liquid hydrogen 99.8 percent sensor dry at-, sec	T - 18	---------
Liquid oxygen 100.2 percent sensor dry at-, sec	-------	T - 23
Ullage pressure at lift-off, psia	21.4	30.6
Density at lift-off[b], lb/ft^3	4.20	68.8
Weight in tank at time sensor indicates dry, lb	5281.0	25 521.0
Liquid hydrogen boiloff to vent valve lock, lb	4	--------
Liquid oxygen boiloff to lift-off, lb	------	9
Ullage volume at lift-off, ft^3	11.2	6.6
Weight at lift-off[c], lb	5277.0	25 512.0

(b) SI Units

Sensor required to be wet at T - 90 sec, percent	99.80	--------
Sensor required to be wet at T - 75 sec, percent	------	100.20
Sensor vehicle station number	174.99	373.16
Tank volume at sensor[a], m^3	35.59	10.50
Ullage volume at sensor, m^3	0.32	0.19
Liquid hydrogen 99.8 percent sensor dry at-, sec	T - 18	--------
Liquid oxygen 100.2 percent sensor dry at-, sec	------	T - 23
Ullage pressure at lift-off, N/cm^2 abs	14.74	21.08
Density at lift-off[b], kg/m^3	67.2	1100.8
Weight in tank at time sensor indicates dry, kg	2395.5	11 576.3
Liquid hydrogen boiloff to vent valve lock, kg	1.8	--------
Liquid oxygen boiloff to lift-off, kg	------	4.1
Ullage volume at lift-off, m^3	0.32	0.20
Weight at lift-off[c], kg	2393.6	11 572.2

[a]Volumes include 1.85 ft^3 (0.052 m^3) liquid oxygen and 2.53 ft^3 (0.0716 m^3) liquid hydrogen for lines from boost pumps to engine turbopump inlet valves.

[b]These are effective densities for boiling liquid hydrogen and liquid oxygen.

[c]Preflight estimates were 5301 lb (2404.5 kg) of liquid hydrogen and 25 447 lb (11 542.7 kg) liquid oxygen.

Atlas Propellant Utilization System

System description. - The Atlas propellant utilization system, shown in figure V-17, was used to ensure near simultaneous propellant depletion and minimum burnable residuals at sustainer engine cutoff. This was accomplished by controlling propellant mixture ratio (oxidizer/fuel flow rate) to the sustainer engine. The system consisted of two mercury manometer assemblies which sensed fuel and oxidizer head pressures, a computer-comparator package, a hydraulically actuated propellant utilization (fuel) valve, sensing lines, and associated electrical harnessing. During flight, the manometers sensed propellant head pressures which were indicative of propellant mass. The mass ratio was then compared with a reference ratio in the computer-comparator, and if needed, a correction signal was sent to the valve controlling the main fuel flow to the sustainer engine. The oxidizer flow was regulated by the head suppression valve. This head suppression valve sensed propellant utilization valve movement and moved in a direction opposite to that of the propellant utilization valve, thus altering propellant mixture ratio but maintaining a constant total propellant mass flow to the sustainer engine.

System performance. - The Atlas propellant utilization system performance during the AC-7 flight was satisfactory. The propellant utilization valve angle position during flight is shown in figure V-18. The propellant consumption during flight was controlled to a nearly simultaneous depletion of liquid oxygen and fuel. A characteristic liquid oxygen depletion was evident on this flight, as shown in figure V-19. Although the sustainer engine cutoff signal was generated by the fuel level sensors in the Atlas fuel tank (fuel depletion sensors), the sustainer liquid oxygen pump inlet pressure had dropped to about two-thirds of its normal operating pressure by engine cutoff. This pressure drop along with the sustainer engine pump speed rise indicated that the sustainer began running out of usable liquid oxygen about 6 seconds prior to engine cutoff.

Atlas propellant residuals. - The nearly simultaneous depletion of usable propellants resulted in total propellant residuals of 385 pounds (174.6 kg) of liquid oxygen and 137 pounds (62.1 kg of fuel. These values are based on densities of 68.6 pounds per cubic foot (1099 kg/m^3) for liquid oxygen and 50 pounds per cubic foot (800.9 kg/m^3) for fuel at this time in flight. The liquid oxygen residual was calculated by using the propellant utilization head sensing port uncovery as a reference point. The fuel residual represents the amount between the fuel depletion sensors and the sustainer engine pump inlet.

Centaur Propellant Utilization System

System description. - The Centaur propellant utilization system was used during flight to optimize propellant consumption for minimum residuals. The system is shown schematically in figure V-20. It was also used during tanking to indicate propellant levels. In flight, the mass of propellant remaining in each tank was sensed by a capacitance probe and compared in a bridge circuit. If the mass ratio of propellants remaining in the tanks varied from a predetermined value (oxidizer to fuel ratio, 5.0 to 1), an error signal was sent to the proportional servopositioner which controlled the liquid oxygen flow control valve. If the mass ratio in the tanks was greater than 5 to 1, the liquid oxygen flow rate was increased to return the ratio to 5 to 1. If the ratio was less than 5 to 1, the liquid oxygen flow rate was decreased. Since the sensing probes did not extend to the top of the tanks, system control was not affected until approximately 90 seconds after main engine start. During this 90-second period of engine burn, the liquid oxygen flow control valves were locked at a propellant mixture ratio of 5 to 1.

System performance. - Prelaunch checks and calibrations of the system were within specification. The in-flight operation of the propellant utilization system was satisfactory. The system liquid oxygen valve positions during flight are shown in figure V-21. The valves were unlocked by the programmer at approximately main engine start plus 90 seconds. At this time, system control was effected. Probe uncovery (liquid levels passing the top of the probe) occurred as expected at approximately main engine start plus 90 seconds. The valves were locked at the mixture ratio position of 5 to 1 by the programmer at approximately 30 seconds prior to engine cutoff because the probes did not extend to the bottom of the tank.

System accuracy. - The Centaur propellant utilization system controlled propellant consumption so that the burnable residual propellants were within 7 pounds (3.17 kg) of hydrogen of a mixture ratio (oxygen/hydrogen) of 5 to 1 at engine cutoff.

Propellant residuals. - The propellant residuals remaining at Centaur engine cutoff were calculated by using the times that the propellant levels passed the bottoms of the probes as reference points. The residuals are summarized in table V-VII.

TABLE V-VII. - CENTAUR PROPELLANT RESIDUALS, AC-7

Residuals at engine cutoff	Propellant	
	Liquid oxygen	Liquid hydrogen
Total propellant[a], lb; kg	270; 122.5	131; 59.4
Burnable propellant[a], lb; kg	202; 91.6	59; 26.8
Burn time, sec	3.6	5.7

[a]Values are ±10 percent.

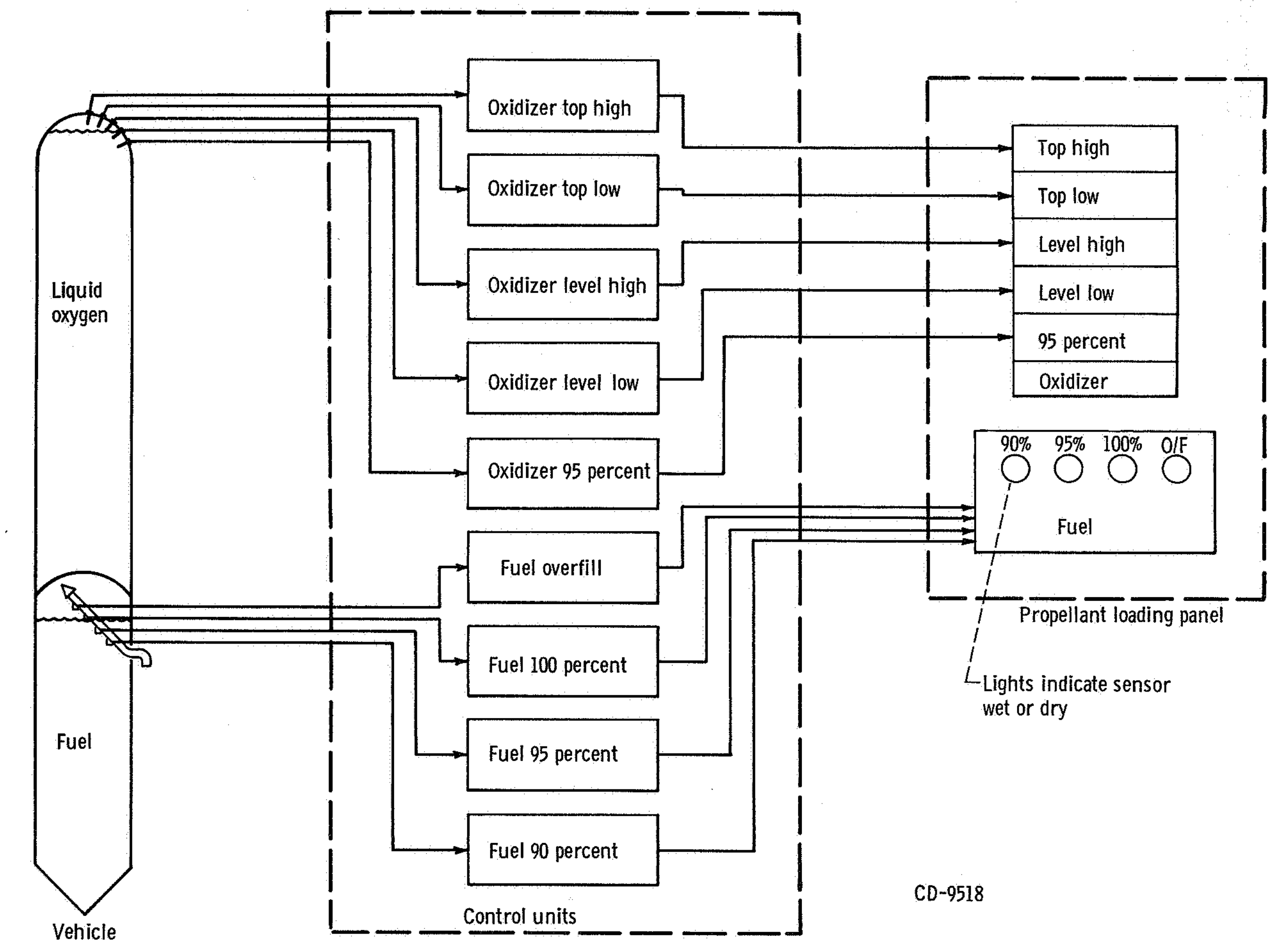

Figure V-15. - First-stage Atlas propellant loading level indicating system, AC-7. (Percent levels shown are percent of desired flight, not of tank volume.)

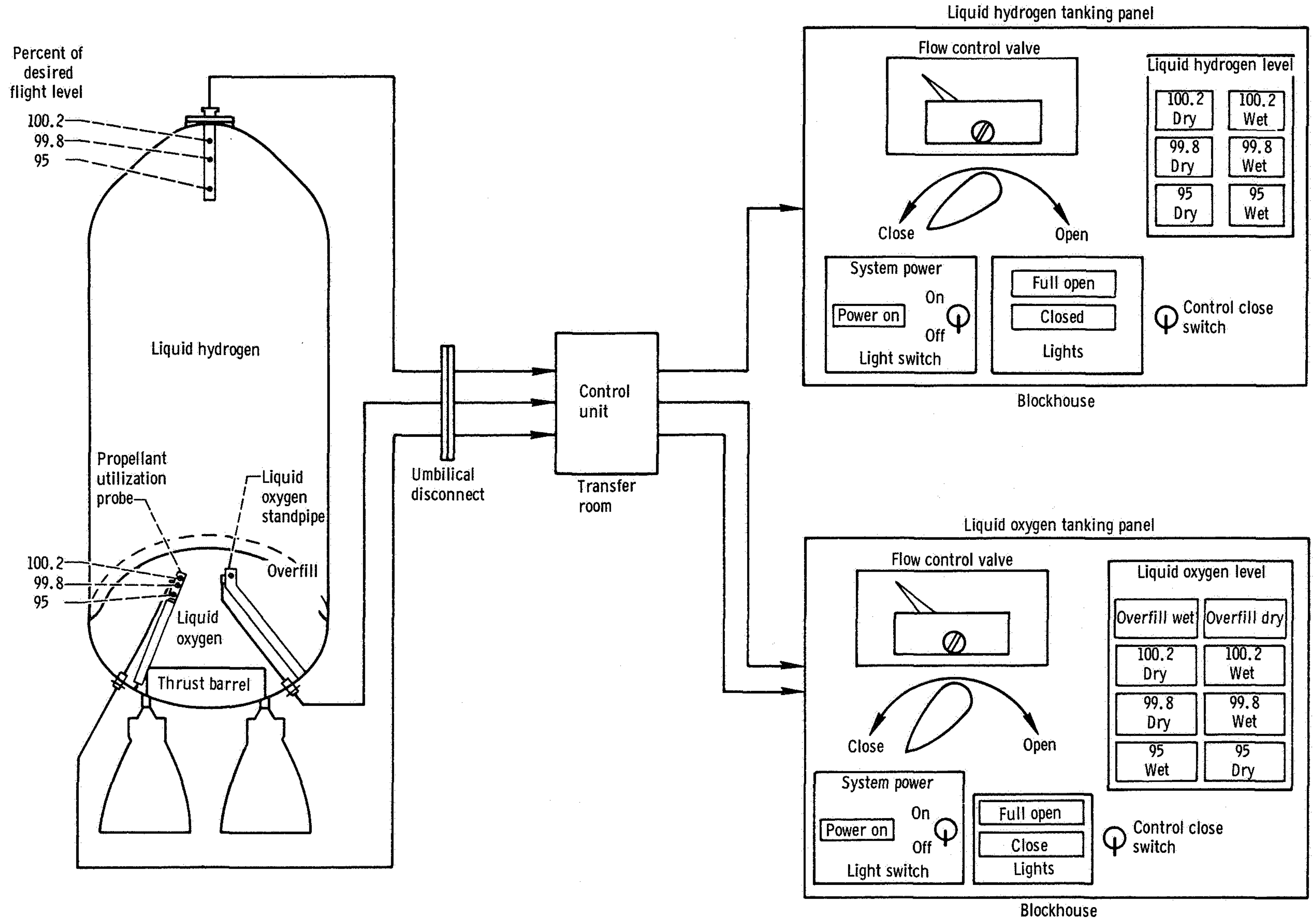

Figure V-16. - Centaur propellant loading level indicating system, AC-7. (All point sensors are dual element.)

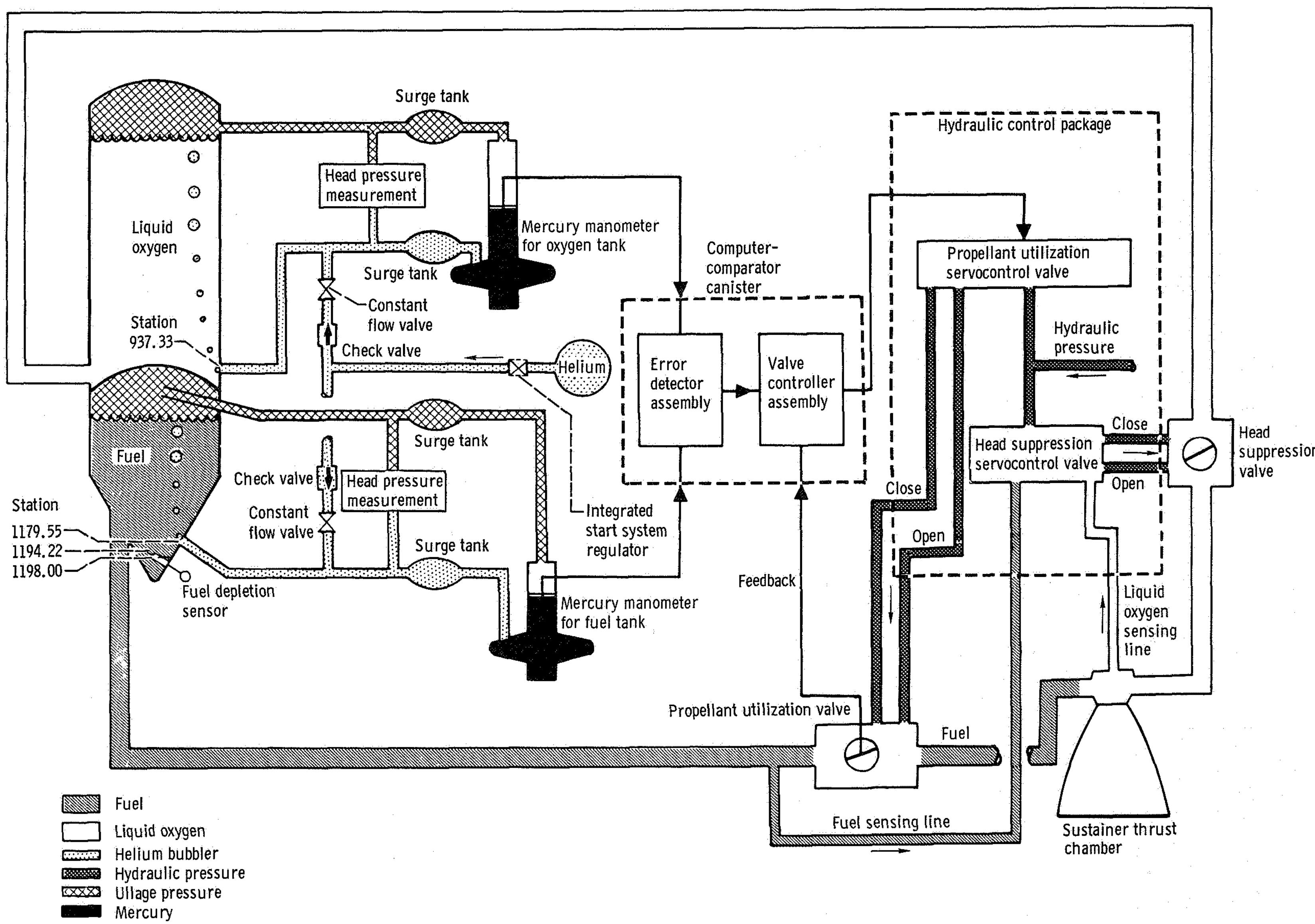

Figure V-17. - Atlas propellant utilization system, AC-7.

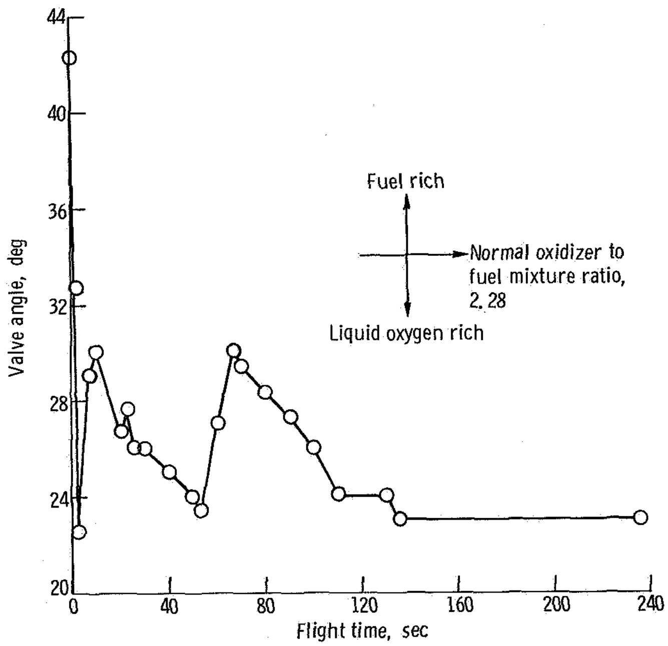

Figure V-18. - Atlas propellant utilization valve angle during flight, AC-7.

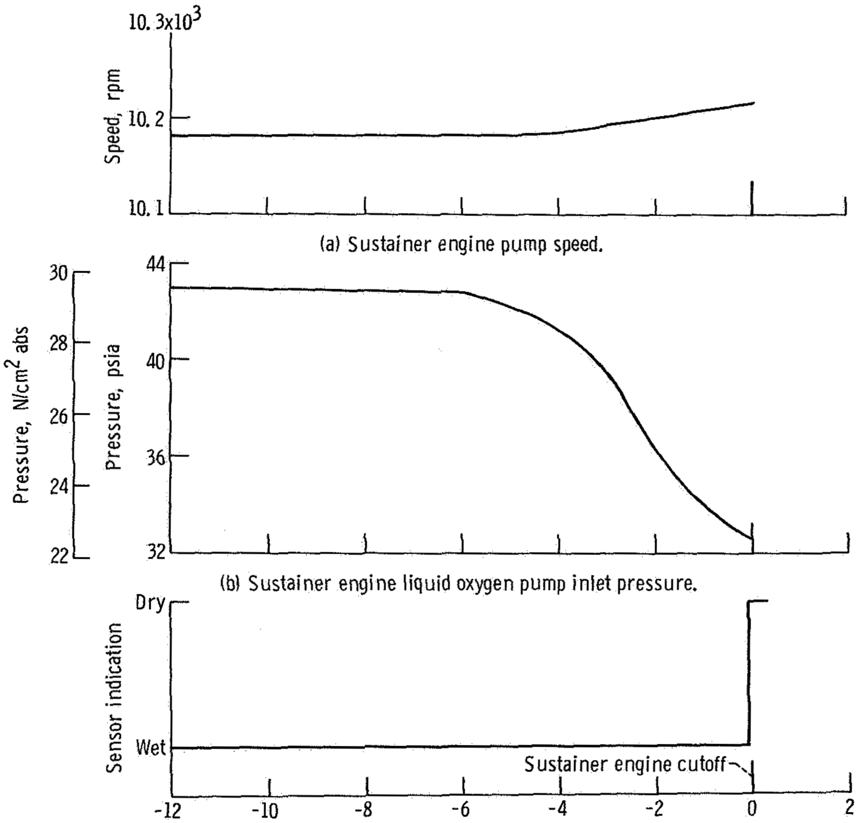

(c) Atlas fuel depletion sensors.

Figure V-19. - Sustainer engine liquid oxygen depletion characteristics at engine cutoff.

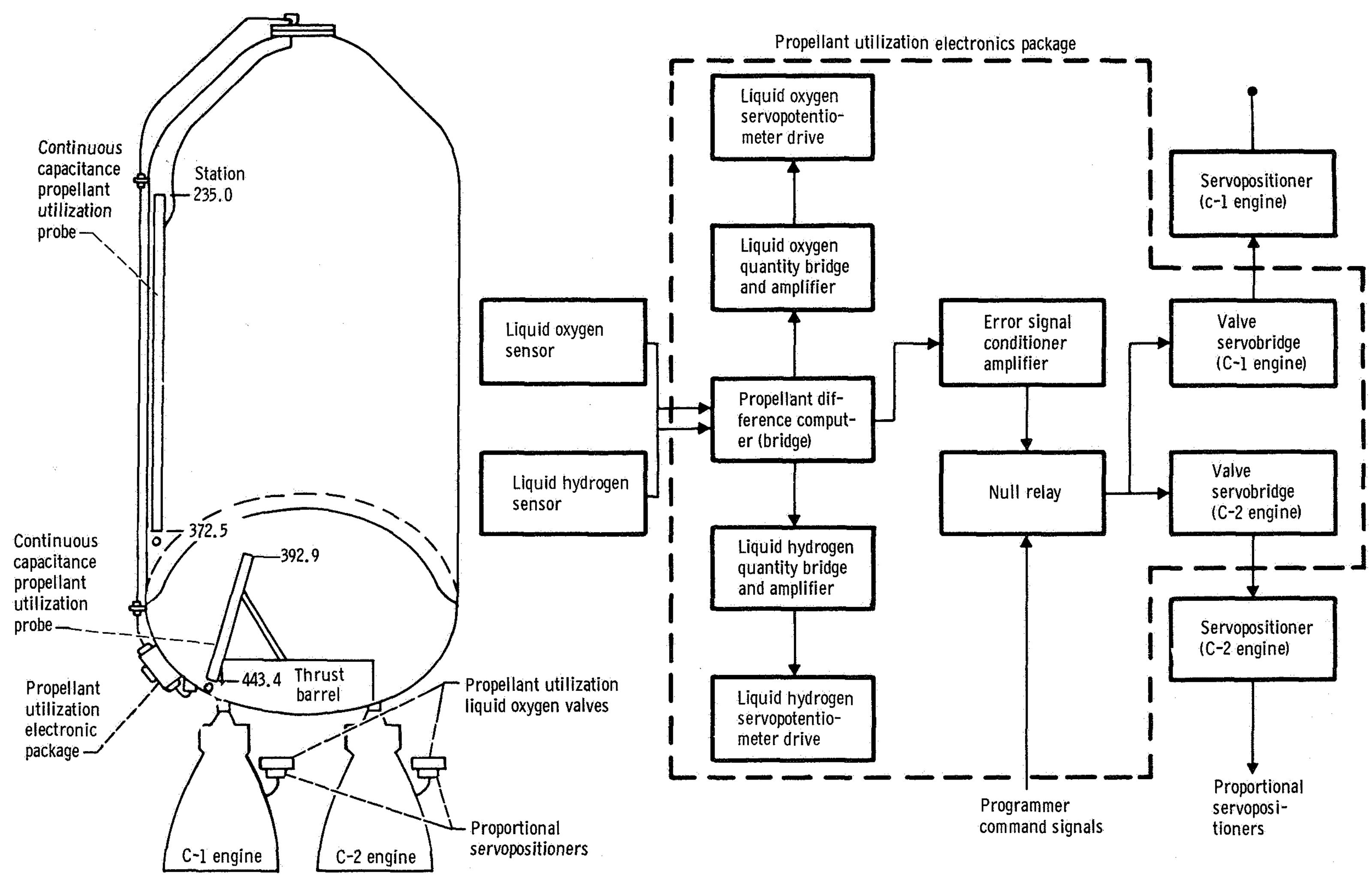

Figure V-20. - Centaur propellant utilization system, AC-7.

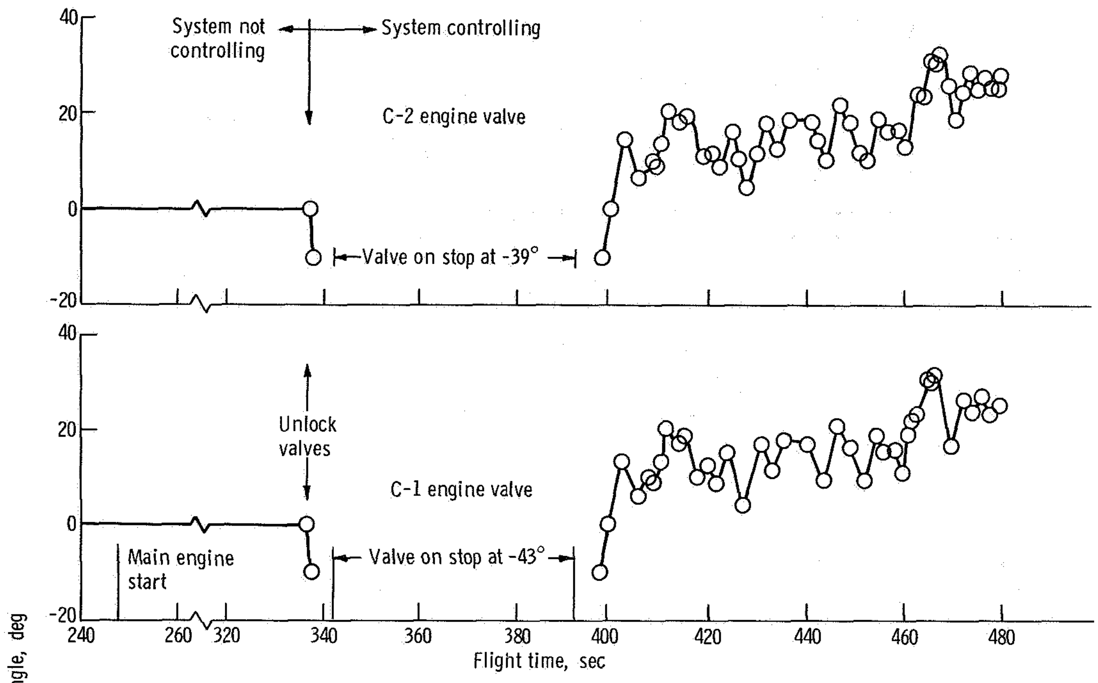

(a) Time, 240 to 480 seconds.

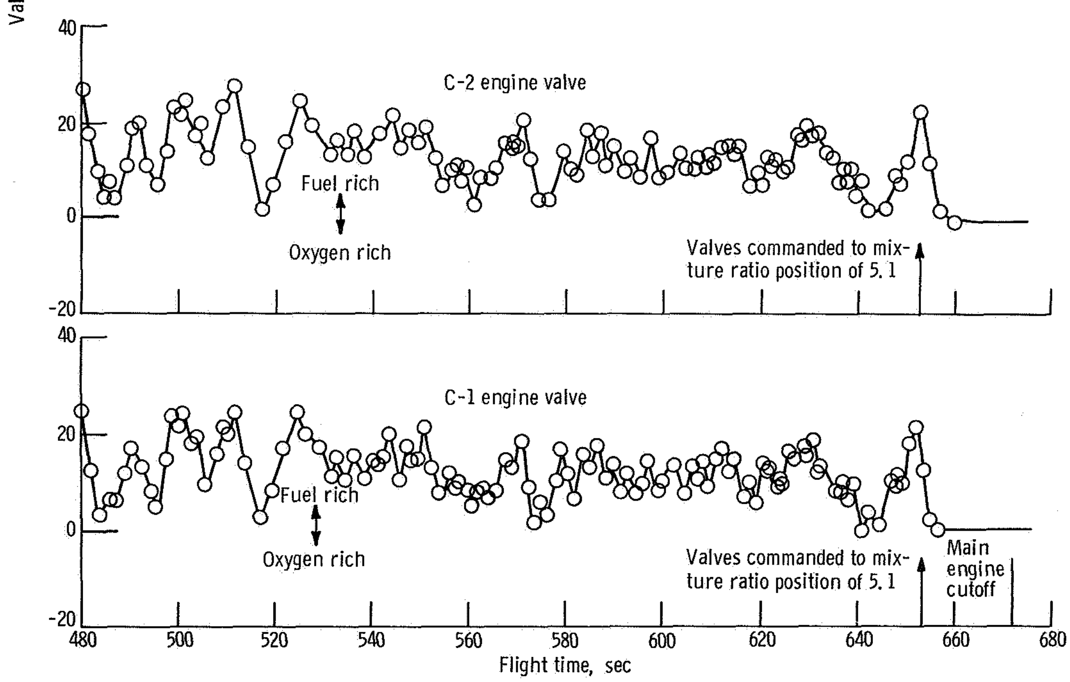

(b) Time, 480 to 680 seconds.

Figure V-21. - Centaur propellant utilization system valve angles, AC-7. Positive valve angles are fuel rich; negative valve angles are oxygen rich.

PNEUMATIC SYSTEMS

by William A. Groesbeck and Merle L. Jones

Atlas

System description. - The Atlas pneumatic system, shown in figure V-22, supplied helium at regulated pressures for several pressurization and control functions. The propellant tanks were pressurized to provide sufficient pressure to prevent propellant pump cavitation and to maintain stability of the pressure supported tank structure. Pressurized helium was bled off the fuel tank pressurization duct to pressurize the hydraulic reservoirs and turbopump lubrication tanks. Helium was supplied to these systems from six bottles mounted in the jettisonable booster section. Prior to launch, the bottles were chilled with liquid nitrogen to increase the stored mass of helium. The cold gas was heated and expanded by a heat exchanger in the booster engine turbine exhaust duct before being supplied to the tank pressure regulators.

A separate system provided pressurized helium to pneumatic regulators in the booster and sustainer engine control systems. Helium for this purpose was supplied from a bottle mounted in the sustainer section.

Propellant tank pressurization. - Control of propellant tank pressures was switched from ground to airborne systems at T - 60 seconds. At this time, however, the liquid oxygen boiloff valve failed to close, preventing an increase in ullage pressure to flight level and caused a countdown delay. Repeated manual cycling of the valve corrected the problem, which was attributed to momentary icing of the valve controller which prevented it from closing.

Ullage pressure profiles, shown in figure V-23, indicated that tank pressures were maintained satisfactorily during flight. The fuel tank pressure was stable at about 60.4 psig (41.6 N/cm^2 gage) until termination of pneumatic control at booster staging. From about T - 2 minutes to T + 20 seconds, the liquid oxygen pneumatic regulator was biased by a slight helium bleed flow into the ullage pressure sensing line. This bias caused the regulator to control oxygen tank pressure at a lower level than the regulator setting. Reducing the oxidizer tank pressure caused an increase in the differential pressure across the intermediate bulkhead. The increased differential pressure ensured against bulkhead reversal due to launch transient loads and an initially large liquid oxygen head pressure. At T + 20 seconds, when the launch transient loads had passed, liquid oxygen head pressure was less, the bias was removed, and the regulator increased tank pressure to within the normal range of 28.5 to 31.0 psig (19.6 to 21.4 N/cm^2 gage). This pressure provided sufficient vehicle structural strength to withstand bending loads for the remainder of the ascent.

TABLE V-VIII. - ATLAS PNEUMATIC SYSTEM DATA, AC-7

(a) U. S. Customary Units

Parameter	Time from lift-off, sec				
	T - 10	Requirement at T - 0	T - 0	Booster engine cutoff T + 142.6	Sustainer engine cutoff and vernier engine cutoff T + 235.1
Oxygen tank ullage pressure, psig	-----	23.3 to 28.5	26.0	31.0	32.6
Fuel tank ullage pressure, psig	61.1	57.8 to 61.5	60.4	60.4	49.7
Intermediate bulkhead differential pressure, psi	18.5	-----------	14.0	17.5	18.0
Booster controls pneumatic regulator outlet pressure, psig	733	715 to 785	733	732	----
Sustainer controls pneumatic regulator outlet pressure, psig	----- -----	565 to 635	627	617	617
Controls bottle pressure, psig	-----	2900 to 3400	3260	2955	2830
Booster bottle pressure, psig	3325	3100 to 3400	3290	1008	----
Booster bottle temperature, ^{o}F	-312	-304 (maximum)	-312	-365	----
Staging bottle pressure, psig	3341	2900 to 3400	3341	----	----

(b) SI Units

Oxygen tank ullage pressure, N/cm^2 gage	-----	16.1 to 19.7	17.9	21.4	22.5
Fuel tank ullage pressure, N/cm^2 gage	42.1	39.9 to 42.4	41.6	41.6	34.1
Intermediate bulkhead differential pressure, N/cm^2	12.8	-----------	9.7	12.1	12.4
Booster controls pneumatic regulator outlet pressure, N/cm^2 gage	505	493 to 541	505	505	----
Sustainer controls pneumatic regulator outlet pressure, N/cm^2 gage	-----	390 to 438	432	425	425
Controls bottle pressure, N/cm^2 gage	-----	2000 to 2344	2248	2037	1951
Booster bottle pressure, N/cm^2 gage	2293	2137 to 2344	2268	695	----
Booster bottle temperature, ^{o}K	82	87 (maximum)	82	53	----
Staging bottle pressure, N/cm^2 gage	2304	2000 to 2344	2304	----	----

Liquid oxygen tank pressure increased above the regulator control band at T + 83 seconds as the result of normal gas boiloff. At T + 107 seconds and a pressure of 33.3 psig (22.9 N/cm^2 gage), the system relief valve opened and slowly bled tank pressure down to 31.0 psig (21.4 N/cm^2 gage) at booster engine cutoff. Immediately after booster engine cutoff, the ullage pressure rose abruptly because of a reduction in liquid oxygen consumption rate and also an increased boiloff rate. The increase in boiloff rate resulted from a decrease in hydrostatic head due to a reduction in vehicle acceleration.

Engine control regulators. - The booster and sustainer pneumatic regulators provided the required helium pressures for engine control throughout the flight. Performance values are shown in table V-VIII.

Centaur

System description. - The Centaur pneumatic system, shown schematically in figure V-24, was used to supply helium gas at regulated pressures or flow rates for propellant tank pressurization, actuation of engine control valves, pressurization of hydrogen peroxide storage bottle, and purge systems.

Propellant tank pressure control was necessary to prevent rupture of the tank, to maintain sufficient pressure at the boost pump inlets, and to meet the requirements of the pressure-stabilized tank structure. Tank pressures were regulated by a dual vent valve configuration on the hydrogen tank and by a single vent valve on the oxygen tank. The oxygen valve and the primary hydrogen valve were each equipped with a solenoid which, on programmer command, could position the valve into either a locked closed (nonregulating) or open (normal regulating) mode. The secondary hydrogen vent valve was able to regulate at all times but at a higher control range. The control range for this secondary valve was selected to guard against overpressure in the tank when the primary vent valve was in the locked closed nonregulating mode. The primary vent valve was programmed to lock closed at given times in order to (1) allow tank pressure buildup during the atmospheric ascent, (2) limit hydrogen venting to nonhazardous times, times, (3) allow pressure pulsing of the tanks, and (4) avoid vehicle disturbance torques as a result of venting after Centaur main engine cutoff. The pressure pulsing of the propellant tanks was affected by a controlled injection of helium gas into the ullage.

Pneumatic pressure supplied through the engine controls regulator was used to actuate the propellant inlet valves, the engine cooldown valves, and the main fuel shutoff valve. The engine controls regulator also supplied helium to a second regulator for pressurization of the bladder-type hydrogen peroxide storage bottle.

The purge system was separate from the pressurization system. This system supplied helium gas from a ground source (until T - 9.9 sec) for purging the cavity between the hydrogen tank and the insulation panels, the seal and cavity between the nose fairing and forward bulkhead insulation, the propellant feed lines and boost pumps, engine chilldown vent ducts, and thrust chambers and hydraulic power packages. Purging the cavities under the insulation panels was vital to prevent cryopumping nitrogen or air which could freeze the jettisonable panels to the tank. This portion of the purge system is shown in figure V-25. At T - 9.9 seconds, the purge was transferred to an airborne bottle supply which blew down and extended the purge through most of the atmospheric ascent.

Propellant tank pressurization. - The pressure profiles for the hydrogen and oxygen tanks during the flight are shown in figure V-26. Pressure regulation was well within specification, and overboard discharge of the propellant boiloff gases during the boost flight phase was accomplished without incident.

Tank pressures just prior to lift-off were 30.6 psia (21.1 N/cm^2 abs) in the oxygen tank and 21.4 psia (14.8 N/cm^2 abs) in the hydrogen tank. At T - 6.8 seconds, the primary hydrogen vent valve was put into a closed, or nonregulating, mode and the tank pressure began increasing at an average rate of 5.1 psi per minute (3.5 $(N/cm^2)/min$). Closing the vent valve just prior to lift-off was necessary to provide increased tank pressure for minimum required structural strength during the atmospheric ascent and to avoid possible fire hazards of hydrogen venting. A hydrogen plume from the vent early in flight, while the vehicle velocity was low, could have washed back over the vehicle and possibly been exposed to an ignition source (see ref. 2).

The first scheduled blowdown of the hydrogen tank occurred at T + 68.7 seconds, when the primary vent valve was programmed back to the open or normal regulating mode. Prior to the blowdown, however, at T + 47.5 seconds, the tank pressure reached the control range of the secondary vent valve and was regulated by that valve between 26.1 and 25.3 psia (18.0 and 17.4 N/cm^2 abs) until the scheduled tank blowdown. This regulating range was within the required specification of 24.8 to 26.8 psia (17.1 to 18.5 N/cm^2 abs). After the blowdown, the tank pressure gradually decayed until the next time the vent valve was programmed. During this period of decay, the pressure remained within the allowable primary vent valve operating range of 19.0 to 21.5 psia (13.1 to 14.8 N/cm^2 abs).

The primary hydrogen vent valve was again closed at T + 142.2 seconds to prevent vented hydrogen gas from mixing with the residual gaseous oxygen which envelopes a large portion of the vehicle during booster engine staging. During this nonventing period which lasted until T + 149.0 seconds, the hydrogen tank ullage pressure increased from 20.0 to 21.6 psia (13.8 to 14.9 N/cm^2 abs).

Oxygen tank pressures were controlled throughout the boost flight phase with the vent valve in the open or normal regulating mode. The liquid oxygen was in a near-thermal equilibrium state, and venting was regular. During Atlas booster engine shutdown, the sudden reduction in vehicle acceleration produced a decrease in hydrostatic head which in turn caused a resultant increase in liquid oxygen boiloff. This increased boiloff caused the ullage pressure to rise from 30.4 to 32.8 psia (21.0 to 22.6 N/cm^2 abs).

During the ascent, the Centaur propellants are at near-saturation conditions. Consequently, the reduction in hydrostatic pressure at sustainer engine cutoff could cause the propellants to boil in the bottom of the tank. However, to prevent this propellant boiling and to avoid boost pump cavitation (boost pumps were started prior to sustainer engine cutoff), helium gas was injected into the tanks to keep the ullage pressure above saturation. This pressure pulsing of the tanks, also called "burping," was controlled by metering helium flow through a 0.089-inch- (3.5-mm-) diameter orifice in the line to the hydrogen tank, and a 0.043-inch- (1.69-mm-) diameter orifice in the line to the oxygen tank.

The primary hydrogen vent valve was closed again at sustainer engine cutoff, T + 235.1 seconds, and the tank pressure was pulsed for 1 second. This pressure pulse increased the ullage pressure from 19.7 to 20.4 psia (13.6 to 14.1 N/cm^2 abs).

Oxygen tank pressure pulsing, however, was more involved because of a very small ullage volume, a maximum pressure limit, and a much higher pressure pulse requirement. The pressure pulse required to offset the reduction in hydrostatic pressure in the oxygen tank at sustainer engine cutoff was more than in the hydrogen tank because of the greater density of the liquid oxygen. Consequently, a higher ullage pressure was necessary to hold the pressure above saturation during staging. To guard against overpressure when pulsing the small ullage, the pressure pulse was limited by a pressure sensitive switch which operated between the limits of 38 and 40 psia (26.2 and 27.6 N/cm^2 abs). The oxygen tank vent valve was closed and pressure pulsing of the tank was started coincident with boost pump start at T + 204.2 seconds. The ullage pressure increased abruptly from 30.4 to 39.7 psia (21.0 to 27.4 N/cm^2 abs) and was controlled well within the specified range of the switch. After the pressure pulsing, the tank pressure increased to 40.0 psia (27.6 N/cm^2 abs) as a result of the heat generated by the boost pump operation. At sustainer engine cutoff, the drop in acceleration caused a corresponding drop in hydrostatic head resulting in increased boiloff. The increased boiloff caused the pressure to increase further to 40.7 psia (28.1 N/cm^2 abs).

Ullage pressures in both propellant tanks decayed normally during main engine firing. At main engine cutoff, the ullage pressure in the hydrogen tank was down to 14.2 psia (9.8 N/cm^2 abs) and 24.8 psia (17.1 N/cm^2 abs) in the oxygen tank. After engine cutoff, ullage pressures increased gradually at an average rate of 0.71 and 0.197 psi (0.489 and 0.136 N/cm^2 abs) in the hydrogen and oxygen tanks, respectively.

At T + 992.6 seconds, the Centaur had completed its turnaround and the retrothrust maneuver was initiated. In this maneuver the residual propellants in the tanks were ejected through the engines, creating a thrust in a direction opposite to the flight velocity vector. During the first portion of the retromaneuver, the ullage pressure curves are relatively flat indicating liquid or two-phase flow out of the tank. The pressure drop, due to the volumetric outflow rate of the liquid, merely offset the pressure rise due to boiloff. Then as the liquid cleared the lines, the greater volumetric flow of the gas caused a distinct decrease in ullage pressure. At T + 1040 seconds, the hydrogen ullage pressure began a steady decline indicating a transition to single-phase gas flow. The transition point in the oxygen tank was reached at T + 1090 seconds. At T + 1242.6 seconds, the engine valves were closed and the retromaneuver was terminated. The oxygen and primary hydrogen vent valves were commanded from the closed to the open or normal regulating mode. A summary of the pneumatic tank pressurization data is given in table V-IX.

Engine and hydrogen peroxide control regulators. - The engine controls and hydrogen peroxide bottle pressure regulators maintained required system pressure throughout the flight. The engine controls regulator provided helium to the engine valves at a pressure of 451 to 457 psia (311 to 315 N/cm^2 abs). The hydrogen peroxide bottle regulator maintained a bottle pressure of 312 to 315 psia (215 to 217 N/cm^2 abs) after the Centaur main engine started. These pressures were well within the required control range. A summary of the regulator pressure data for various flight times is given in table V-IX.

Pneumatic purges. - The pneumatic purge system was controlled by ground support equipment to provide the necessary component conditioning prior to launch. The required helium environment during prelaunch was maintained by using a purge rate of 110 pounds per hour (49.9 kg/hr). This purge rate provided an insulation panel differential pressure of 0.25 psi (0.17 N/cm^2) which was well above the minimum allowable of 0.03 psi (0.02 N/cm^2) required for launch. The pneumatic purge was switched from the ground to airborne system at T - 9.9 seconds by enabling blowdown of the airborne helium purge bottle. The purge then continued until the helium supply was depleted, by which time the vehicle had cleared the atmosphere.

TABLE V-IX. - CENTAUR PNEUMATIC SYSTEM DATA, AC-7

(a) U.S. Customary Units

Parameter	Time from lift-off, sec				
	Requirement at T - 0	T - 10	Booster engine cutoff T + 142.6	Centaur main engine start T + 242.6	Centaur main engine cutoff T + 686.2
Engine control regulator output pressure, psia	455 to 490	467	463	457	451
Hydrogen peroxide supply bottle pressure regulator output, psia	312 to 330	326	----	----	----
Hydrogen peroxide supply bottle pneumatic pressure, psia	360 (maximum)	326	324	315	312
Helium supply bottle pressure, psia	2600 to 2950	2800	2790	2530	2480
Helium supply (pneumatic pressurization bottle), lb	-----------	4.86	4.86	4.57	4.56
Insulation panel purge differential pressure, psi	0.03 (minimum)	0.25	----	----	----
Hydrogen ullage pressure, psia	19.7 to 22.0	21.4	20.0	20.0	14.2
Oxygen ullage pressure, psia	29.2 to 32.3	30.6	30.4	38.1	24.8

(b) SI Units

Engine control regulator output pressure, N/cm^2 abs	314 to 338	322	319	315	311
Hydrogen peroxide supply bottle pressure regulator output, N/cm^2 abs	215 to 228	225	----	----	----
Hydrogen peroxide supply bottle pneumatic pressure, N/cm^2 abs	248 (maximum)	225	223	217	215
Helium supply bottle pressure, N/cm^2 abs	1793 to 2034	1931	1924	1744	1710
Helium supply (pneumatic pressurization bottle, kg	-----------	2.21	2.21	2.08	2.07
Insulation panel purge differential pressure, N/cm^2	0.02 (minimum)	0.17	----	----	----
Hydrogen ullage pressure, N/cm^2 abs	13.6 to 15.2	14.8	13.8	13.8	9.8
Oxygen ullage pressure, N/cm^2 abs	20.1 to 22.3	21.1	21.0	26.3	17.1

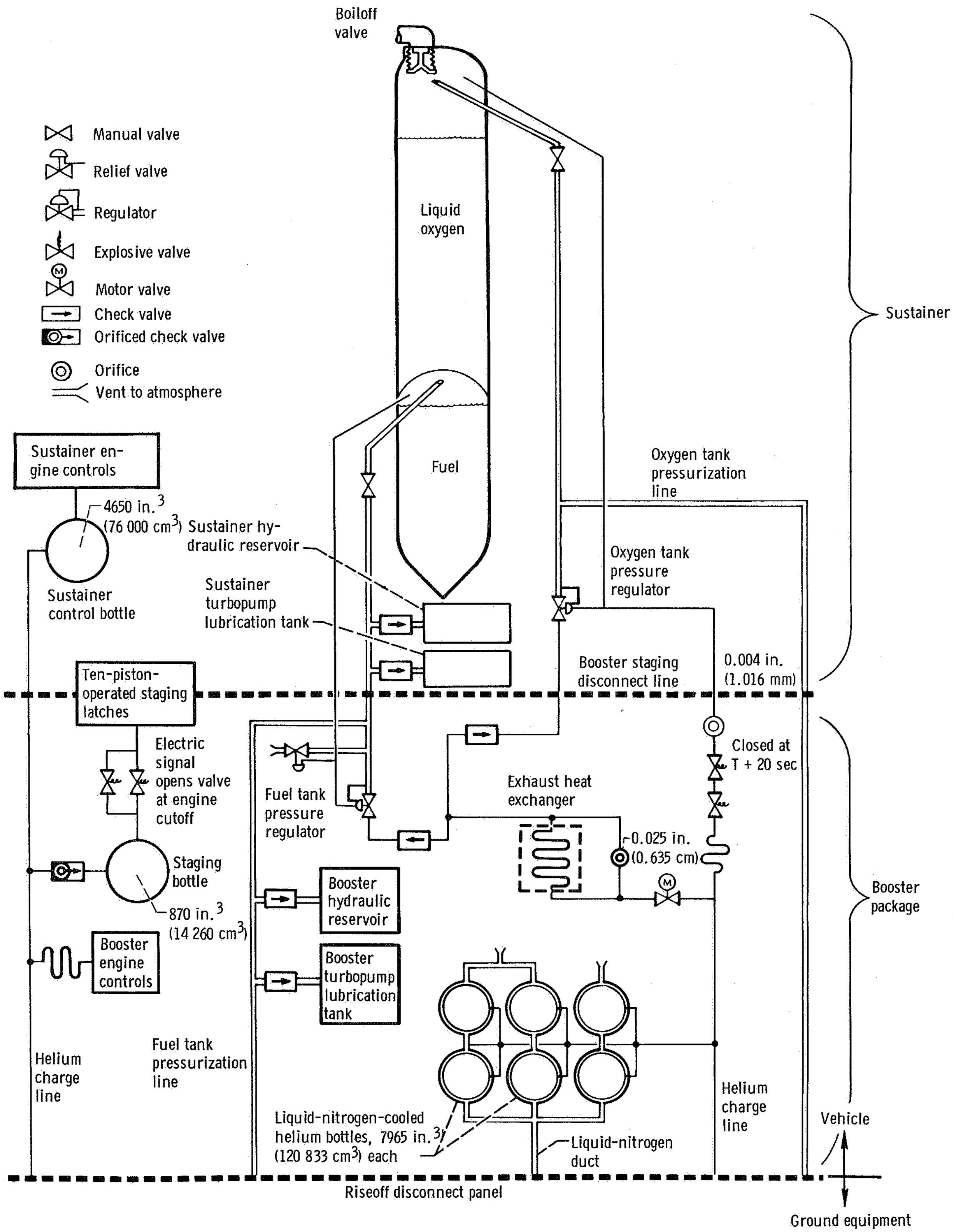

Figure V-22. - Atlas vehicle pneumatic system, AC-7.

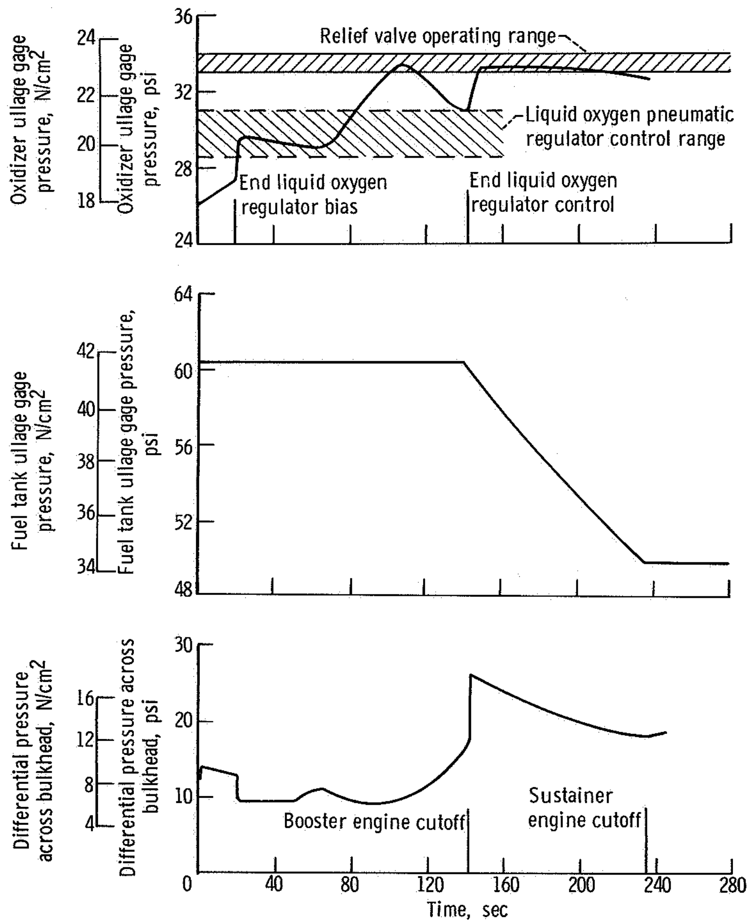

Figure V-23. - Atlas oxygen and fuel tank ullage pressures, AC-7.

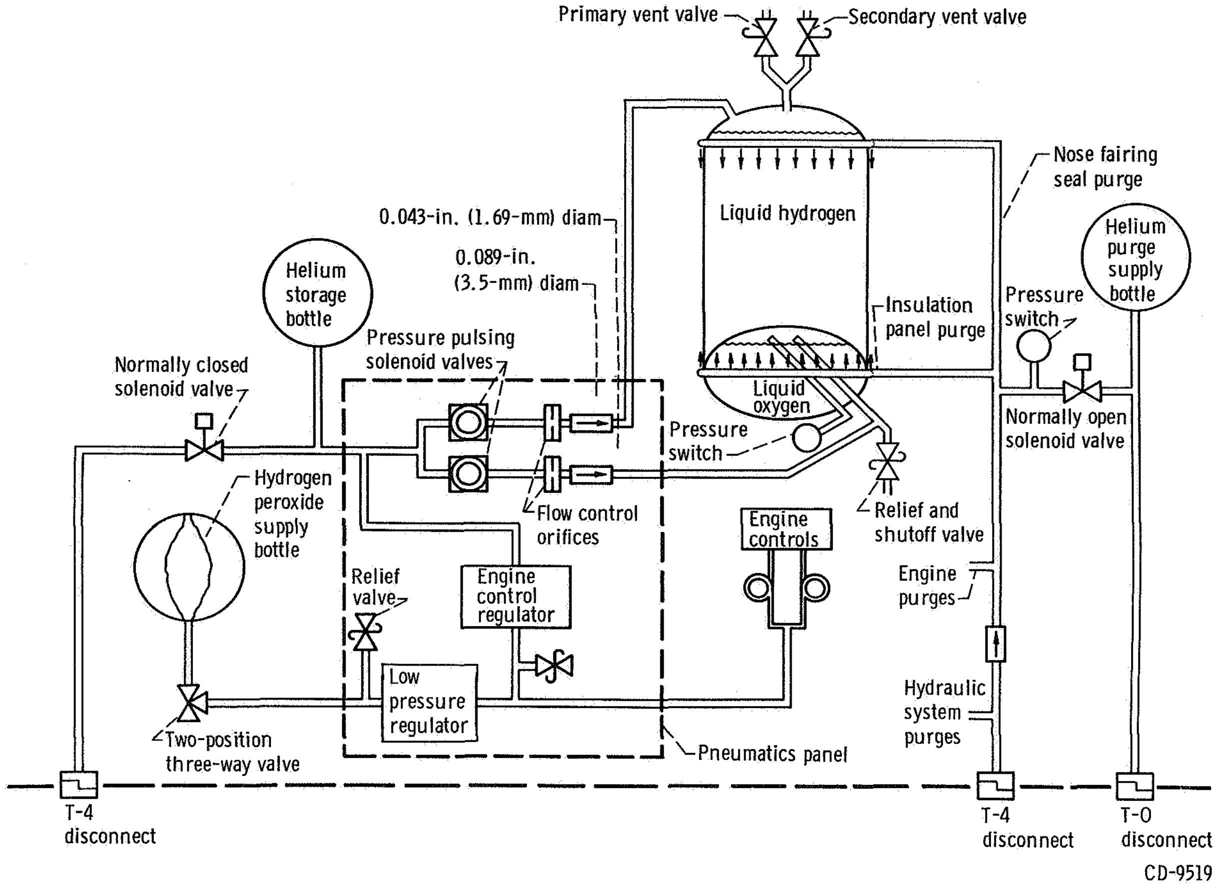

Figure V-24. - Centaur pneumatic system, AC-7.

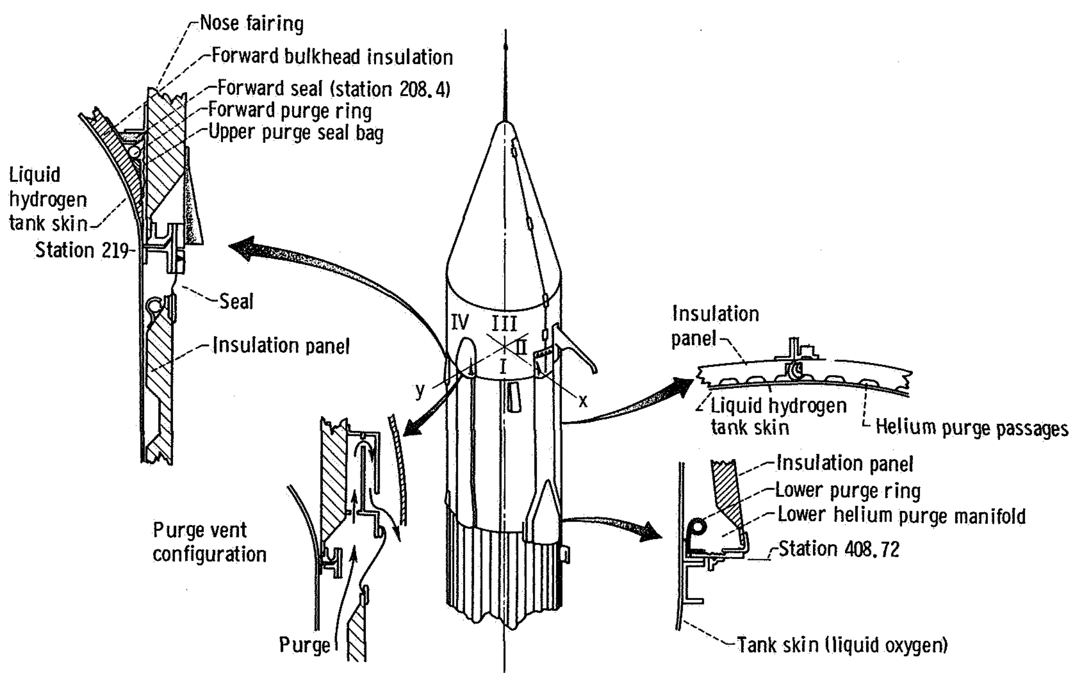

Figure 25. - Nose fairing and insulation panel helium purge systems, AC-7.

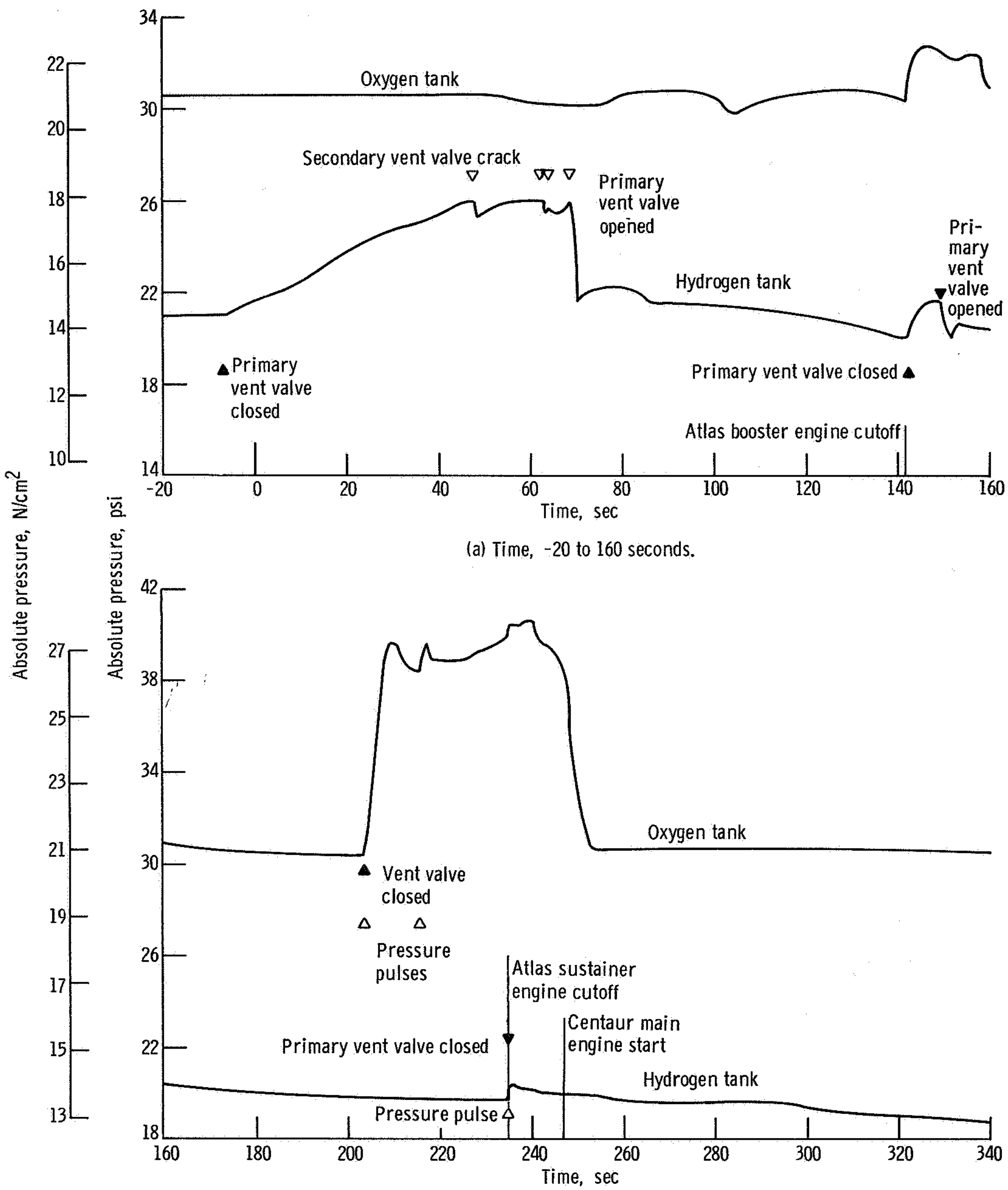

(a) Time, -20 to 160 seconds.

(b) Time, 160 to 340 seconds.

Figure V-26. - Centaur fuel and oxidizer tank ullage pressures, AC-7.

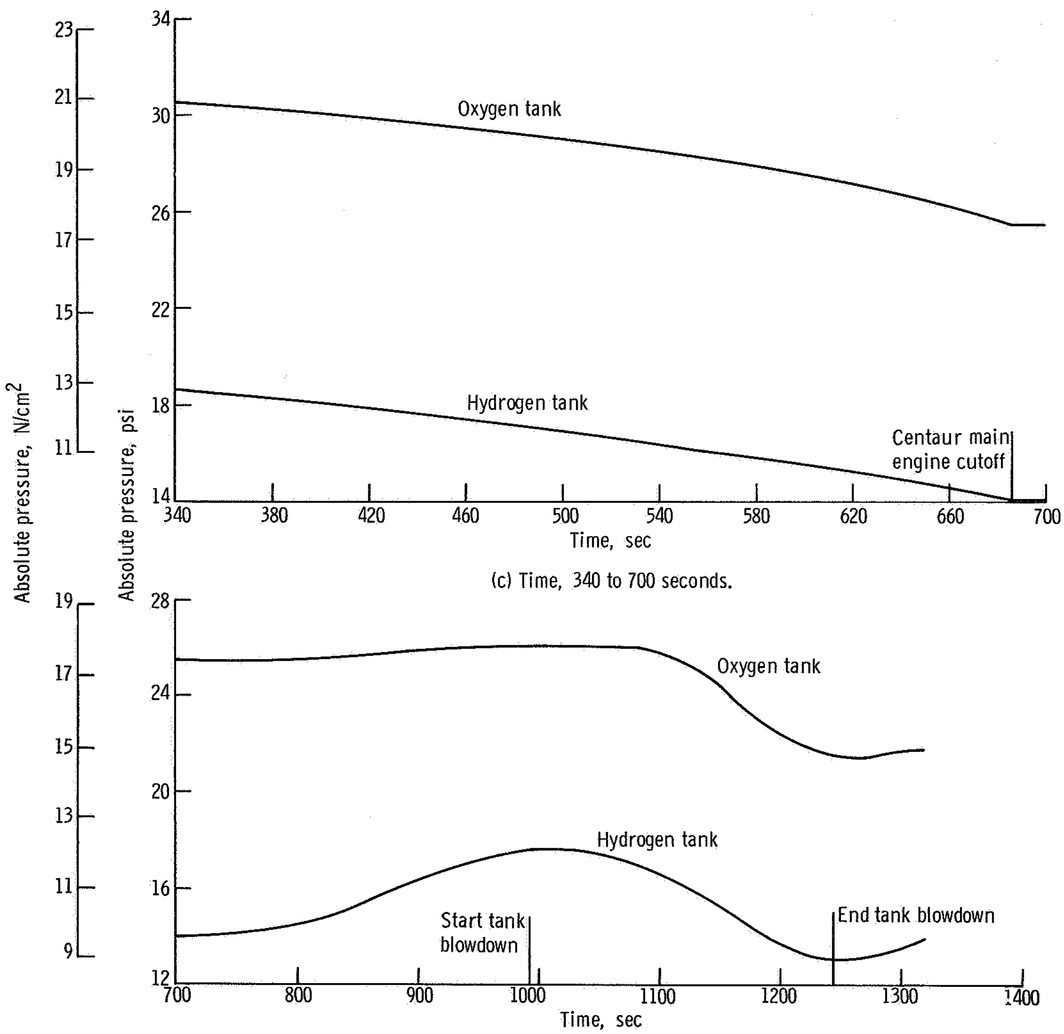

(c) Time, 340 to 700 seconds.

(d) Time, 700 to 1400 seconds.

Figure V-26. - Concluded.

HYDRAULIC SYSTEMS

by Eugene J. Cieslewicz

Atlas

System description. - Two hydraulic systems, shown in figure V-27, were used on the Atlas vehicle to supply fluid power for operation of sustainer engine control valves and for thrust vector control of all engines. One system was used for the booster engine and the other for the sustainer engine and the vernier engines.

The booster hydraulic system provided power solely for gimbaling the two thrust chambers. System pressure was supplied by a single, pressure-compensated, variable-displacement pump driven by the engine turbopump accessory drive. Additional components of the system included a high-pressure relief valve, two accumulators, and a reservoir. Engine gimbaling in response to flight control commands was accomplished by servocylinders providing separate pitch and yaw control for each thrust chamber. The maximum booster engine gimbal angle capability was 5° in both the pitch and yaw planes.

The sustainer stage used a system similar to that of the booster but in addition provided hydraulic power for sustainer engine control valves and gimbaling of the two vernier engines.

Sustainer gimbal control was electrically nulled until booster engine cutoff. At this time, disturbances created by booster differential cutoff were damped by gimbaling the sustainer and vernier engines. The sustainer engine was electrically nulled a second time for 0.7 second during booster stage jettison. Vernier engine roll control was maintained throughout the flight by differential gimbaling. Actuator limit travel of the vernier engine was $\pm 70^{\circ}$.

System performance. - Hydraulic system pressure data for both the booster and sustainer circuits are shown in figure V-28. Pressures were stable throughout the boost flight phase. The transition of fluid power from ground to airborne hydraulic systems was normal. Pump discharge pressures increased from 1950 psia (1345 N/cm^2 abs) at T - 2 seconds to flight levels of 3100 psia (2130 N/cm^2 abs) in less than 2 seconds. Starting transients produced a normal overshoot of about 5 percent with the pump discharge pressures stabilizing at 3075 psia (2120 N/cm^2 abs) in the sustainer hydraulic circuit and 3100 psia (2138 N/cm^2 abs) in the booster hydraulic circuit.

Engine gimbaling requirements during flight were generally less than 1° in the pitch and yaw planes. An exception of 1.7° occurred during the period of maximum dynamic pressure in the pitch plane. The excursions were less than expected and were well within the engine gimbal limits.

Centaur

System description. - Two separate but identical hydraulic systems, as shown in figure V-29, were used on the Centaur stage. One system for each engine was used to gimbal the thrust chambers for pitch, yaw, and roll control. Each system was composed of two servocylinders, high and low pressure pumps, reservoirs, and an engine coupled power package which contained an accumulator, pressure intensifying bootstrap piston, and relief valves for pressure regulation. Hydraulic pressure and flow were provided by a constant-displacement vane-type pump driven by the liquid oxygen turbopump drive shaft. An electrically powered secondary recirculation pump was also used to provide low pressure for engine gimbaling requirements during prelaunch checkout, to aline the engines prior to main engine start, and for limited thrust vector control during the propellant tank blowdown portion of the Centaur retrothrust maneuver. Maximum engine gimbal capability was $\pm 3^{\circ}$.

System performance. - Performance of both hydraulic systems on the Centaur stage was satisfactory until 160 seconds after main engine ignition. The system pressure data is shown in figures V-30 and V-31. At this time, the pressure of the C-2 package started to drop slowly from 1090 psia (752 N/cm^2 abs) to a low of 1045 psia (721 N/cm^2 abs) at 230 seconds after main engine ignition. This small drop in pressure, however, did not affect the system performance. The C-1 package maintained a steady output of 1095 psia (755 N/cm^2 abs) throughout the flight. By 350 seconds after main engine ignition, the C-2 system pressure had recovered to 1120 psia (772 N/cm^2 abs). The only reasonable explanation for the loss and recovery of system pressure is the possibility of an internal leak around the pressure intensifying bootstrap piston. A weakness in this area was found subsequent to this flight and has been corrected by utilizing a more effective seal. All future power packages will contain the new seal configuration.

The drift in C-2 system pressure was not sufficient to jeopardize servocylinder performance since the available differential pressure exceeded the minimum 950 psia (655 N/cm^2 abs). At lift-off plus 235.6 seconds, the electrically driven hydraulic pumps were activated to provide low pressure hydraulic power for alining the Centaur engines prior to Atlas Centaur separation. Pressures, as shown in figures V-30 and V-31, rose to 115 and 130 psia (79.3 to 79.6 N/cm^2 abs), respectively, in the C-1 and C-2 packages.

Thermal conditioning of the system prior to launch was maintained by ambient helium purges and by operation of the low pressure recirculation pumps. The hydraulic manifold temperatures at main engine ignition, as shown in figures V-30 and V-31, were approximately 56° F (286° K). These temperatures were well above the minimum required limit of 20° F (266° K). When the main pumps were started, the manifold temperatures increased normally to 162° F (345° K) and 166° F (347° K) for C-1 and C-2, respectively, at main engine cutoff.

After main engine cutoff, the hydraulic system was inactive until the start of propellant tank blowdown at T + 992.6 seconds. The electrically driven recirculation pumps were then turned on to provide low pressure hydraulic power for alining the engines and providing limited thrust vector control during the retrothrust blowdown maneuver. This limited control supplemented the primary hydrogen peroxide attitude control system and helped to reduce the duty cycle on these engines.

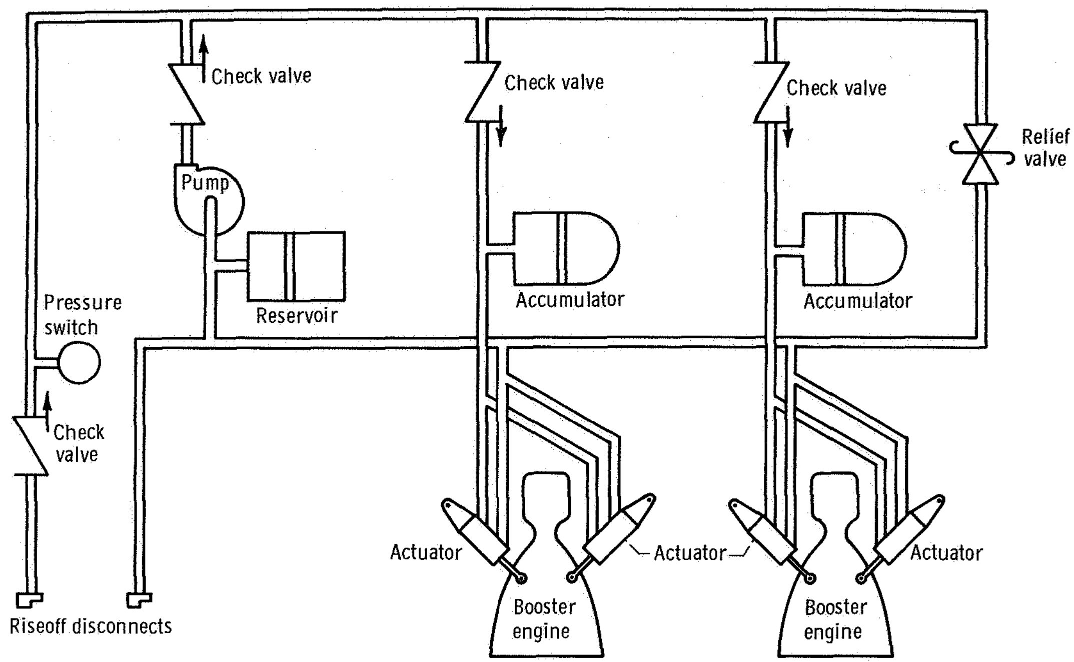

(a) Booster.

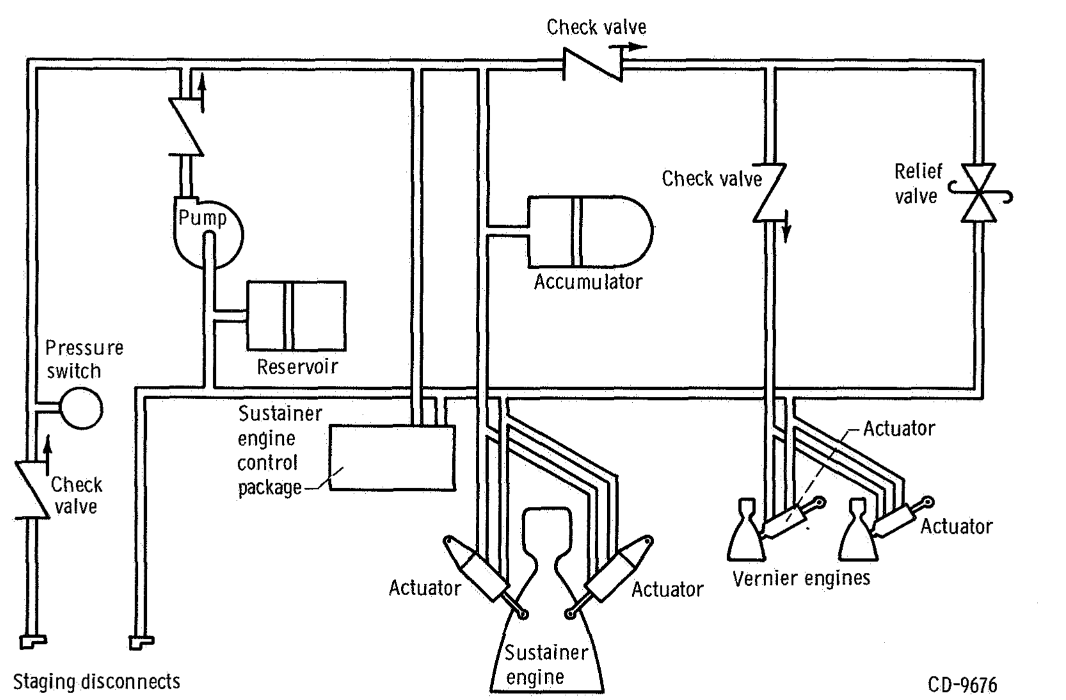

(b) Sustainer.

Figure V-27. - Atlas hydraulic system, AC-7.

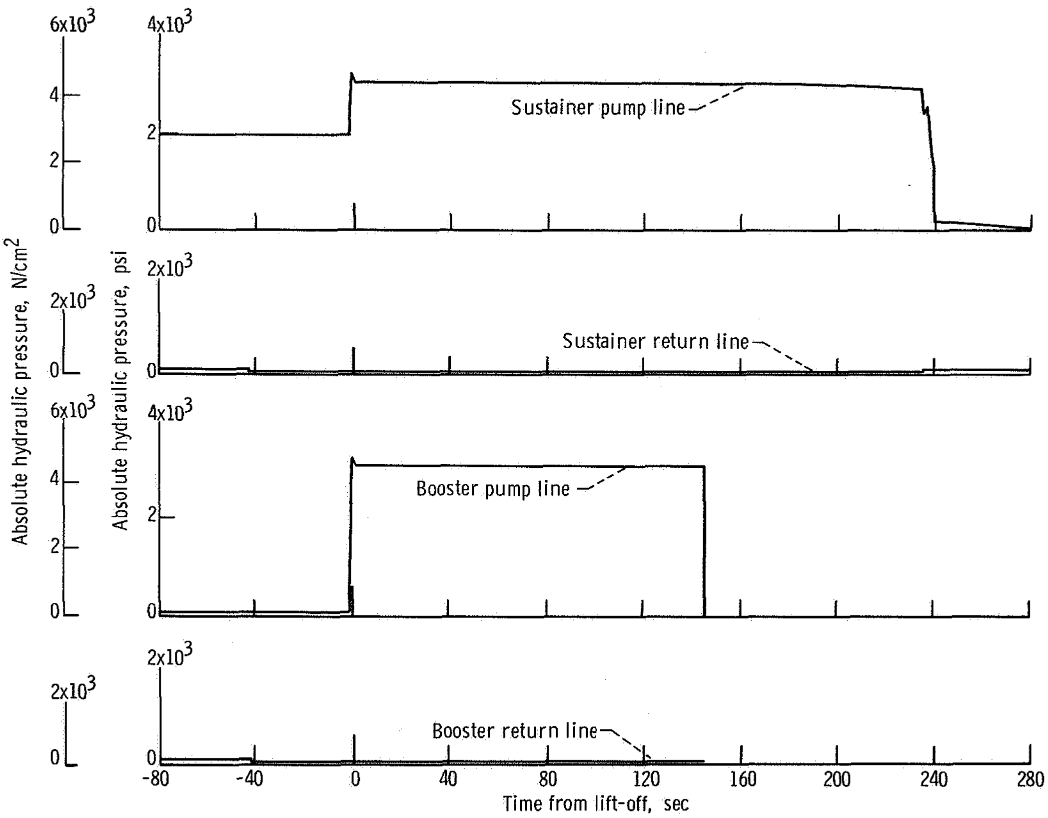

Figure V-28. - Atlas hydraulic system pressures, AC-7.

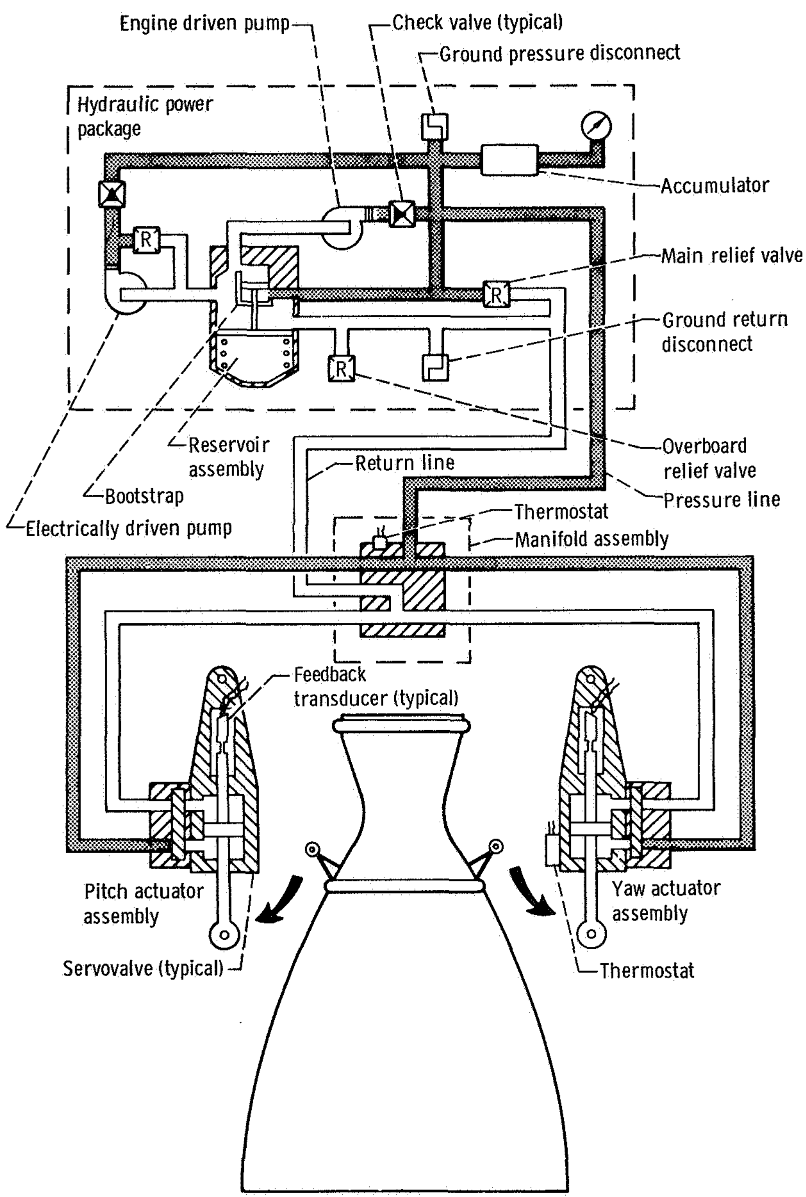

Figure V-29. - Centaur hydraulic system, AC-7.

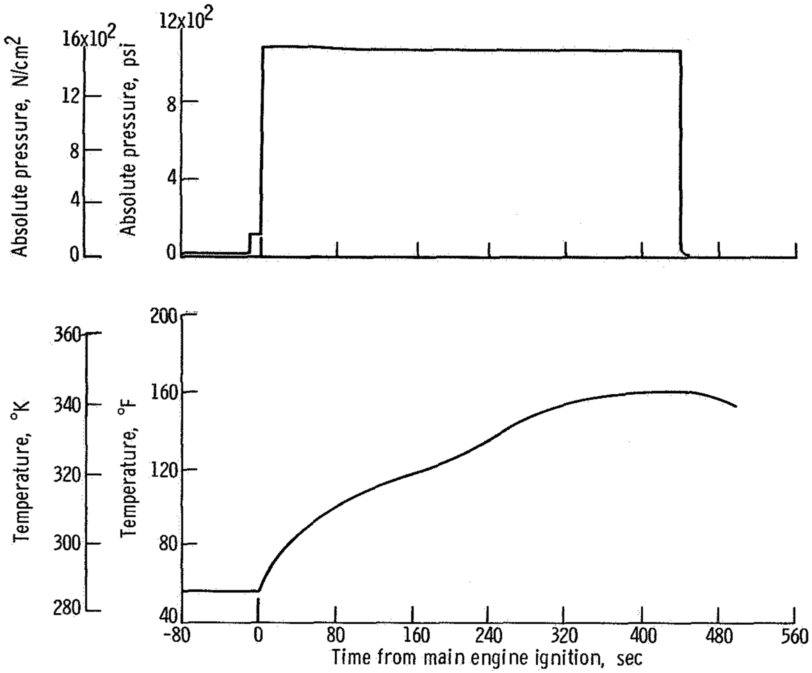

Figure V-30. - C-1 hydraulic system pressure and temperature, AC-7.

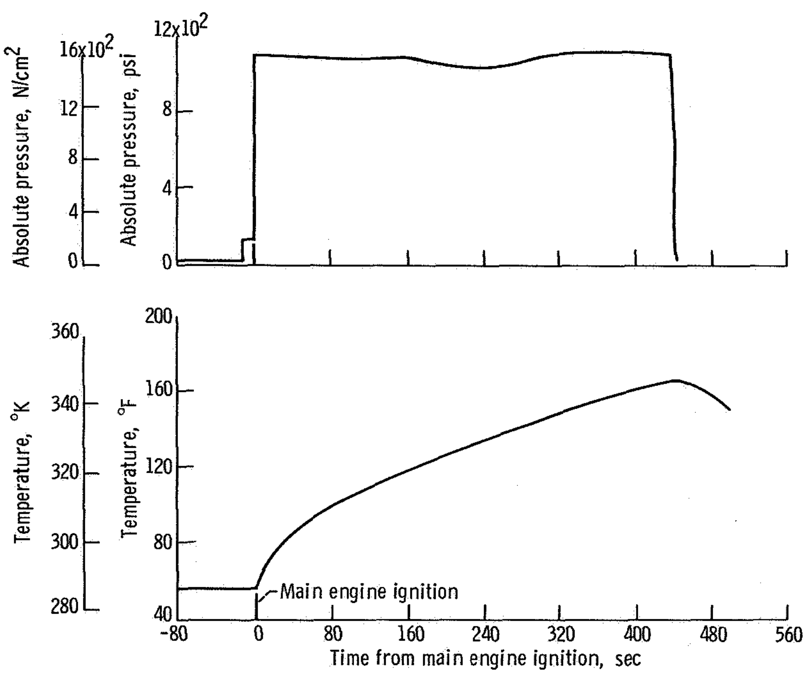

Figure V-31. - C-2 hydraulic system pressure and temperature, AC-7.

VEHICLE STRUCTURES

by Robert C. Edwards, Theodore F. Gerus, and Dana H. Benjamin

System Description

Vehicle structures include the basic Atlas and Centaur tanks and all bolt-on and jettisonable hardware attached. The Atlas and Centaur propellant tanks provided the primary vehicle structure. Both stages used pressure stabilized tank sections of monocoque construction. These propellant tanks had a minimum pressure requirement for various periods of flight to maintain structural stability. The structural capability of the tank as a pressure vessel limited the maximum allowable pressure in the propellant tanks.

Vehicle Structural Loads

Centaur tank pressure criteria. - The maximum allowable and minimum required tank pressures are predicted on the maximum design flight loads being imposed on the vehicle with appropriate factors of safety included. The pertinent maximum allowable and minimum required tank pressures along with AC-7 tank pressure profiles at various locations are given in figure V-32. Figure V-33 indicates the area of the tank structure which determines the maximum allowable and minimum required tank pressures.

The liquid oxygen tank pressure was of greatest concern at booster engine cutoff at which time it approached most closely the maximum design allowable. The maximum allowable liquid oxygen tank pressure was 33.0 psia (22.7 N/cm^2 abs) at booster engine cutoff, whereas the actual AC-7 liquid oxygen tank pressure, as shown in figure V-32, was 30.4 psia (20.9 N/cm^2 abs). The minimum required liquid oxygen tank pressure was not a critical factor during any period of flight.

The liquid hydrogen tank pressure reached a value closest to the allowable design maximum just prior to the primary hydrogen vent valve being opened at T + 68.7 seconds. The maximum allowable pressure was 25.0 psia (17.2 N/cm^2 abs) plus the nose fairing internal pressure. At T + 68.7 seconds, the nose fairing internal pressure was 3.0 psia (2.1 N/cm^2 abs); thus, the maximum allowable liquid hydrogen tank pressure was 28.0 psia (19.3 N/cm^2 abs). This pressure is determined by the hoop stress capability of the forward bulkhead conical section. The actual liquid hydrogen tank pressure at this time was 26.0 psia (17.9 N/cm^2 abs).

The minimum required liquid hydrogen tank pressure was of primary importance at the following times: prelaunch, launch, first hydrogen vent valve opening (at T + 68.7

sec), and nose fairing jettison:

(1) Prior to launch, the insulation panel pretensioning imposed local bending stresses on the liquid hydrogen cylindrical skin. The minimum required liquid hydrogen tank pressure at this time was 19.0 psia (13.1 N/cm^2 abs); the actual tank pressure was 20.9 psia (14.4 N/cm^2 abs).

(2) During the launch phase (T + 0 to T + 10 sec), the payload caused compression loads on the forward bulkhead due to inertia and lateral vibration. The minimum required liquid hydrogen tank pressure, was 20.5 psia (14.1 N/cm^2 abs) at T + 10 seconds; at this time the actual tank pressure was 22.4 psia (15.4 N/cm^2 abs).

(3) Just after the primary hydrogen vent valve was opened at T + 68.7 seconds, the inertia and bending compression loads were critical at station 409.6 on the cylindrical skin. The minimum required liquid hydrogen tank pressure was 20.3 psia (14.0 N/cm^2 abs). The actual tank pressure at this time was 21.6 psia (14.9 N/cm^2 abs).

(4) At nose fairing jettison, the nose fairing exerted inboard radial loads at station 219. The minimum required tank pressure at this time was 18.5 psia (12.8 N/cm^2 abs); the actual tank pressure was 19.8 psia (13.7 N/cm^2 abs).

The maximum and minimum differential pressures between the liquid oxygen and liquid hydrogen tanks were limited by the strength of the Centaur intermediate bulkhead. The liquid oxygen tank pressure must always be greater than the liquid hydrogen tank pressure for stability (to prevent bulkhead reversal), and maximum pressure differential was limited by the bulkhead material strength.

The desirable minimum differential pressure across the intermediate bulkhead was 2.0 psi (1.4 N/cm^2). Before the primary hydrogen vent valve was opened at T + 68.7 seconds, the actual differential pressure across the intermediate bulkhead was 4.1 psi (2.8 N/cm^2). The maximum allowable differential pressure across the intermediate bulkhead was 23.0 psi (15.9 N/cm^2). During step pressurization of the liquid oxygen tank, the actual differential pressure was 20.8 psi (14.3 N/cm^2) at T + 235 seconds.

Atlas tank pressure criteria. - The Atlas intermediate bulkhead differential pressure, shown in figure V-34, remained well above the minimum allowable of 2.0 psi (1.4 N/cm^2) throughout the critical lift-off period when the Atlas liquid oxygen mass was subjected to longitudinal oscillations. Thereafter the bulkhead differential pressure varied between a minimum of 9.0 psi (6.2 N/cm^2) at T + 90 seconds and a maximum of 26.5 psi (18.2 N/cm^2) at booster engine cutoff.

Design flight loads produced the greatest bending stresses in the Atlas liquid oxygen tank between T + 60 and T + 80 seconds. Controlled tank pressures during that time, as shown in figure V-35, were above the minimums required for resisting the maximum design flight loads. The minimum differential between required and actual pressures occurred at T + 80 seconds, when the liquid oxygen tank pressure was 33.5 psia (23.1 N/cm^2 abs) and the minimum allowable was 31.8 psia (21.9 N/cm^2 abs). The maximum allowable liquid oxygen pressure was most closely approached at T + 100 seconds. At This time, the tank pressure was 33.4 psia (23.0 N/cm^2 abs). The allowable maximum pressure was 36.6 psia (25.2 N/cm^2 abs).

Quasi-steady-state load factors. - The longitudinal load factor buildup was as expected. A maximum value of 5.65 g's was reached at booster engine cutoff which was within $\pm 3\ \sigma$ range (5.62 to 5.78 g's).

Atlas launcher transients. - During release of the vehicle at lift-off, launcher mechanism forces transmitted through the kick struts caused longitudinal and lateral oscillations and thus, additional loads on the vehicle and its components. The booster fuel staging valve and fuel manifold support struts were also instrumented on AC-7. Launcher transients were measured because of relatively high longitudinal g forces on the vehicle and high lateral g forces, on the payload model, experienced on the AC-6 flight.

The maximum launcher kick strut load was 31 200 pounds (138 000 N), and the longitudinal oscillation measured on the Atlas at approximately the time of peak kick strut load was 0.56 peak to peak. A comparison of these parameters for this flight and previous flights is shown in table V-X. The accelerations in table V-X are all within allowable limits for the vehicle. Poppet clearance in the fuel staging valve was within allowable limits, as shown and compared with AC-8 and AC-10 in table V-XI with a minimum of 1.77 inches (4.5 cm) at the time of kick strut second peak load. Three of the four manifold strut load measurements were functional and indicated normal loads (table V-XI) referenced to pretanking conditions, for vehicle lift-off and release.

TABLE V-X. - LOADS ON LAUNCHER KICK STRUTS AT LIFT-OFF, AC-7

Flight	Maximum kick strut loads, lb (N)		Longitudinal acceleration, g's peak to peak	Accelerometer location vehicle station
	B-1	B-2		
AC-8	29 000 (128 900)	30 000 (133 400)	0.58	173
AC-10	28 000 (124 400)	25 600 (113 800)	.81	1043
AC-7	31 200 (138 800)	29 600 (131 600)	.56	1043

TABLE V-XI. - LOADS ON BOOSTER FUEL STAGING VALVE SUPPORT STRUTS AND VALVE POPPET CLEARANCE AT LAUNCH, AC-7

Flight	Maximum loads[a] on valve support struts, lb (N)				Valve poppet clearance, in (cm)	
	P-2	P-4	P-5	P-6	Pretanking measurement	Minimum during launch
AC-8	+2250 (+10 000)	-1400 (-6230)	----------	+650 (+2880)	1.67 (4.24)	1.64 (4.16)
AC-10	+2550 (+11 300)	------------	+150 (+667)	-150 (-667)	1.68 (4.27)	1.70 (4.32)
AC-7	-------------	-1300 (-5780)	-90 (-400)	-200 (-890)	1.77 (4.50)	1.77 (4.50)

[a]Tension loads denoted by +; compression loads denoted by -.

Vehicle Dynamic Loads

The Atlas-Centaur launch vehicle may receive dynamic loading from several sources. These loads fall into three major categories: (1) external loads, such as aerodynamic and acoustic loads; (2) loads due to transients, such as engines starting and stopping and separation transients; and (3) loads due to dynamic coupling between major systems.

Previous flights of the Atlas-Centaur had shown that these loads were within the structural limits. For this flight, an operational one, only a limited number of flight measurements of dynamic loads and local spacecraft vibrations were made. However, these few data indicate accurately the structural loading of the vehicle. The response indicated by the data taken at fixed locations and using the analytical model which has been set up permit computation of the dynamic loads which occur throughout the vehicle. The measurement instruments and the parameters measured are listed in the following table:

Measurement instrument	Parameter measured
Low frequency range accelerometer	Launch vehicle longitudinal vibration
Centaur pitch rate gyro	Launch vehicle pitch plane vibration
Centaur yaw rate gyro	Launch vehicle yaw plane vibration
High frequency range accelerometer	Local spacecraft vibrations
Angle of attack	Vehicle aerodynamic loads

Launch vehicle longitudinal vibrations, as measured on the Centaur forward bulkhead, are shown in figure V-36. The frequency and amplitude of the vibrations measured on this flight are compared with three other representative flights.

Launch vehicle longitudinal vibrations were excited during launcher release (see previous discussion, Atlas launcher transients, p. 76). The amplitude and frequency of these vibrations were near those observed during other flights. Calculations using the analytical model show that Atlas intermediate bulkhead pressure fluctuations were the most significant effects produced by the launcher induced longitudinal vibrations. The maximum fluctuation computed was 4.3 psia (2.96 N/cm^2 abs). Since the steady-state bulkhead differential pressure measured at this time was 14.5 psi (10 N/cm^2) (see fig. V-34), the minimum differential pressure was 10.2 psi (7 N/cm^2). The minimum differential pressure across the bulkhead allowed for this flight (which includes an allowance for errors) was 2.0 psi (1.3 N/cm^2).

During Atlas flight between T + 107 and T + 130 seconds, intermittent longitudinal vibrations of 0.1 g (zero to peak) at a frequency of 12 hertz were observed. These vibrations are believed to be caused by dynamic coupling (commonly referred to as POGO) of structure, engines, and propellant lines. The level and frequency of the vibrations are similar for the four vehicles shown in figure V-36, because the vehicle configuration has not changed from flight to flight. These vibrations at the amplitudes measured do not produce significant vehicle loads (see ref. 3).

During booster engine thrust decay, short duration transient longitudinal vibrations of 2.2 g's at a frequency of 90 hertz were observed. The analytical models did not indicate a significant structural loading due to this transient.

During the boost phase of flight, the vehicle vibrates in the pitch and yaw planes as an integral unit at all its natural frequencies. Previous analyses and tests have defined these natural frequencies or modes and the shapes which the vehicle assumes when the modes are excited. The rate gyros on the Centaur which sense the local rate of change of slope were used as instruments to sense the level of these modes. The maximum first mode excitation was seen in the pitch plane at T + 137 seconds (fig. V-37). The level was about 1.3 percent of the allowable deflection. The maximum second mode excitation was seen in the yaw plane at T + 27 seconds (fig. V-38). The yaw level was about 18 percent of the allowable deflection.

Angles of attack were calculated by using two differential pressures measured on the nose fairing and the total pressure obtained from a trajectory reconstruction. Computed angles of attack are shown in figures V-39 and V-40. Predicted values are shown for comparison. The difference between actual and predicted values of angles of attack are within the expected dispersion values for all significant times in flight. Expected angles of attack were calculated by using upper wind data obtained from a weather balloon released at T - 2 hours. The balloon was released to obtain upper wind information as close to flight time as possible for a postflight evaluation.

Vehicle bending moments were computed by using computed angle of attack, engine gimbal data, vehicle weights, and vehicle stiffnesses. The vehicle bending moments computed were added to axial load equivalent moments and moments resulting from random dispersions. The most significant dispersions considered were launch vehicle performance uncertainties, vehicle center-of-gravity offset, and wind gusts. The total equivalent predicted bending moment was divided by the bending moment allowable to obtain the structural capability ratio, as shown in figure V-41. The structural capability ratio shown in figure V-41 is greatest between T + 52 and T + 67 seconds due to high aerodynamic loads during this period. The maximum structural capability ratio of 0.78 was computed by using predicted axial loads and moments due to random dispersions. Since the angles of attack measured in flight were within the expected dispersion values, it can be assumed that the structural capability ratio did not exceed 0.78.

Five high frequency piezoelectric accelerometers were installed on the Surveyor spacecraft and payload adapter to determine the in-flight vibration environment. Two measurements provided satisfactory data throughout Atlas-Centaur flight; however, because these two measurements were time shared throughout flight, the transients that were of greatest interest were either not sampled or sampled by one of the accelerometers that had failed.

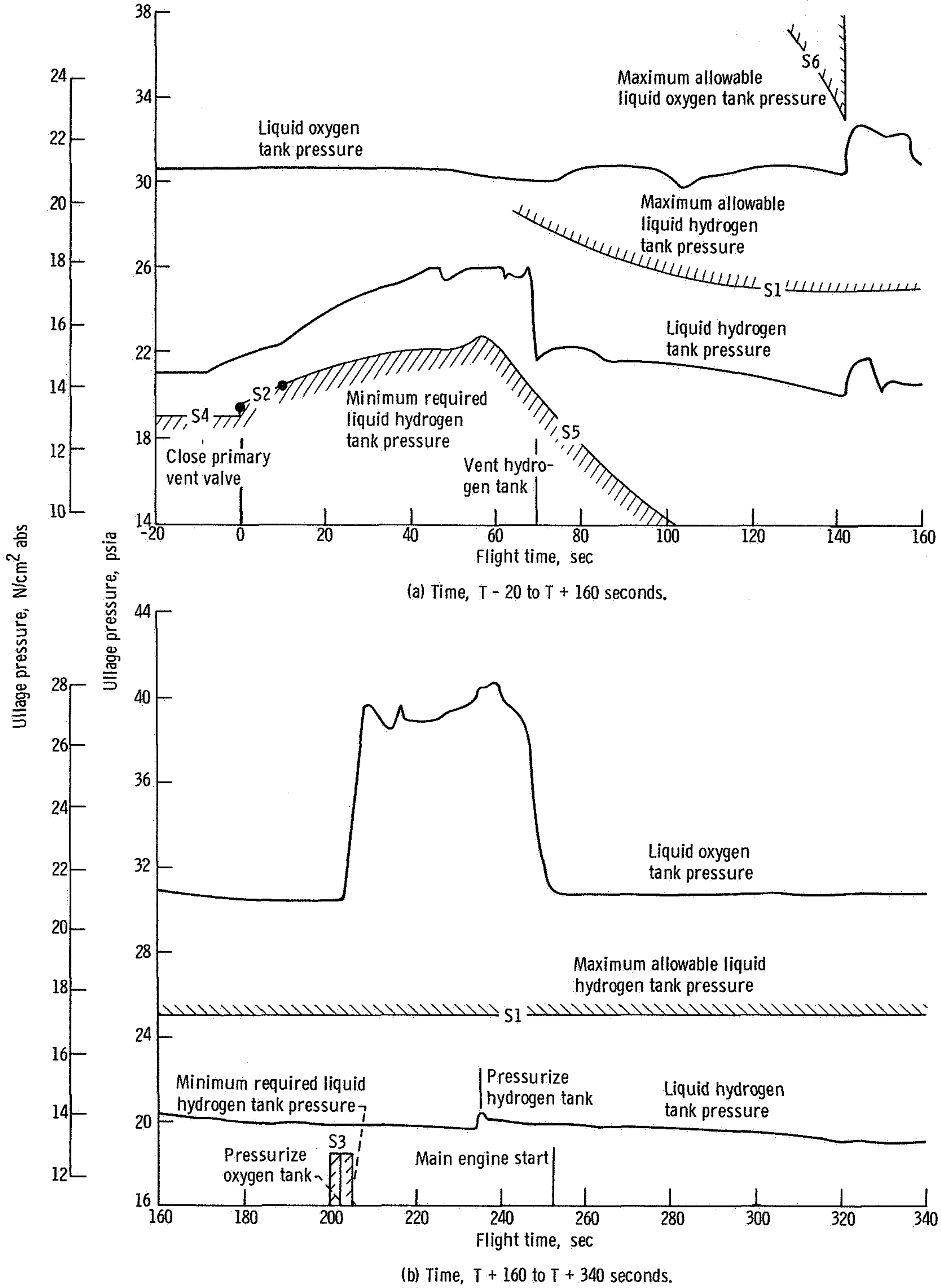

Figure V-32. - Centaur liquid hydrogen and liquid oxygen tank ullage pressure, AC-7. (S1, S2, etc. are defined in fig. V-33.)

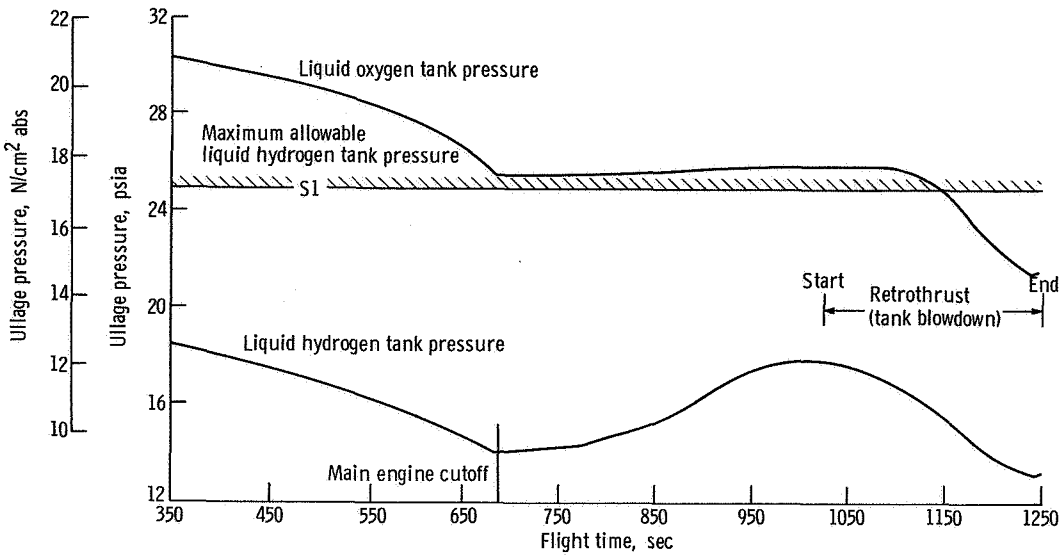

(c) Time, T + 350 to T + 1250 seconds.

Figure V-32. - Concluded.

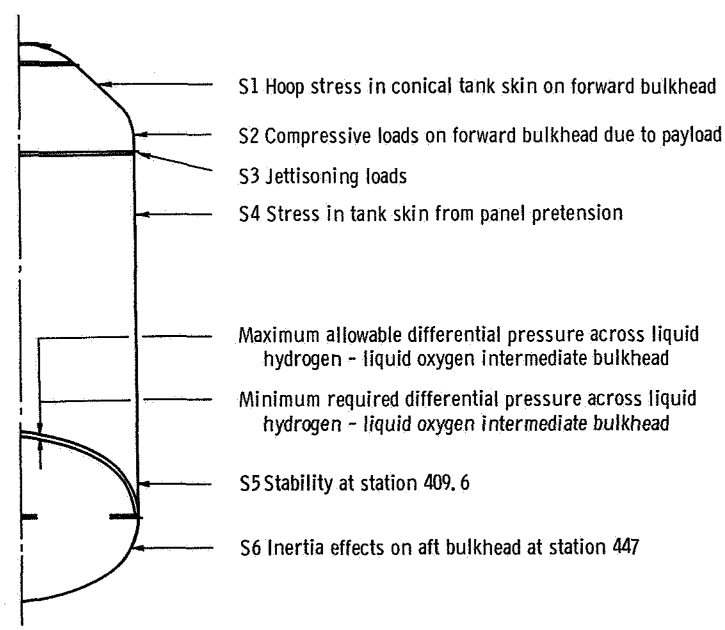

Figure V-33. - Tank areas which determined allowable pressures, AC-7.

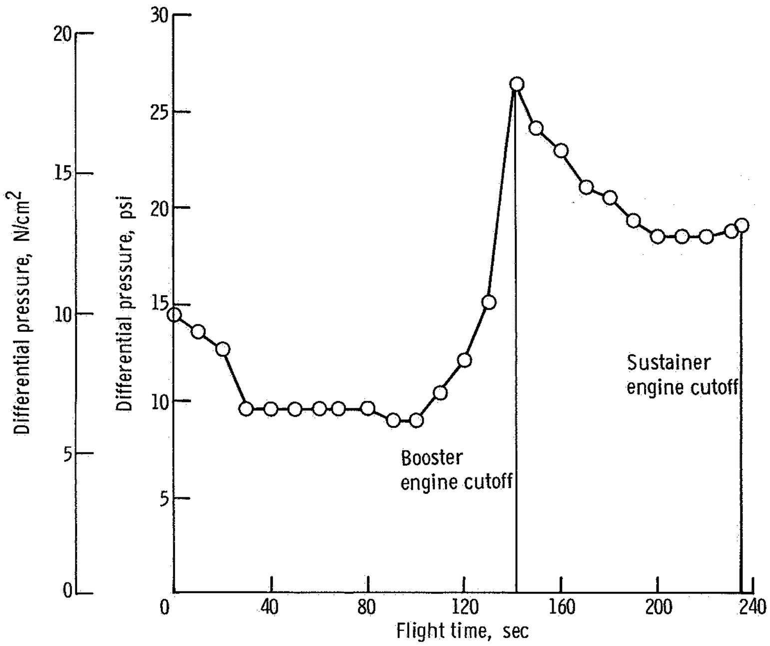

Figure V-34. - Atlas intermediate bulkhead differential pressure, AC-7.

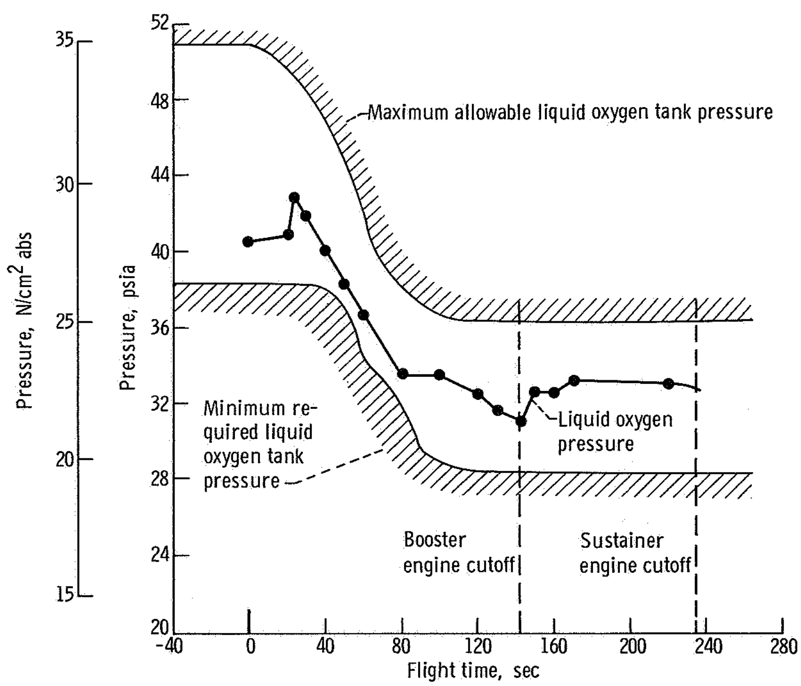

Figure V-35. - Atlas liquid oxygen tank pressure, AC-7.

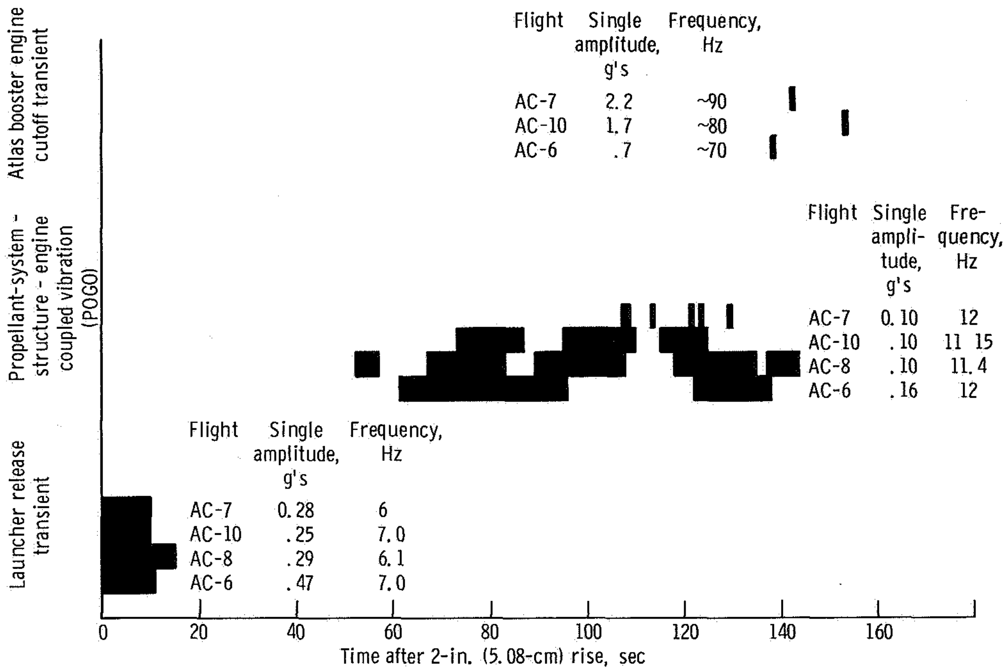

Figure V-36. - Longitudinal vibrations for Atlas-Centaur flights. (Length of bars indicates duration of vibration).

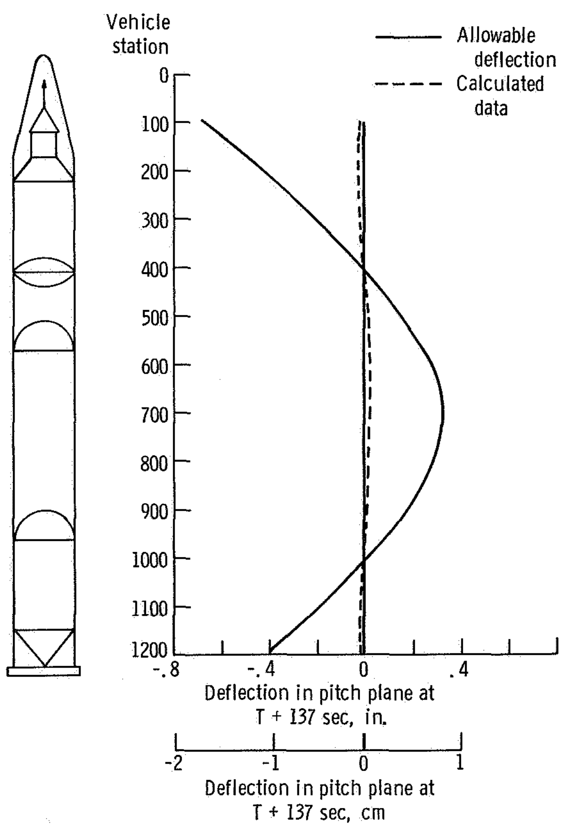

Figure V-37. - Maximum pitch plane first bending mode amplitudes, AC-7.

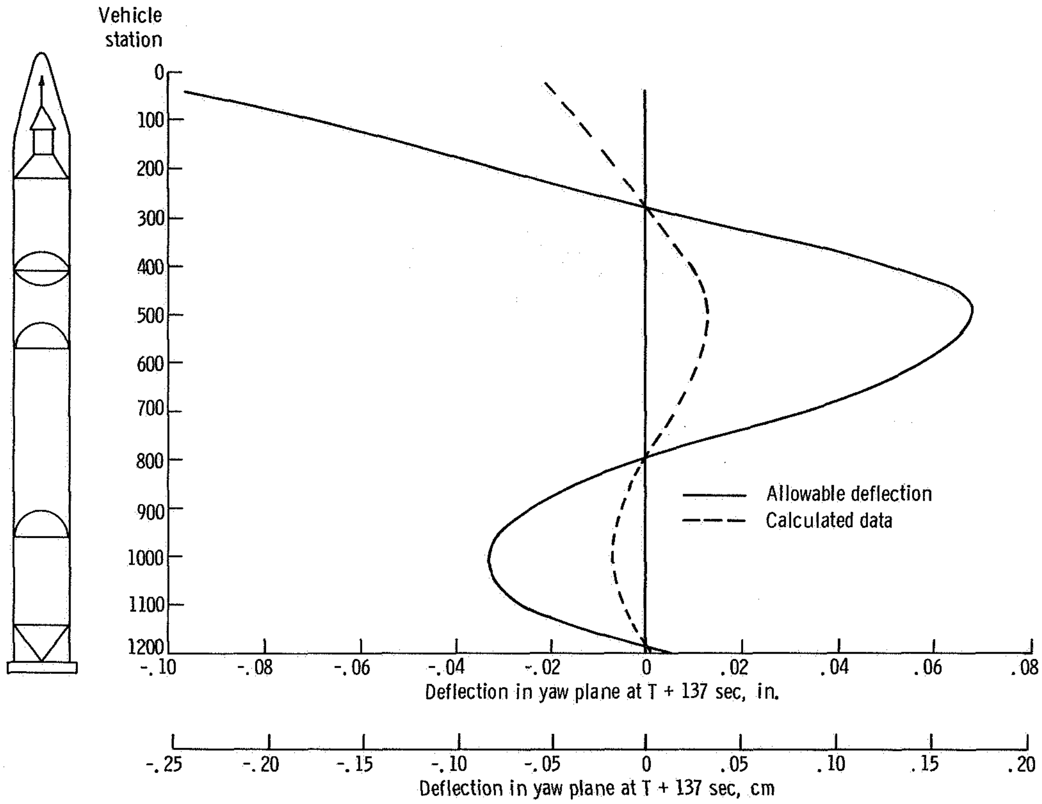

Figure V-38. - Maximum yaw plane second bending mode amplitudes, AC-7.

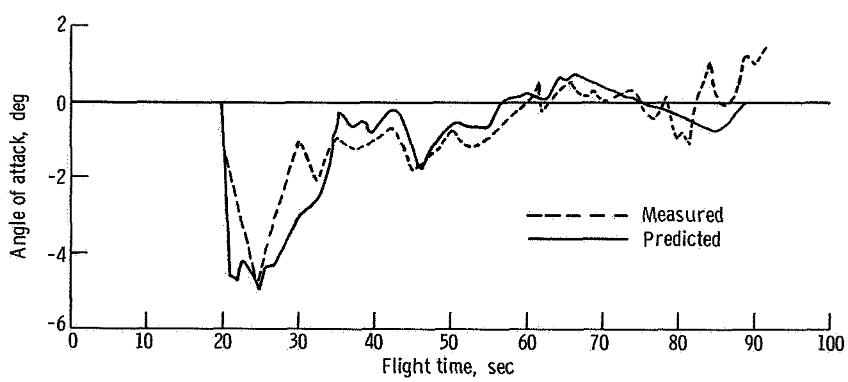

Figure V-39. - Pitch angles of attack, AC-7.

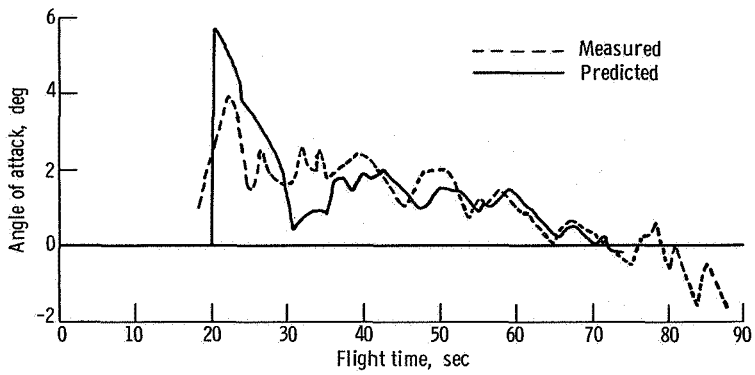

Figure V-40. - Yaw angles of attack, AC-7.

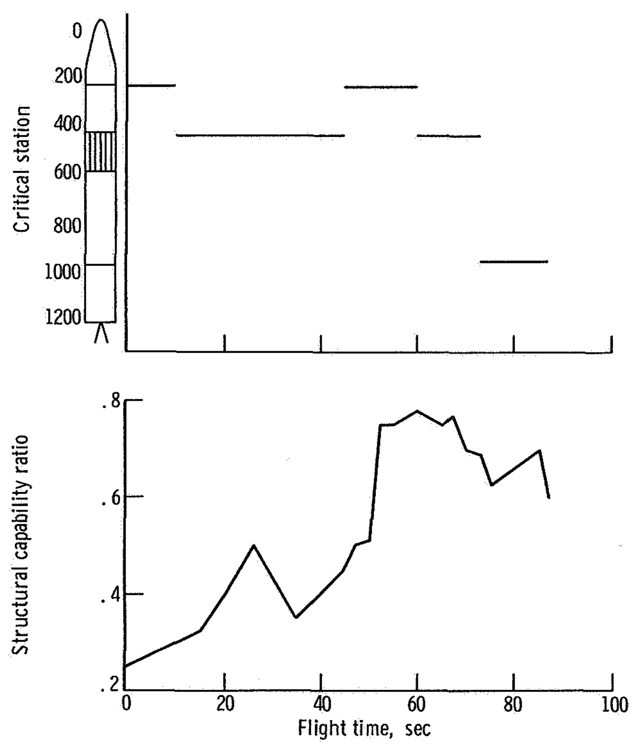

Figure V-41. - Maximum predicted structural capability ratio [(Total equivalent predicted bending moment)/(Bending moment allowable)] and critical station, AC-7.

SEPARATION SYSTEMS

by Thomas L. Seeholzer

System Description

The Atlas-Centaur vehicle required the separation of stages and certain jettisonable structures during the launch phase. Systems were required for (1) insulation panel separation, (2) nose fairing separation, (3) Atlas-Centaur separation, and (4) spacecraft separation.

Four insulation panels were separated by a flexible linear shaped charge located at the forward, aft, and longitudinal seams. Each panel was jettisoned about two interstage adapter hinge points (fig. V-42). On actuation of the shaped charge, the in-flight purge pressure under the panels, together with the energy from the elasticity in the panels which were under pretension, exerted a force causing their rotation about the hinge points. After approximately 45° of rotation, the panels are free from the Centaur vehicle.

Nose fairing jettison was accomplished by nitrogen gas powered thrustors located at the forward end of the fairings, one in each cone half. The thrustors exerted a force causing the fairing halves to pivot outboard around their respective hinge points. After approximately 35° of rotation, the fairings separated from the Centaur vehicle. Prior to thrustor actuation, the aft circumferential connection to the Centaur tank was severed by firing a flexible linear shaped charge (fig. V-43). The nose fairing split line was opened by release of eight pyrotechnically operated pin puller latches.

Atlas-Centaur separation was accomplished by a flexible linear shaped charge which cut the interstage adapter circumferentially near its forward end. The Atlas and interstage adapters were then separated from Centaur by retrorockets which fired approximately 0.1 second later (fig. V-44).

The spacecraft was separated from Centaur by three pyrotechnically operated pin puller latches mounted on the forward payload adapter. Separation force was provided by three mechanical spring assemblies, which have a 1-inch (2.54-cm) stroke, that were mounted adjacent to each separation latch on the forward adapter (fig. V-45).

System Performance

Insulation panel separation. - A review of the flight data indicated that all four panels separated and jettisoned normally. Four breakwires were attached to the insulation panel hinge arms and the interstage adapter to record panel separation, as shown in figure V-46.

One breakwire on each of the four panels recorded panel separation after 35° of panel rotation. The data indicated panel rotational velocities of approximately 80 degrees per second compared with 75 to 87 degrees per second experienced on the AC-10 flight.

Nose fairing separation. - Separation of the nose fairing occurred at T + 203.15 seconds. Thrustor bottles fired at T + 202.90 seconds. Nose fairing jettison was verified by disconnect wires telemetered on a commutated channel. They showed that jettison occurred between T + 202.19 and T + 203.15 seconds. These wires, incorporated for the first time on this flight, were part of the electrical connectors in each of the nose fairing halves and were located on the y-y axis about 35° forward of the hinge point. Connectors separated after approximately 4° of fairing rotation. Other applicable instrumentation as Atlas vehicle rate gyros and accelerometers indicated a normal fairing separation. As expected, no indication of pressure buildup in the payload compartment occurred at nose fairing thrustor bottle actuation, as shown in figure V-47.

Atlas-Centaur separation. - Vehicle staging was initiated by the firing of the linear shaped charge at T + 237 seconds which severed the interstage adapter at station 413. The retrorockets mounted around the aft end of the Atlas fired approximately 0.1 second later to decelerate the booster. Accelerometer data indicated that all eight retrorockets ignited. The critical motion was in pitch as there was less radial clearance between the interstage adapter and the Centaur in the y-z plane. The gyros indicated no discernible rotation between the two stages as the Atlas cleared the Centaur.

The steering gyros mounted on the Atlas indicated approximately 0.21° of rotation about the yaw axis at the time it cleared the Centaur. This rotation created a lateral displacement at the forward end of the interstage adapter of 2.1 inches (5.3 cm).

Spacecraft separation. - Centaur-Surveyor separation was accomplished at T+752.6 seconds. Data from extensometers on the separation spring assemblies indicated all three separation latches actuated within 1 millisecond of each other. The three jettison spring assemblies were calibrated prior to flight, as shown in figure V-48. The springs operated normally during flight and yielded approximately identical data for stroke against time, as shown in figure V-49. The separation was normal producing no significant spring induced angular rate in the spacecraft.

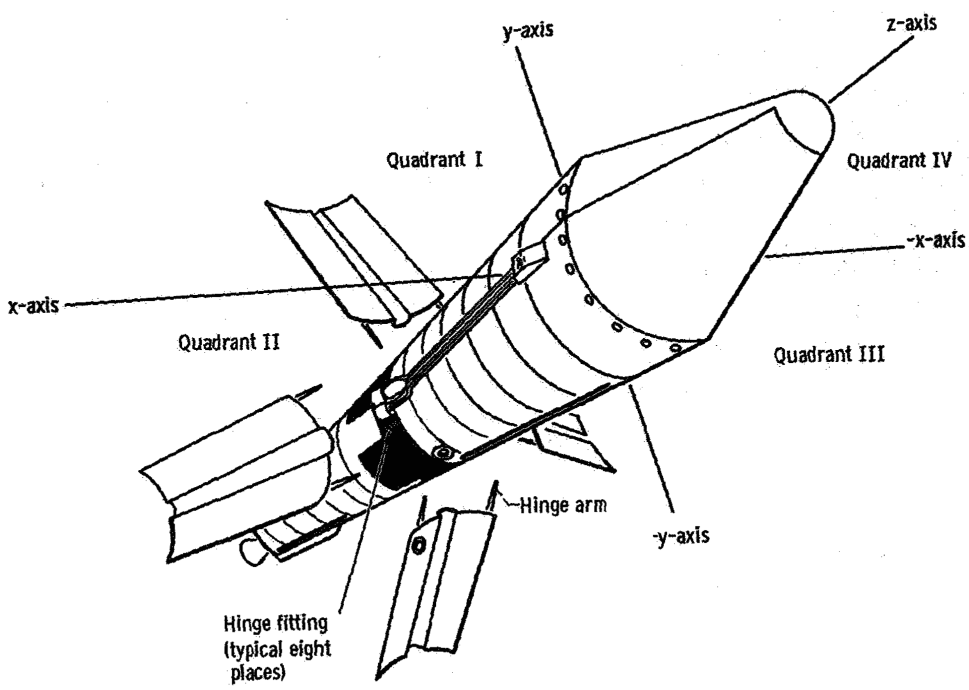

Figure V-42. - Jettisonable insulation panel system, AC-7.

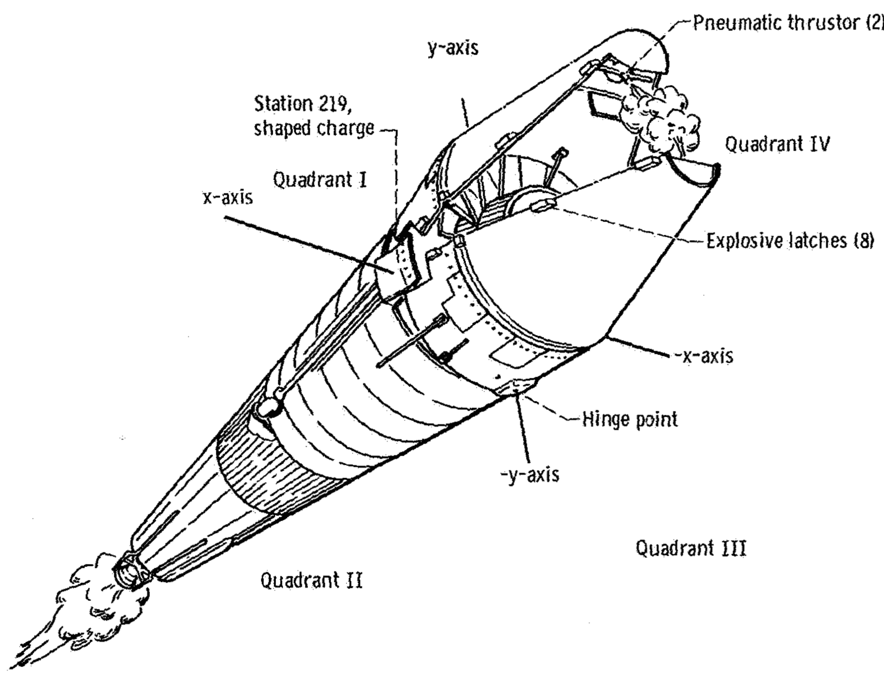

Figure V-43. - Surveyor nose fairing jettison, AC-7.

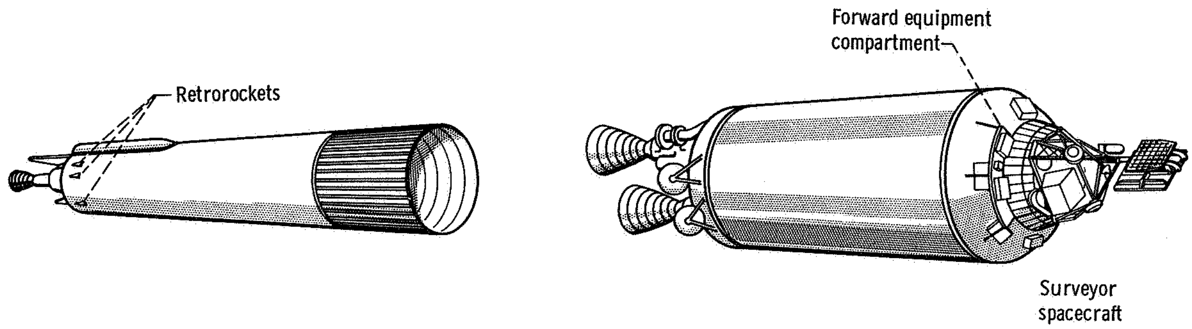

Figure V-44. - Atlas-Centaur separation, AC-7.

CD-9521

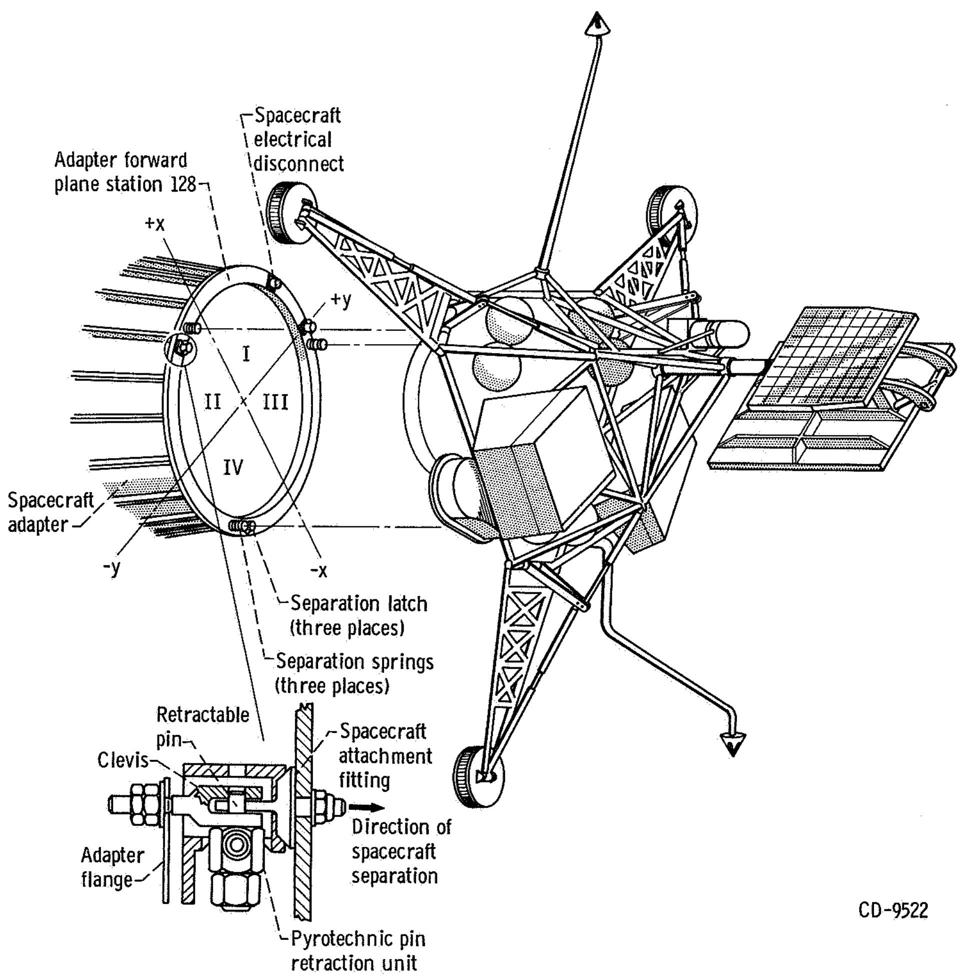

CD-9522

Figure V-45. - Centaur-Surveyor separation, AC-7.

Breakwire	Quadrant location		Break time, sec
	Panel	Hinge arm	
A	2-3	III	T + 176.49
B	1-2	I	T + 176.51
C	3-4	III	T + 176.51
D	4-1	I	T + 176.51

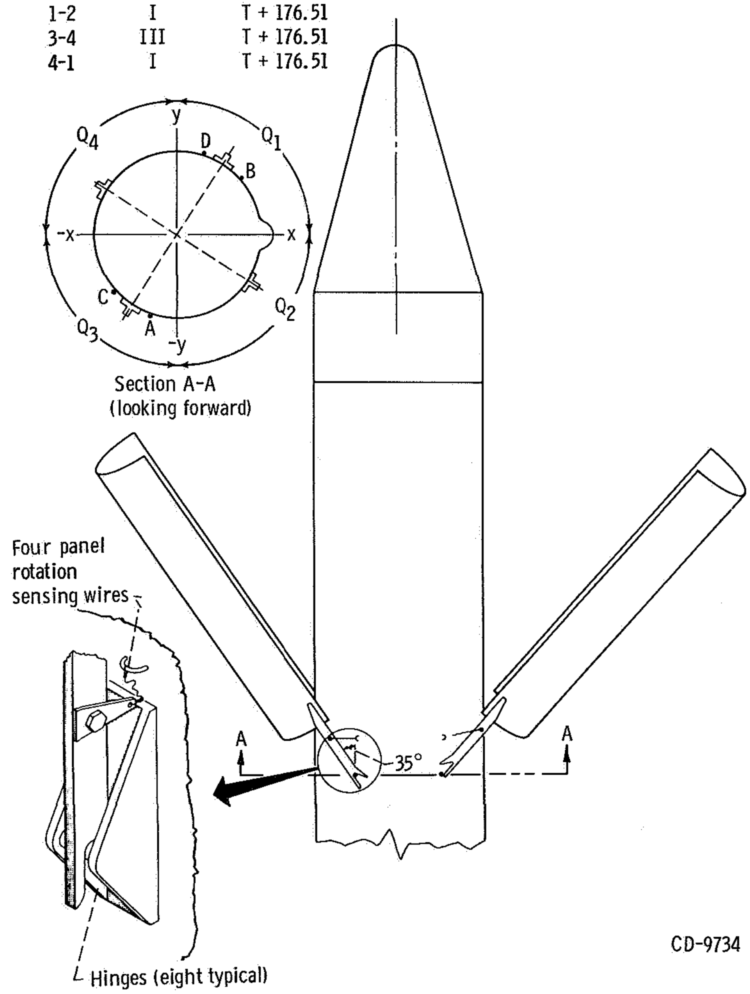

Figure V-46. - Insulation panel breakwire locations, AC-7.

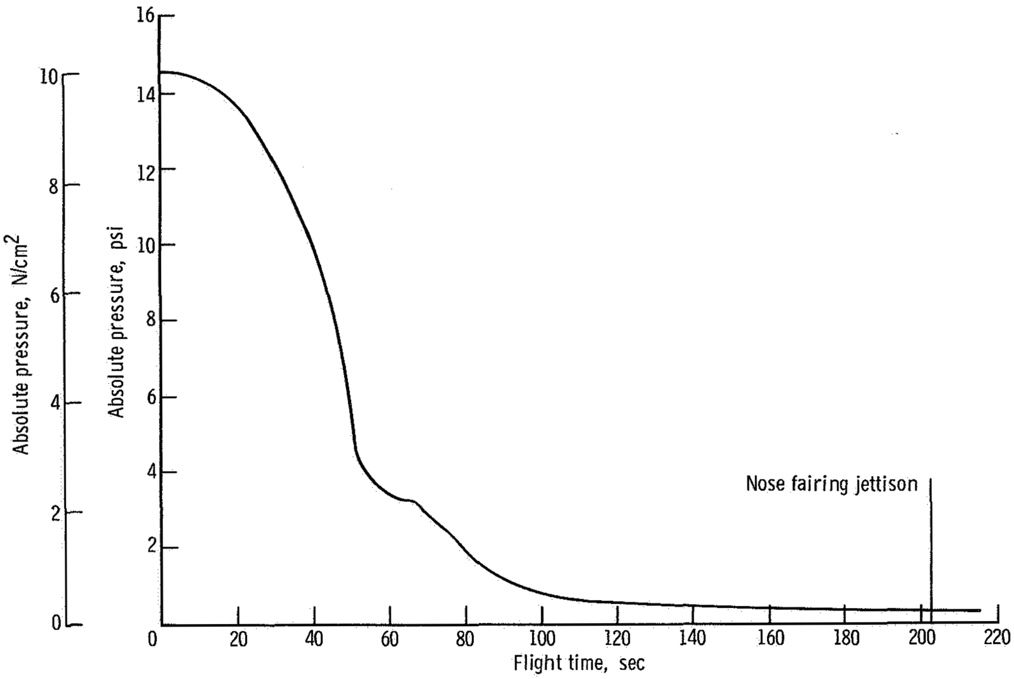

Figure V-47. - Payload compartment pressure, AC-7.

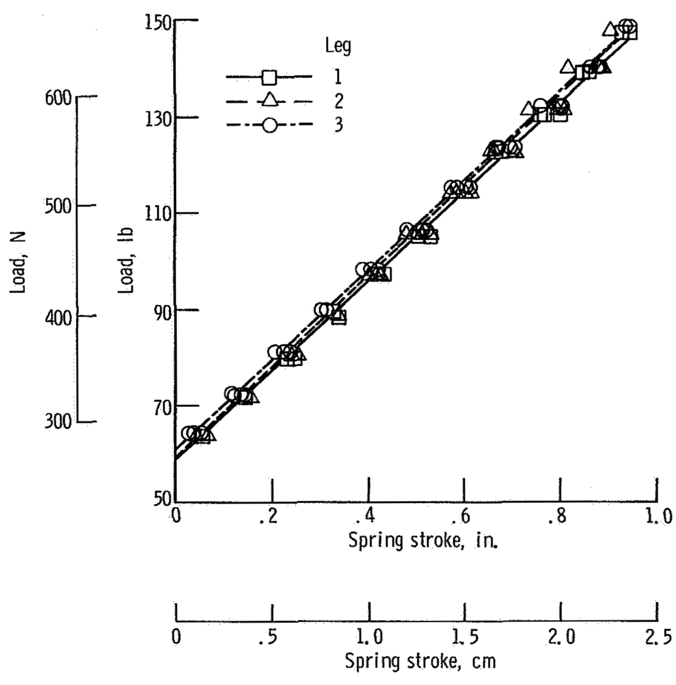

Figure V-48. - Surveyor jettison spring calibration data at Eastern Test Range, AC-7.

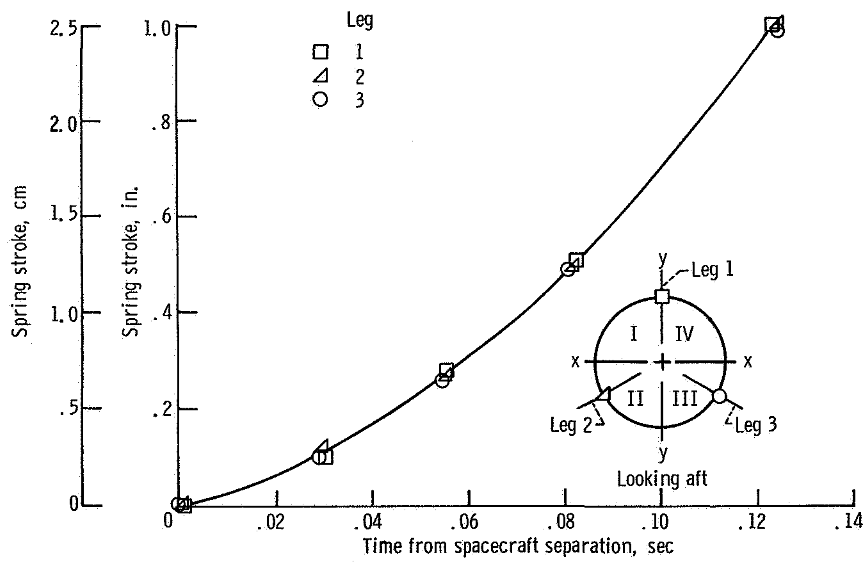

Figure V-49. - Centaur-Surveyor separation spring motion, AC-7.

ELECTRICAL SYSTEMS

by Robert Freedman, John E. Moss, Jr., and John B. Nechvatal

Power Sources and Distribution

Atlas system description. - Atlas electrical power requirements were supplied by one main battery, one telemetry battery, two range safety command batteries, and a rotary inverter. Transfer of the electrical load from external to internal battery power was satisfactorily accomplished by the power changeover switch at T - 2 minutes.

Atlas system performance. - The Atlas main missile battery supplied the requirements of the dependent systems at near normal voltage levels. The battery voltage was 27.9 volts at lift-off, rose to 28.2 volts at sustainer engine cutoff, then dropped to a low of 26.6 volts at retrorocket firing.

The three batteries which supplied the telemetry and range safety command systems provided normal voltage levels throughout Atlas flight. The voltage at lift-off was 28.2 volts for the telemetry system, 28.2 volts for range safety command system 1, and 28.3 volts for range safety command system 2.

The rotary inverter, supplying the airborne 400 hertz power, operated within established voltage and frequency parameters. The voltage at lift-off was 115.4 volts with a decline to 114.9 volts at end of data acquisition. The inverter frequency at lift-off was 402.1 hertz and rose to 403 hertz at the end of programmed Atlas flight. The gradual rise in frequency is typical for this component, as noted on earlier flights and during ground testing. The required difference of 1.3 to 3.7 hertz between Atlas and Centaur inverter frequencies was properly maintained to avoid generation of undesirable beat frequencies in the autopilot system. If a beat frequency occurred in resonance with the slosh or natural frequencies of the vehicle, false commands would be given to the autopilot resulting in possible degradation of vehicle stability.

Centaur system description. - The Centaur electrical power system consisted of a main battery, two range safety command batteries, two pyrotechnic batteries, a main power changeover switch, and a solid-state inverter. The inverter supplied 400 hertz power to the guidance, flight control, and propellant utilization systems.

Centaur system performance. - System operation was satisfactory throughout the flight. Transfer of the Centaur electrical loads from external power to the internal battery was accomplished by the power changeover switch within 250 milliseconds. Transient voltages were small. The umbilical disconnects operated satisfactorily on command.

The main battery voltage level at lift-off was 28.2 volts. It dropped to a low of 27.5 volts at main engine start, then recovered to 28.1 volts during Centaur powered flight.

Comparison of the preflight battery load profiles with the actual AC-7 flight profile shows close correlation between sequential events. Battery current at lift-off was 43 amperes. It reached a normal peak at T + 235 seconds, as shown in the load profile (fig. V-50). The profile exhibited an unexpected current surge coincident with mechanical separation of the spacecraft. An abnormally high current demand (varying from 13 to 20 A above normal) was apparent immediately following pyrotechnic firing at T + 752.6 seconds. Analysis has isolated the anomaly to the spacecraft separation pyrotechnic circuit. This circuit is provided by Centaur. A short circuit at the output side of the pyrotechnic relay assembly is postulated since the fault did not appear until the relay was energized.

The backup AC-7 pyrotechnic relay assembly was depotted and inspected for possible areas where short circuits could occur without being detected in the nine preflight checkout tests of the relay and assembly. Examination revealed that wire clearances on the thermal relay terminal board were marginal even on the backup relay assembly. One thermal relay switch was almost shorted out by an adjacent terminal wire.

From examination of the AC-7 backup pyrotechnic relay box and the history jacket for the flight article, it has been concluded that such a fault was probable. The component history jacket showed that a diode was replaced. In so doing, it is possible to short out adjacent terminals. This would have the effect of bypassing the normally closed contacts of a thermal relay, and external measurement would not reveal the parallel paths. Should the associated squibs short circuit on firing, which is common, the thermal relay contacts would open, but the fault current would continue to flow through the shorted terminals.

The thermal relay board, in the pyrotechnic relay assembly, was redesigned for AC-9, AC-11, and following flights, which greatly reduces the possibility of adjacent terminal shorts on the terminal board. The AC-7 style turret terminal is shown in figure V-51. The terminal design has been changed by bringing wires up through the hollow cores of the bifurcated terminal rather than by wrapping them around the turret terminal, as shown in figure V-52. The tendency toward excess solder or wire bulge is thus minimized. The reliability of the pyrotechnic system operation has been improved for AC-11 and following flights by redesigning to provide for firing the squibs by redundant relays.

The pyrotechnic battery voltages were 36.5 and 36.4 volts, respectively, at lift-off. (Minimum specification limit is 34.7 V.) Proper operation of the pyrotechnic batteries and relay system was verified by the successful jettison of the insulation panels and nose fairing.

Performance of the two range safety command batteries was satisfactory as verified by proper command receiver operation during launch and flight. The battery voltages were 32.6 and 32.5 volts, respectively, with the receivers in operation. (Minimum specification limit is 30 V).

The solid-state Centaur inverter, supplying 400 hertz power to the guidance, autopilot, and propellant utilization systems, operated satisfactorily throughout the flight. Telemetered voltage levels compared closely with values recorded during preflight testing. The three-phase voltages at lift-off were as follows: phase A, 115.7 volts; phase B, 115.5 volts; and phase C, 114.9 volts. Phase A and B voltages rose slightly during flight (0.3 V for phase A and 0.2 V for phase B) while phase C voltage remained nearly constant.

The inverter frequency remained constant at 400.0 hertz throughout the flight. Inverter temperature was 104° F (313° K) prior to hydrogen tanking and then cooled to 82° F (300° K) at lift-off.

Instrumentation and Telemetry

Atlas system description. - The Atlas telemetry system consisted of a single PAM/FM/FM unit transmitting at 229.9 megahertz. The former designation PAM refers to Pulse Amplitude Modulation, a technique of sampling data to allow better utilization of the data handling capacity of the telemetry system. The designation FM/FM (Frequency Modulation/Frequency Modulation) refers to the technique of frequency modulating a transmitter with the output of several subcarrier oscillators, which, in turn, have been frequency modulated by data signals. All operational measurements were transmitted by two antennas, one in each pod.

Atlas system performance. - The performance of the Atlas telemetry system was satisfactory. Transmitter frequency remained within limits, and signal strength was adequate throughout the flight. Locations of ground and ship stations are shown in figure V-53. Telemetry coverage was continuous, as shown in figure V-54. The commutator for channel eleven, mainly temperature measurements, exceeded its upper speed limit, but data quality did not deteriorate since the shift was gradual. A summary of the 110 Atlas measurements that were telemetered is given in table V-XII.

Centaur system description. - For the AC-7 operational flight, Centaur telemetry consisted of one PAM/FM/FM unit transmitting at 225.7 megahertz. A block diagram of the Centaur telemetry system is shown in figure V-55. All measurements were transmitted by the Centaur antenna mounted on a ground plane on top of the umbilical island. Figure V-56 shows the location of antennas on the Centaur.

Centaur system performance. - Analysis indicated satisfactory telemetry performance for the system. Centaur telemetry coverage is shown in figure V-57. A summary of 134 measurements telemetered by Centaur is given in table V-XIII. The following three Centaur vibration measurements failed:

(1) The accelerometer on the payload adapter at station 130 showed no activity during

TABLE V-XII. - ATLAS MEASUREMENT SUMMARY, AC-7

Airborne systems	Number and type of measurement									
	Acceleration	Rotation rate	Deflection	Vibration	Pressure	Frequency	Rate	Temperature	Voltage	Discrete	Totals
Airframe				1	9			11		8	29
Range safety									2	1	3
Electrical						1			2		3
Pneumatics					7			2			9
Hydraulics					6						6
Propulsion		3	2		20			2		7	34
Flight control			11				3			7	21
Axial acceleration	1										1
Propellants	1				2				1		4
Totals	2	3	13	1	44	1	3	15	5	23	110

TABLE V-XIII. - CENTAUR MEASUREMENT SUMMARY, AC-7

Airborne systems	Number and type of measurement										
	Rotation rate	Current	Deflection	Vibration	Pressure	Frequency	Rate	Temperature	Voltage	Discrete	Digital	Totals
Airframe					1			2		3		6
Range safety									2	6		8
Electrical		1				1			4			6
Pneumatics					7			4		2		13
Hydraulics					2			2				4
Guidance								1	18	3	1	23
Propulsion	4				12					8		24
Flight control							3		4	28		35
Stage separation			1									1
Propellants			2						2			4
Spacecraft			3	5		1		1				10
Totals	4	1	6	5	22	2	3	10	30	50	1	134

launch. The telemeter trace read 50 percent information bandwidth with no variation when expected - at lift-off. This indicated that the charge amplifier was operating, and that the electrical leads which carry signals to the telemetry package were intact. This measurement was checked end-to-end prior to encapsulation of the spacecraft and was operating satisfactorily. It is possible that the transducer or the coaxial cable and connector were damaged during spacecraft encapsulation.

(2) Spacecraft retromotor attachment 1 and 2 (z-axis measurements) remained at 50 percent information bandwidth during the flight, except for occasional voltage excursions. This indicated that the charge amplifier had gone into saturation. This type of saturation is often caused by a bad coaxial cable or a loose coaxial connection at either the transducer or charge amplifier.

Tracking

System description. - The airborne tracking beacon was a C-band radar transponder providing real-time position and velocity data to the range safety tracking system impact predictor. The system provided data for use in Deep Space Network acquisition of the spacecraft and for guidance and flight trajectory analysis. The airborne system included a lightweight transponder, circulator (to channel receiving and sending signals), power divider, and two antennas located on opposite sides of the tank. The location of the Centaur antennas is shown in figure V-56. The ground and ship stations are shown in figure V-53.

System performance. - Continuous coverage was obtained to T + 938 seconds. Intermittent tracking thereafter is attributed to insufficient signal strength caused by poor aspect angles (Radar sees the C-band Antenna Pattern at a lower than optimum gain point) and increasing slant range. C-band radar coverage is shown in figure V-58.

Flight Termination System (Destruct)

System description. - The Atlas and Centaur stages each contained independent vehicle borne flight termination systems which are designed to function simultaneously on receipt of command signals from the ground stations. These systems included receivers and batteries whose operation was entirely independent of the main vehicle power system.

The Atlas and Centaur flight termination system provided a means of shutting down the engines only, or shutting down the engines and destroying the vehicle. When the vehicle is destroyed in the event of a flight malfunction, the tank is ruptured with a shaped charge, and the liquid propellants of the first and second stages are dispersed. In addition, the upper stage system has the capability to destroy the Surveyor spacecraft engine prior to spacecraft separation. These functions can be commanded by the range safety officer.

System performance. - The Atlas and Centaur-Surveyor range safety command systems were prepared to execute commands throughout the flight, as shown in telemetered data. Neither engine cutoff nor destruct commands were sent by the range transmitter, nor were inadvertent commands generated at the vehicle. The command from Antigua to disable the flight termination system (destruct) shortly after Centaur main engine cutoff was properly received and executed. Figure V-59 depicts verified reception of the transmitted signal from various ground stations in supporting the range safety command system.

Signal strength at the Atlas and Centaur range safety command receivers was excellent throughout the flight as indicated by telemetry measurements. Telemetered data indicated that the Centaur receivers were deactivated at approximately T + 696 seconds, thus confirming that the disable command was transmitted from the Antigua station. The Surveyor destructor, controlled by the upper stage receivers, was also deactivated when the command to disable the range safety command system was sent from Antigua.

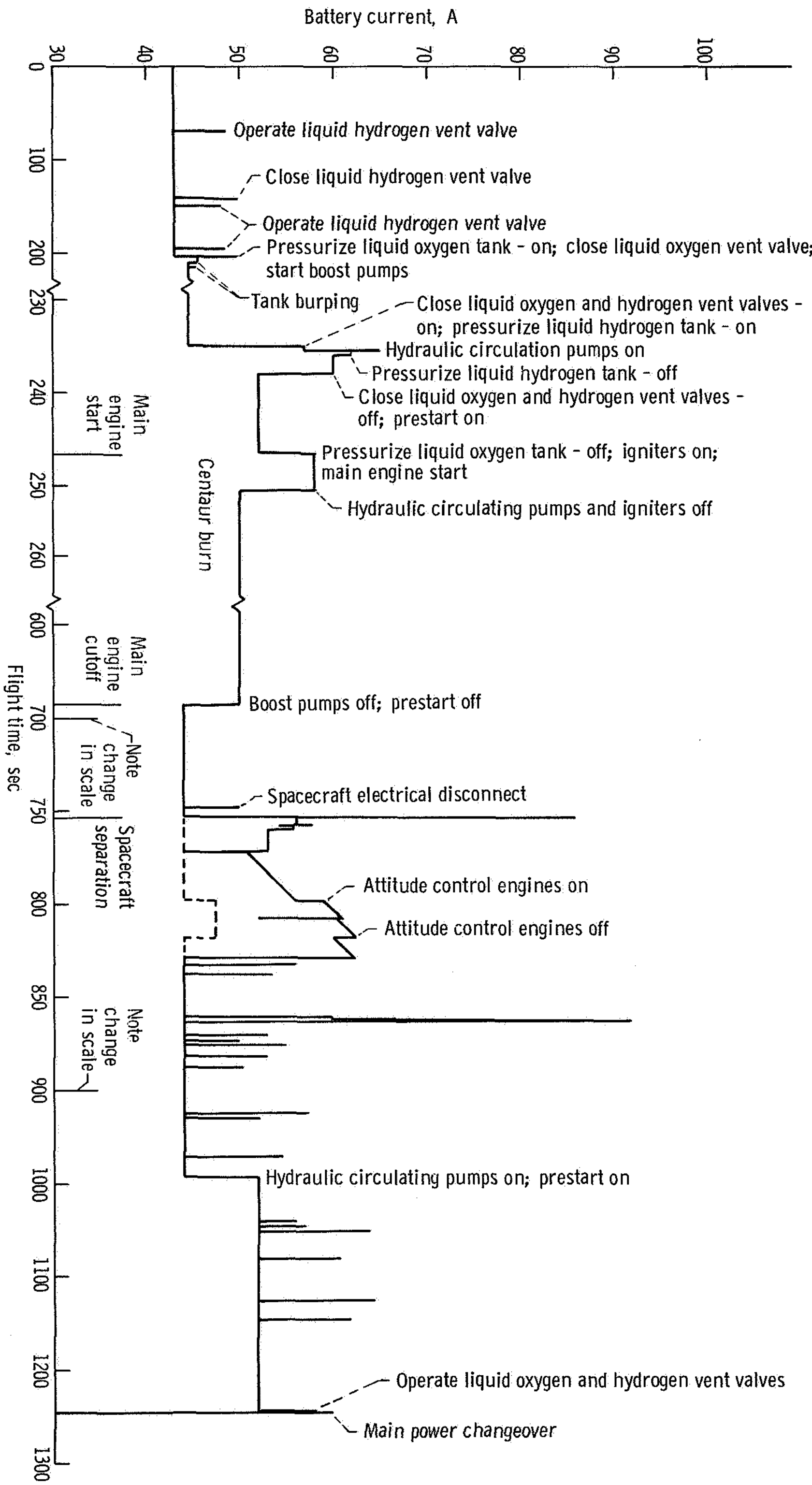

Figure V-50. - Centaur main battery load profile, AC-7.

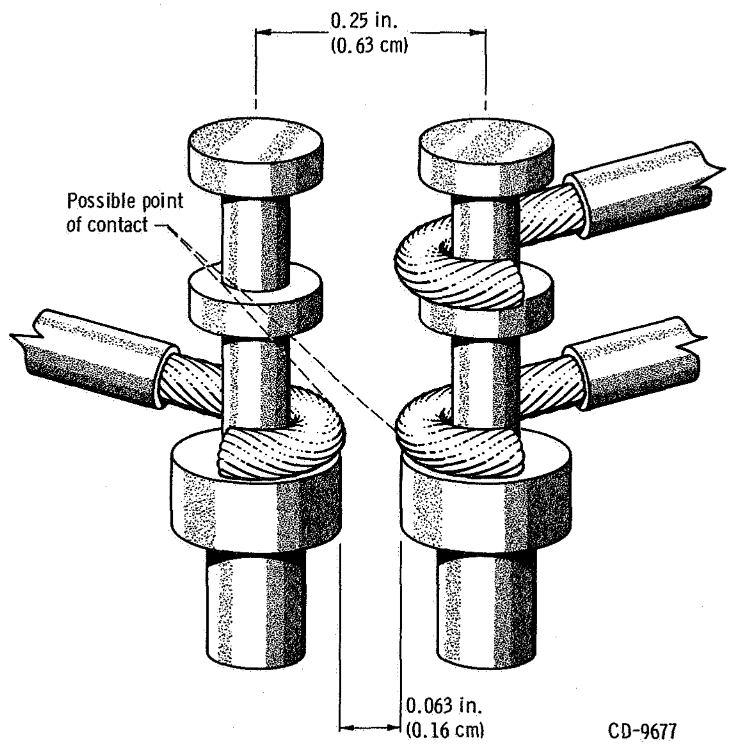

Figure V-51. - Turret type terminal.

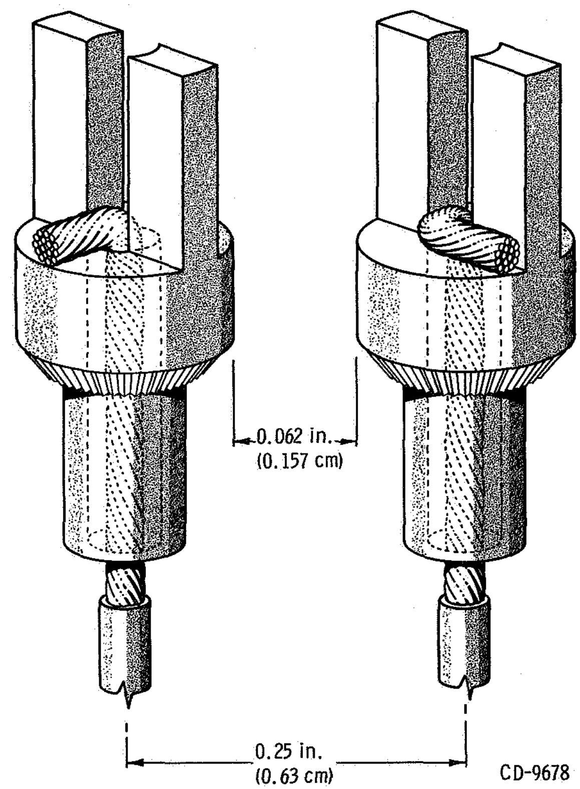

Figure V-52. - Bifurcated type terminal (bottom route connection).

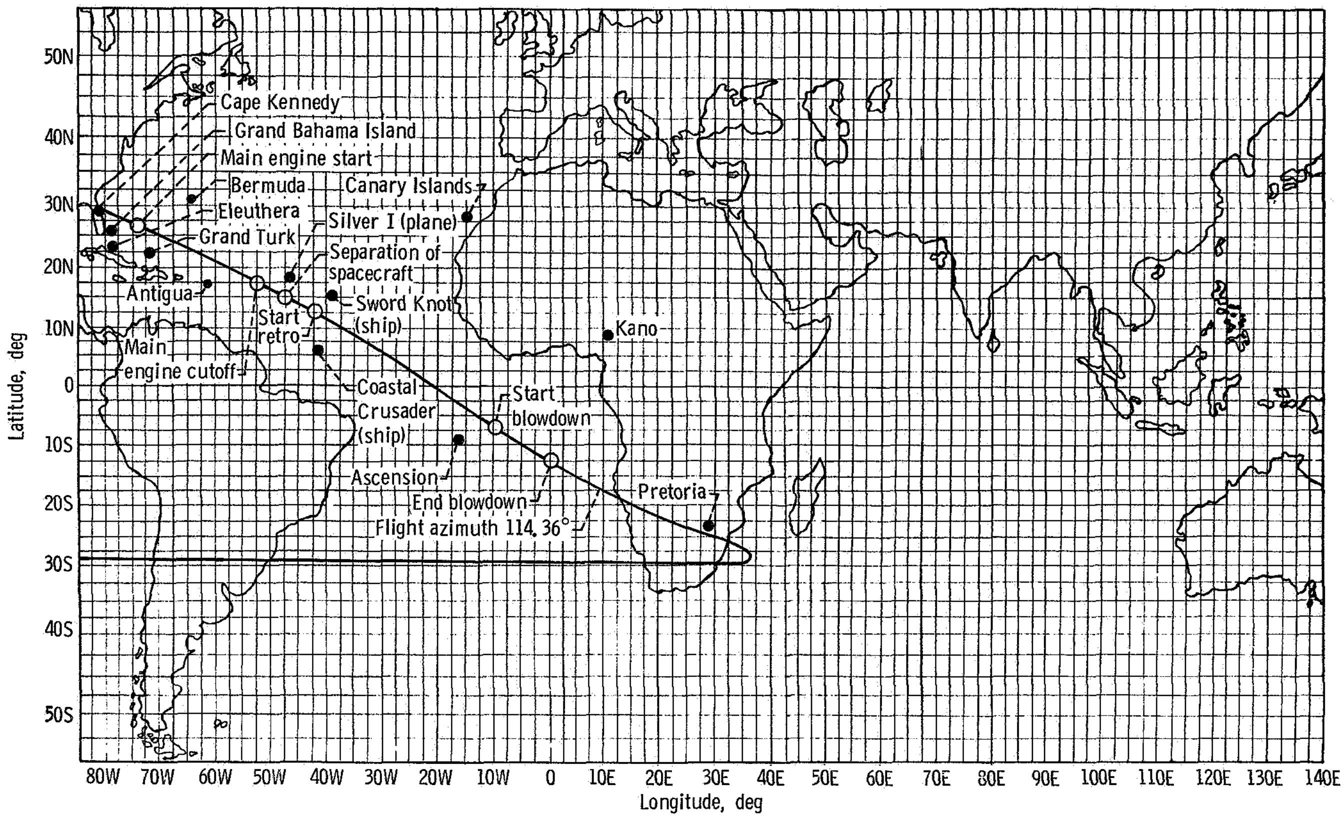

Figure V-53. - Location of ground and ship stations and vehicle trajectory Earth track, AC-7.

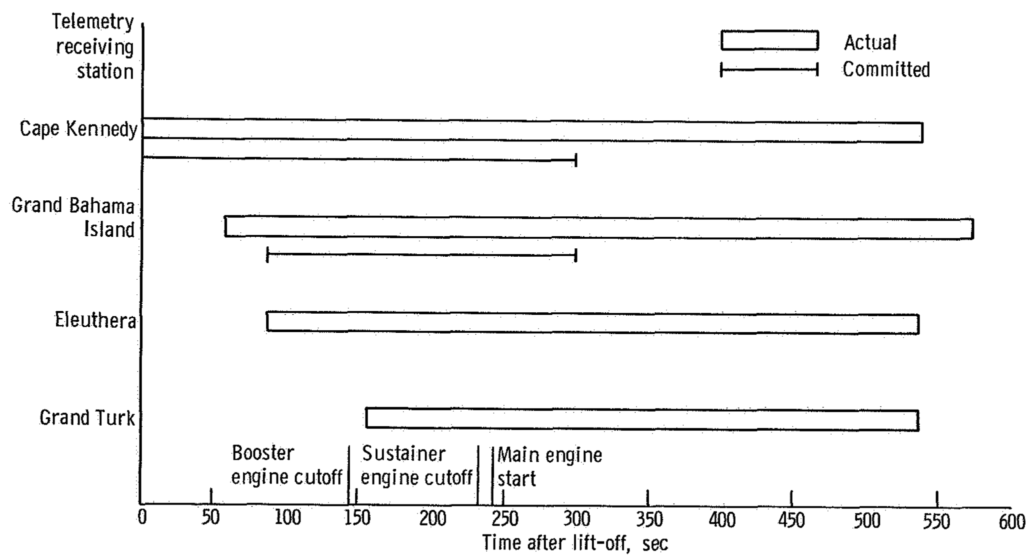

Figure V-54. - Atlas telemetry coverage, AC-7. Eleuthera and Grand Turk stations were not committed - tracked for best obtainable data.

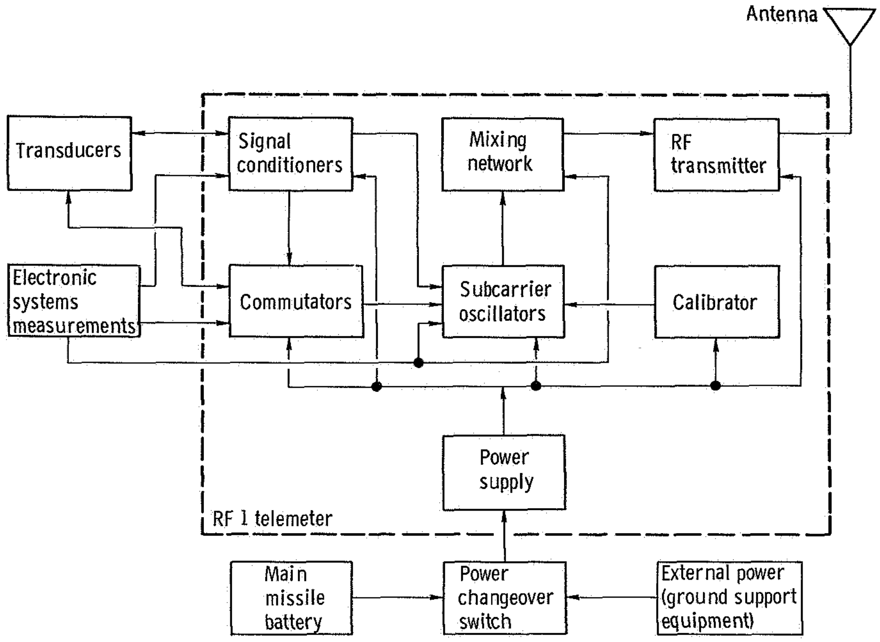

Figure V-55. - Centaur telemetry system block diagram, AC-7.

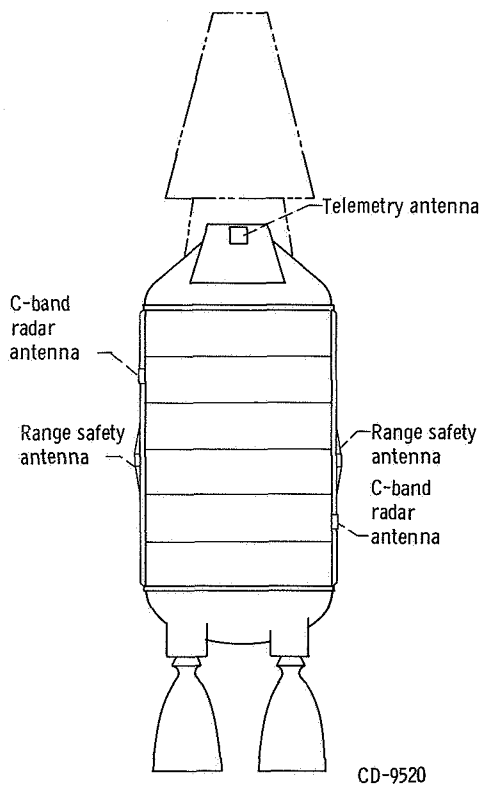

Figure V-56. - Location of Centaur antennas, AC-7.

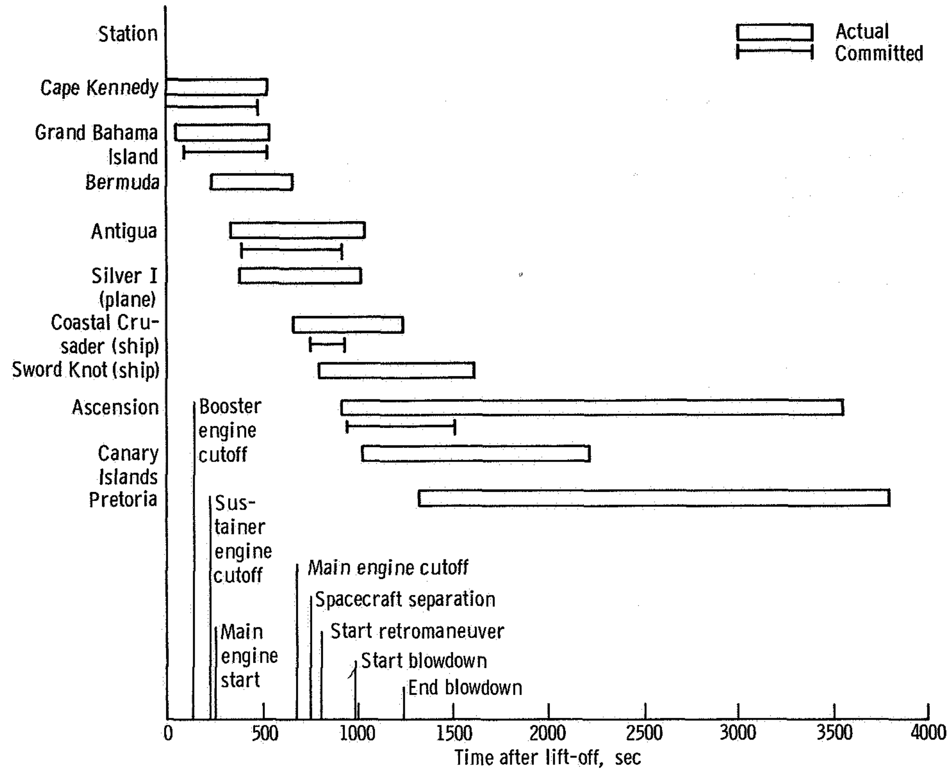

Figure V-57. - Centaur telemetry coverage, AC-7. Bermuda, Silver I, Sword Knot, Canary Islands, and Pretoria were not committed - tracked for best obtainable.

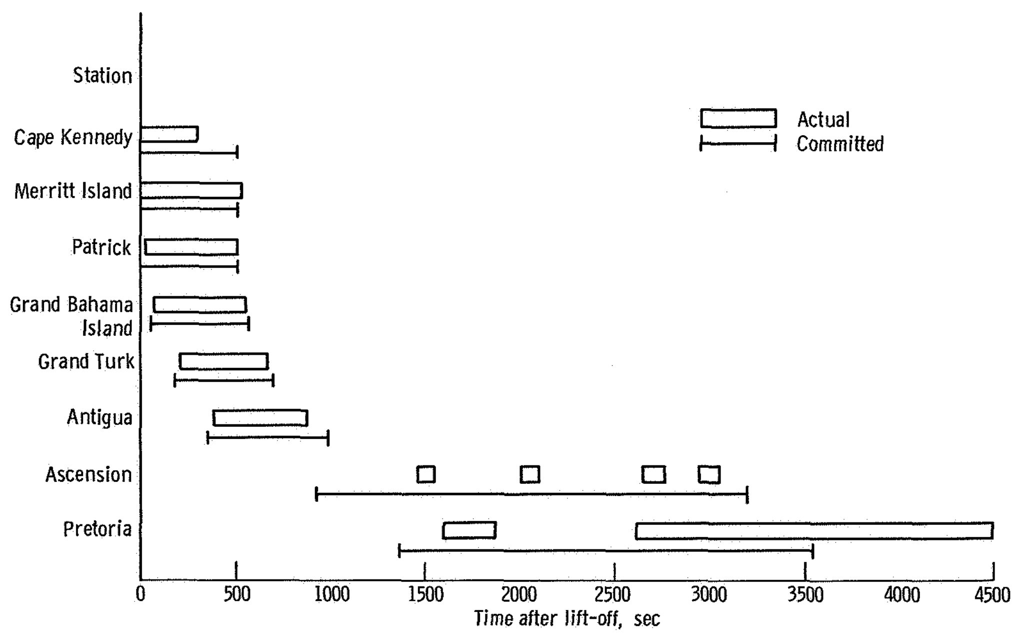

Figure V-58. - C-band radar coverage, AC-7. (Automatic beacon track only).

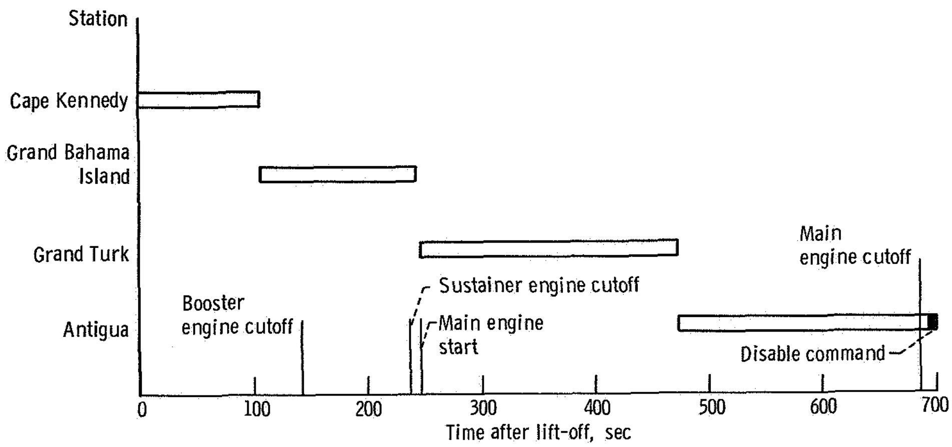

Figure V-59. - Range safety command system transmitter coverage, AC-7.

GUIDANCE AND FLIGHT CONTROL SYSTEMS

by Donald F. Garman, Theodore F. Gerus, and Sanford F. Tingley

The functions of the guidance and flight control systems were to stabilize, control, and sequence flight events of the Atlas-Centaur vehicle from lift-off through completion of the Centaur retromaneuver after spacecraft separation. These functions were accomplished by using a self-contained inertial guidance system in the Centaur stage and individual flight control systems in the Atlas and Centaur stages. The objective was to guide the launch vehicle to the injection point and establish the required launch vehicle velocity necessary to place the Surveyor spacecraft in a lunar transfer orbit. The systems had the capability to compensate for trajectory dispersions resulting from thrust misalinement, winds, and performance variations in Atlas and Centaur. A direct-ascent mission was used for the AC-7 flight. Three modes of operation were used for stabilization and control of the launch vehicle. These modes were rate stabilization, open loop control, and closed loop control. These modes are shown in simplified block diagram form in figure V-60 and the time periods of each mode are shown in figure V-61.

The purpose of the rate stabilization mode was to maintain the vehicle with near zero rotational rates about the vehicle pitch, yaw, and roll axes. Rate stabilization was done by sensing rotational rates with rate gyros (one for each axis) and gimbaling the engines during powered flight to counter any vehicle angular rates. After main engine cutoff, the hydrogen peroxide attitude control system was used to counter any vehicle angular rates. The rate stabilization mode was used only for short periods of time after Atlas-Centaur separation and after Centaur main engine cutoff.

The open loop control mode was accomplished by combining the rate gyro information with displacement information. Rate integrating gyros (one each for pitch, yaw, and roll axes) were used to provide a reference attitude from which vehicle angular displacement was measured. Engine gimbaling provided direction thrust which resulted in vehicle movement to zero out the rate integrating gyro attitude error. The reference attitude was programmed to vary in discrete steps as a function of time. The reference attitude commanded the vehicle to go from a vertical attitude toward a horizontal attitude and also to roll the vehicle to the required launch azimuth angle. This mode of operation was open loop control since there was no method to measure the actual angle through which the vehicle rotated and compare it to the commanded angle. The open loop control mode was used only during Atlas booster phase of the flight.

Closed loop control was accomplished by combining the rate gyro information with displacement information from the guidance system. This displacement information was the difference between the desired position and the actual position of the vehicle as measured by the guidance system. The term "closed loop control" denotes this method of operation where the error signal was generated by the difference between the desired or command signal and the measured output of the system. Closed loop control was used during Atlas sustainer and Centaur phases of flight. This type of control was used for only two axes, pitch and yaw. During Atlas sustainer phase the roll displacement information was provided by the Atlas rate integrating gyro. During the Centaur phase of the flight, the roll axis was stabilized only by rate gyro information. Figure V-62 is a simplified diagram of the guidance-flight control systems interface showing the summation points for the three modes of operation.

The sequencing of flight events was another shared function between the flight control systems and the guidance system. Sharing was used in the sense that one system could initiate a period of performance, such as main engine start, and another system could terminate that period of performance, such as main engine cutoff. Table V-XIV lists the main events commanded by these systems and identifies the system that originated the command for the discrete flight event.

The following sections are organized to present the description and performance of each system in order of (1) guidance system, (2) Atlas flight control system, and (3) Centaur flight control system.

TABLE V-XIV. - GUIDANCE AND FLIGHT CONTROL SYSTEMS SHARED DISCRETE COMMANDS, AC-7

Event	Originating source of discrete command
Guidance to flight condition	Guidance launch equipment
Enable Atlas flight control system	42-in. (1.1-m) rise umbilical ejection
Start roll program	Atlas flight control
Start pitch program	Atlas flight control
Booster engine cutoff	Guidance
Start guidance steering	Atlas flight control
Sustainer engine cutoff	Atlas flight control
Atlas-Centaur separation	Atlas flight control
Centaur main engine start	Centaur flight control
Start guidance steering	Centaur flight control
Accept a main engine cutoff command	Centaur flight control
Main engine cutoff	Guidance
Separate spacecraft	Centaur flight control
Provide retromaneuver steering vector	Guidance
Start guidance steering	Centaur flight control
Calibrate telemetry on	Guidance
Calibrate telemetry off	Guidance
Centaur power to external	Centaur flight control

Guidance System

System description. - The AC-7 Centaur guidance system was an inertial system which was completely independent from ground control after entering flight condition approximately 8 seconds before lift-off of the vehicle. The guidance system performed the following functions:

(1) Measured vehicle acceleration in fixed inertial coordinates

(2) Computed vehicle velocity, actual present position, and steering signals

(3) Determined time of discrete events

A simplified block diagram of the guidance system is shown in figure V-63.

Inertial measuring units: The function of measuring vehicle acceleration was accomplished by the following three units of the five units which comprise the complete guidance system:

(1) Inertial platform unit contained the gimbal assembly and gyros and accelerometers

(2) Pulse rebalance, gyro torquer, and power supply unit contained the electronics associated with the accelerometers

(3) Platform electronics unit contained the electronics associated with the gyros

The remaining two units, the navigation computer and the signal conditioner are discussed later in this section.

A platform assembly with four gimbals provided a three-axis coordinate system with a redundant fourth axis. The gimbals were used to isolate the inner or azimuth gimbal from movements of the vehicle airframe. A gimbal diagram is shown in figure V-64. The four gimbals allowed complete rotation of all three vehicle axes about the platform without gimbal lock. Gimbal lock is a condition where two axes coincide and 1 degree of freedom is inadvertently lost. The inertial components, three gyros and three accelerometers, were mounted on the azimuth gimbal. A gyro and an accelerometer were mounted as a pair with the input axes of each pair parallel. These gyro-accelerometer pairs were also alined on three mutually perpendicular (orthogonal) axes corresponding to the three axes of the platform.

The three gyros used were the single degree-of-freedom, floated-gimbal, rate-integrating type. Each of the three axes of the platform was controlled by a gyro, the only function of which was to maintain that axis fixed in inertial space. Control was provided by inputing the gyro signal to a servoamplifier. The output of the amplifier controlled a direct-drive gimbal-torque motor. Since the inner gimbals were fixed to an inertial reference and the outer gimbal was fixed to the vehicle, the angles between the gimbals were used for an analog transformation of steering signals from inertial coordinates to a vehicle coordinate system. The analog transformation was accomplished by resolvers, mounted between gimbals, which produced the sine and cosine functions of the gimbal angles.

The three accelerometers used were the single-axis, viscous-damped, hinged-pendulum type. The accelerometer associated with each axis measured the change in vehicle velocity along that axis as positive or negative pulses, depending on an increase or decrease in vehicle velocity. The accelerometer and its associated electronics were designed so that each rebalance pulse, necessary to center the hinged pendulum, represented a unit of change in velocity of approximately 0.1 foot per second (0.03 m/sec). These pulses of incremental velocity were then routed to the navigation computer unit for further processing to provide the outputs of the guidance system.

During launch countdown, the inertial measuring units were alined and calibrated for initial conditions. The azimuth axis of the platform, to which the desired flight trajectory was referenced, was established by ground based optical alinement equipment. The remaining two axes of the platform were alined to the local vertical by using the two appropriate accelerometers. The platform was then controlled to center the outputs of these accelerometers. Each gyro was calibrated for constant torque drift rate and mass unbalance along the input axis. The accelerometers were calibrated for misalinement of input axes, and the scale factor and zero bias offset of each accelerometer was determined. These prelaunch determined constants were stored in the navigation computer for use during flight.

Navigation computer unit: The navigation computer unit was a serial, binary, digital machine with a magnetic drum memory. The memory drum had a capacity of 2816 words (25 bits per word) of permanent storage, 256 words of temporary storage, and six special purpose tracks. The permanent storage was prerecorded and could not be altered by the computer. The temporary storage track was the working storage of the computer. The incremental velocity pulses from the accelerometers were the information inputs to the navigation computer. The operation of the navigation computer was controlled by a program prerecorded in the permanent memory of the computer. This program allowed the computer to perform three basic operations which are described by the prelaunch equations, and guidance equations.

The prelaunch equations established the initial conditions for the navigation and guidance equations to begin navigating and guiding at approximately 8 seconds prior to lift-off. This conditioning included selecting a reference trajectory, inserting launch pad values of position, and setting various navigation and guidance functions to predetermine initial values.

The navigation equations computed present velocity and present position. The present (current) velocity was determined by algebraically summing the incremental velocity pulses from the accelerometers and then performing an integration on the computed velocity to determine present position. Corrections for the calibrated gyro and accelerometer constants were also made during the velocity and position determination to improve the navigation accuracy. As an example, the velocity information derived from the accelerometer data was adjusted to compensate for the accelerometer scale factors and zero offset biases that were measured during the launch countdown. The direction of the velocity was also adjusted to compensate for the gyro constant torque drift rates that were measured in the launch countdown.

The function of the guidance equations was to guide the vehicle to the required point in space for injection into the desired lunar trajectory. The guidance equations used were of the modified "velocity-to-be-gained" concept, which involved the difference between the present velocity and the desired velocity. These guidance equations only required as inputs present position, present velocity, and the trajectory injection requirements. The equations were "modified" to optimize other mission constraints. Based on the modified velocity-to-be-gained concept, steering signals were generated to guide the vehicle along an optimized flight path from the present position to the desired injection conditions. The navigation computer used the guidance equations, to initiate five discrete commands: (1) booster engine cutoff, (2) backup sustainer engine cutoff, (3) Centaur main engine cutoff, (4) calibrate telemetry on, and (5) calibrate telemetry off. The booster and backup sustainer engine cutoff discrete commands were issued when the measured vehicle acceleration equaled a predetermined value. The Centaur main engine cutoff discrete command was issued when the computed vehicle energy (using measured vehicle velocity) equaled the orbital energy required for injection into the lunar trajectory. The telemetry discrete commands were issued on predetermined fixed time intervals from the backup sustainer discrete command.

Signal conditioner unit: The signal conditioner unit was the link between the guidance system and the vehicle telemetry system. The signals in the guidance system required modification and scaling to match the input range of the telemetry system.

System performance. - The overall performance of the AC-7 guidance system (designated MGS #16B) was excellent with no discrepancies or anomalies noted.

System accuracy: The guidance system performed within the expected limits. Data from tracking information indicated that the midcourse correction required to be performed 20 hours after injection in order to impact the designed target point was 1.16 meters per second (miss only) or 1.20 meters per second (miss plus time of flight). These midcourse corrections were well within the specified accuracy requirement for a Surveyor mission with a maximum midcourse correction capability of 50 meters per second. Trajectory perigee was designed to be 90±5 nautical miles (167 km) based on spacecraft heating and payload considerations. The actual perigee was 89.2 nautical miles (165 km).

The overall injection velocity error was caused by three main sources: (1) an error in the prediction of engine shutdown impulse, (2) an error due to the computational technique used and influenced by the actual trajectory flown, and (3) an error related to the precision of the guidance system. A separation of these injection errors is shown in the following table:

Error	Miss only, m/sec	Miss plus time of flight, m/sec
Engine shutdown impulse	1.92	5.37
Guidance equations	.13	.24
Guidance hardware	1.18	5.04
Total error (vector summation)	1.16	1.20

The largest injection error appeared to be caused by larger than expected Centaur main engine shutdown impulse. No significant spacecraft separation impulse error appeared to have occurred.

The landing conditions for which the computer program was designed and the landing conditions which would have been achieved had no midcourse correction maneuver been made are listed in the following table:

Landing conditions	Designed	No midcourse correction maneuver
Selenographic latitude	0.00° S	0.05° S
Selenographic longitude	0.67° W	5.32° W
Unbraked impact velocity	2663.0 m/sec	2663.3 m/sec
Flight time to Moon	2 days 14 hr 47 min 54.13 sec	2 days 14 hr 47 min 56.25 sec

These data reflect a projected miss of the designed target of about 76 nautical miles (141 km) an impact velocity error of 0.3 meter per second, and a flight time difference of 2.12 seconds late.

Hardware performance: The navigation computer issued the booster engine cutoff discrete at T + 142.6 seconds. Acceleration of the vehicle at the time of booster engine cutoff discrete was 5.65 g's which was within the expected range of 5.62 to 5.78 g's. The Centaur main engine cutoff discrete was issued at T + 686.24 seconds. The energy error at main engine cutoff was approximately 4000 feet squared per second squared ($372.0\ m^2/sec^2$). This corresponds to a velocity error of -0.06 foot per second (-0.018 m/sec).

Guidance steering was activated 7 seconds after booster engine cutoff was commanded. At this time, a 6° pitchdown maneuver and a 3° yaw-left maneuver were commanded. Minor pitch and yaw commands of 4° or less were commanded at the start of

Centaur powered flight when guidance steering was reactivated. The steering commands were small, less than 1° throughout the periods of Atlas sustainer and Centaur powered flight, which indicated that the thrust vector was properly alined with the desired velocity vector.

The four platform gimbal servoloops operated satisfactorily throughout the flight. The maximum displacement errors were less than 13 arc-seconds. (The dynamic accuracy requirement was 60 arc-sec.) Normal low frequency oscillations (less than 2 Hz) occurred in all four loops. Except for one component, these oscillations were apparently the result of vehicle dynamics. A 1.5-hertz oscillation on gimbal 1, averaging about 5 arc-seconds peak to peak throughout the flight, could not be correlated with vehicle movement. This type of oscillation has been observed on previous flights and does not appear to have any detrimental effect on the system.

The accelerometer loops operated satisfactorily throughout the flight. The maximum accelerometer pendulum excursions were less than 3 arc-seconds.

All the guidance system signals and measurements, which were monitored during flight, were normal and indicated satisfactory operation of the guidance system.

Flight Control Systems

Atlas system description. - The Atlas flight control system provided the primary functions required for vehicle stabilization, control, execution of guidance steering signals, and electronically timed switching sequences.

The Atlas flight control system comprised the following principal units:

(1) The displacement gyro unit consisted of three single-degree-of-freedom, floated, rate-integrating-type gyros, and associated electronics for gain selection and signal amplification. These gyros were mounted to the vehicle airframe in an orthogonal triad configuration alining the input axis of a gyro to its respective vehicle axis of pitch, yaw, or roll.

(2) The rate gyro unit contained three single-degree-of-freedom, floated, rate gyros, and associated electronics. These gyros were mounted in the same manner as the displacement gyro unit.

(3) The servoamplifier unit contained electronics to amplify, filter, integrate, and algebraically sum engine position feedback signals with guidance and/or displacement gyro generated steering signals.

(4) The programmer unit contained a time base electronic timer, arm-safe switch, high, low, and medium power electronic switches, the fixed pitch program, and circuitry to set the roll program from launch ground equipment.

During the Atlas booster phase, pitch and yaw open loop control was accomplished by

TABLE V-XV. - VEHICLE DYNAMIC RESPONSE TO FLIGHT DISTURBANCES

Event	Flight time, sec	Measurement	Rate gyro amplitude (peak to peak), deg/sec	Transient frequency, Hz	Transient duration, sec	Required percent control capability
Lift-off transients	T + 0	Pitch	0.64	(a)	(a)	4
		Yaw	.48	(a)	(a)	2
		Roll	(a)	(a)	(a)	2
42-in. (1.1-m) rise	T + 1	Pitch	0.64	6	2.8	5
		Yaw	.24	(a)	(a)	4
		Roll	1.6 (1.28 zero to peak)	(a)	(a)	4
Maximum aerodynamic loads	T + 79.5	Pitch	1.28	0.4	12	10
		Yaw	1.28	.3	12	9
		Roll	.4	1.25	(a)	9
Booster engine cutoff	T + 142.6	Pitch	0.64	10	1	6
		Yaw	.72	5	Until booster engine jettison	9
		Roll	1.44	.645	Until booster engine jettison	9
Booster engine jettison	T + 145.6	Pitch	0.64	0.77	1.3	(a)
		Yaw	3.84	.835	Until admit guidance	(a)
		Roll	3.44	.91	Until admit guidance	(a)
Start guidance	T + 150.2	Pitch	2.08	1.1	5	10
		Yaw	2.82	1	4.5	26
		Roll	3.68	1	5	21
Insulation panel jettison	T + 176.6	Pitch	0.48	(a)	(a)	2
		Yaw	.8	(a)	(a)	3
		Roll	1.36	4	0.9	7
Nose fairing jettison	T + 203.15	Pitch	[b]3.68	30	1.5	2
		Yaw	.48	(a)	(a)	8
		Roll	.8	5	0.5	6
Sustainer engine cutoff	T + 235.1	Pitch	0.16	(a)	(a)	(a)
		Yaw	Smooth separation			(a)
		Roll	No noticeable transients			(a)

[a]No measurable data or data of negligible magnitude.
[b]May be telemetry noise; if so, only a small rate exists.

gimbaling the booster engines. Roll open loop control was accomplished by gimbaling the booster and vernier engines. During the Atlas sustainer phase, roll open loop control was achieved by differential gimbaling of the vernier engines; pitch and yaw closed loop control was provided by gimbaling the Atlas sustainer engine.

At 42-inch (1.1-m) rise plus 1.0 second, a roll rate of 0.2 degree per second was commanded to rotate the vehicle from the azimuth of the launcher to the azimuth required for the flight trajectory. At T + 15.45 seconds, the roll program was disabled and a pitch program initiated. One of four available seasonal pitch program kits had been selected and installed months prior to launch. These programs allowed a choice in the vehicle pitch trajectory to compensate for expected seasonal differences in upper atmosphere winds. The pitch program was a timed sequence of pitch rates which were designed to control the vehicle during ascent through the atmosphere with acceptable aerodynamic heating conditions and at near zero angle of attack.

The functions performed by the Atlas flight control system to stabilize and control the vehicle were previously discussed in this section. Also discussed was the issuance of discrete commands that had a shared relation to commands issued by the guidance system. In addition to these "shared" commands, many other timed discrete commands were issued by this system.

Atlas system performance. - The flight control system performed satisfactorily throughout the Atlas phase of flight. The control corrections required because of vehicle disturbances were well within the control system capability. Table V-XV summarizes the analysis of flight disturbances. The transient response resulting from each flight event was evaluated in terms of amplitude, frequency, and duration, as observed on rate gyro data. In this table, the percent control capability is the amount of engine gimbal angle used with respect to the total engine gimbal angle capability available. The control capability shown in table V-XV (used at the time of the flight event) includes that necessary for correction of the vehicle disturbance and for steady-state requirements.

The programmer was started at 42-inch (1.1-m) rise which occurred at approximately T + 1 second. At T + 2.2 seconds, an estimated roll rate of -0.68 degree per second was sensed, indicating the roll program had been initiated. The errors in pitch and yaw were damped out by T + 3.8 seconds by using 5 percent of the control capability. The pitch program was observed to start at T + 15.45 seconds with a pitch rate of -0.56 degree per second.

The period of maximum aerodynamic forces for this flight was observed from approximately T + 76 to T + 86 seconds. Ten percent of the control capability was required to overcome both steady-state and transient loading.

The booster engines were cut off at T + 142.6 seconds. The rates imparted to the vehicle by the transients required a maximum of 9 percent of the Atlas sustainer engine gimbal capability. The Atlas booster engines were jettisoned at T + 145.6 seconds. The rates imparted by this disturbance were nearly damped out within 4 seconds.

Prior to the sustainer portion of flight, the Atlas flight control system provided the vehicle displacement reference. At T + 150.2 seconds, the Centaur guidance system was used as the displacement reference. The new displacement command resulting from the change in reference required 21 percent of the total control capability. The maximum vehicle rate during this change was a peak-to-peak roll rate of 3.68 degrees per second. It was discovered that the pitch and yaw commands of the sustainer thrust vector yielded counterclockwise additive roll torques. Although the magnitude of the roll rate of AC-7 was higher than that for previous flights, as well as for the succeeding AC-9 launch, the resulting torques due to Atlas sustainer engine thrust vectors were well within the control capability of the flight control system. The vehicle stabilized on the new reference within 5 seconds.

Insulation panels and nose fairings were jettisoned at T + 176.6 and T + 203.15 seconds, respectively. The maximum vehicle transient observed due to these disturbances was a peak-to-peak roll rate of 1.36 degrees per second. A pitch rate of 3.68 degrees per second observed at this time is believed to be telemetry noise. The maximum control capability used to overcome the jettison forces was 8 percent.

Sustainer engine cutoff occurred at T + 235.1 seconds. Atlas-Centaur separation was smooth with no noticeable transients.

Centaur system description. - The Centaur flight control system provided primary functions required for vehicle stabilization and control during Centaur powered flight, for execution of guidance steering signals, and to provide timed switching sequences for programmed flight events. A simplified block diagram of the Centaur flight control system is shown in figure V-65.

The Centaur flight control system consisted of the following principal units:

(1) The rate gyro unit contained three single-degree-of-freedom, floated, rate gyros with electronics for channel selection limiting and signal amplification. These gyros were mounted to the vehicle in an orthogonal triad configuration alining the input axis of the gyro to its respective vehicle axis of pitch, yaw, or roll.

(2) The servoamplifier unit contained the required electronics to amplify, integrate, and algebraically sum engine position feedback signals with guidance - rate-gyro-generated steering signals and the associated logic and threshold circuitry for control of the hydrogen peroxide engines.

(3) The electromechanical timer unit contained a 400-hertz synchronous motor which provided the time reference. The motor drove a mechanical arrangement of shafts and cams which activated switch contacts. The switches were used as control imputs for the auxiliary electronics unit.

(4) The auxiliary electronics unit contained logic, relay switches, transistor power switches, power supplies, and an arm-safe switch. Signals from these devices then

controlled sequencing of other subsystems. The arm-safe switch electrically isolated the pyrotechnic devices and valve actuators from control switches.

Vehicle steering during Centaur powered flight was by thrust vector control through gimbaling of the two main engines. There were two actuators for each engine to provide pitch, yaw, and roll control. Pitch control was accomplished by moving both engines in the pitch plane. Yaw control was accomplished by moving both engines in the yaw plane, and roll control was accomplished by differentially moving the engines in the yaw plane. Thus, the yaw actuator responded to an algebraically summed yaw-roll command. By controlling the direction of thrust of the main engines, the flight control system maintained the flight of the vehicle on a trajectory directed by the guidance system.

After main engine cutoff, control of the vehicle was maintained by the flight control system by using selected constant thrust hydrogen peroxide engines in an "on-off" mode of operation. This was accomplished by logic circuitry within the flight control system responding to rate and displacement signals.

The functions performed by the Centaur flight control system to stabilize and control the vehicle were previously discussed in this section. Also, discussed was the issuance of discrete commands that had a shared relation to commands issued by the guidance system. In addition to these "shared" commands many other timed discrete commands were issued.

Centaur system performance. - The Centaur flight control system performance was satisfactory throughout the flight. Vehicle stabilization and control were maintained at all times, and all flight programmer discrete events were executed at the required times.

The Centaur programmer was started at Atlas sustainer engine cutoff (T + 235.1 sec) by a discrete from the Atlas programmer. Appropriate commands were issued for pressurizing the hydrogen tank, centering the Centaur engines, engine prestart, chilldown, and main engine start. Vehicle rates sensed in pitch, yaw, and roll were mild during staging and did not exceed 1.5 degrees per second.

Main engine start was commanded at T + 246.58 seconds. Rates due to engine start transients were not greater than 3.00 degrees per second and were corrected by gimbaling the engines less than 1°. When guidance steering was admitted to the Centaur flight control system 4 seconds after engine start, the vehicle attitude was 4.0° nose high and 3.0° nose right of the desired steering vector. This difference was corrected within 4 seconds.

Vehicle steady-state rates during Centaur main engine firing were essentially zero in yaw and roll. Pitch rates in response to closed loop control did not exceed 0.20 degree per second. Approximately 60 seconds prior to engine cutoff, the pitchdown rate decreased as the vehicle approached the desired orbital injection conditions, and the guidance velocity-to-be-gained terms approached zero.

Rates imparted to the vehicle due to engine cutoff transients were mild, indicating a small differential impulse. Maximum disturbance rate was 0.95 degree per second in roll. Coincident with main engine cutoff, closed loop control was terminated. The hydrogen peroxide attitude control system was activated and the engines fired only if vehicle rates exceeded 0.2 degree per second. Vehicle disturbances were almost negligible and the hydrogen peroxide attitude control engines fired only 3 percent of the time.

After Centaur main engine cutoff, the programmer issued commands to prepare the spacecraft for separation, and all required commands were issued properly. At T + 752.58 seconds, the hydrogen peroxide attitude control system was deactivated for 5 seconds and the spacecraft was successfully separated from Centaur. The hydrogen peroxide attitude control system was deactivated during this time to preclude collision of the Centaur vehicle with the spacecraft.

The retromaneuver was initiated at T + 757.7 seconds when the Centaur was commanded to turn approximately 180° to the negative of the injection guidance steering vector. Simultaneously, the attitude control system was activated and began a nose-up, nose-right maneuver toward the new vector. Approximately half way (90°) through the turnaround, two of the 50-pound- (222.4-N-) thrust hydrogen peroxide attitude control engines were commanded to fire to provide 100 pounds (444 N) thrust for 20 seconds, as planned. Guidance gimbal resolver data indicated that the vehicle turned through a total angle of 157° in approximately 102 seconds to the new vector. The total angle and the turnaround time were within the expected dispersions.

At T + 992.6 seconds, the engine prestart valves were opened to allow the residual propellant to blow down through the main engines. Coincident with the start of this blowdown, the engine thrust chambers were gimbaled to aline the thrust vector through the vehicle center of gravity. Thrust from the propellant blowdown provided adequate separation distance between the Centaur stage and the Surveyor spacecraft. Separation distance at the end of 5 hours was 395 nautical miles (730 km). Required separation after 5 hours was greater than 182 nautical miles (336 km) to prevent the Surveyor star sensor from acquiring the reflected light of Centaur rather than the star Canopus.

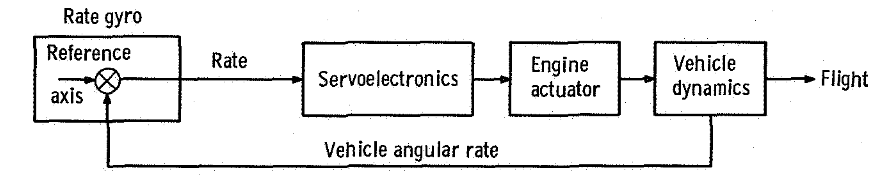

(a) Rate stabilization.

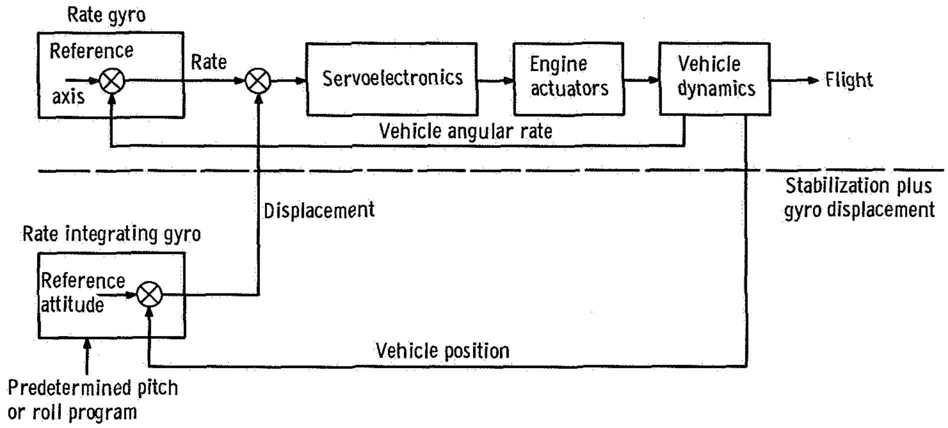

(b) Open loop control.

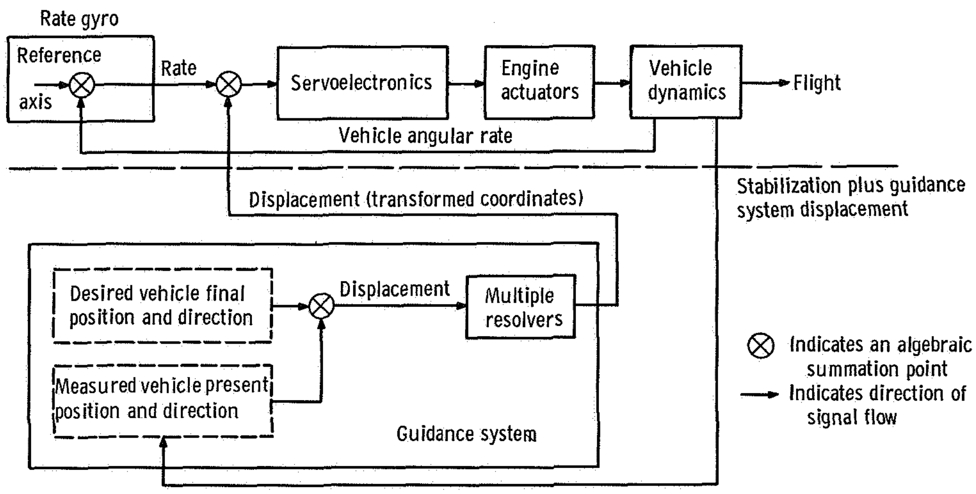

(c) Closed loop control.

Figure V-60. - Guidance and flight control modes of operation, AC-7.

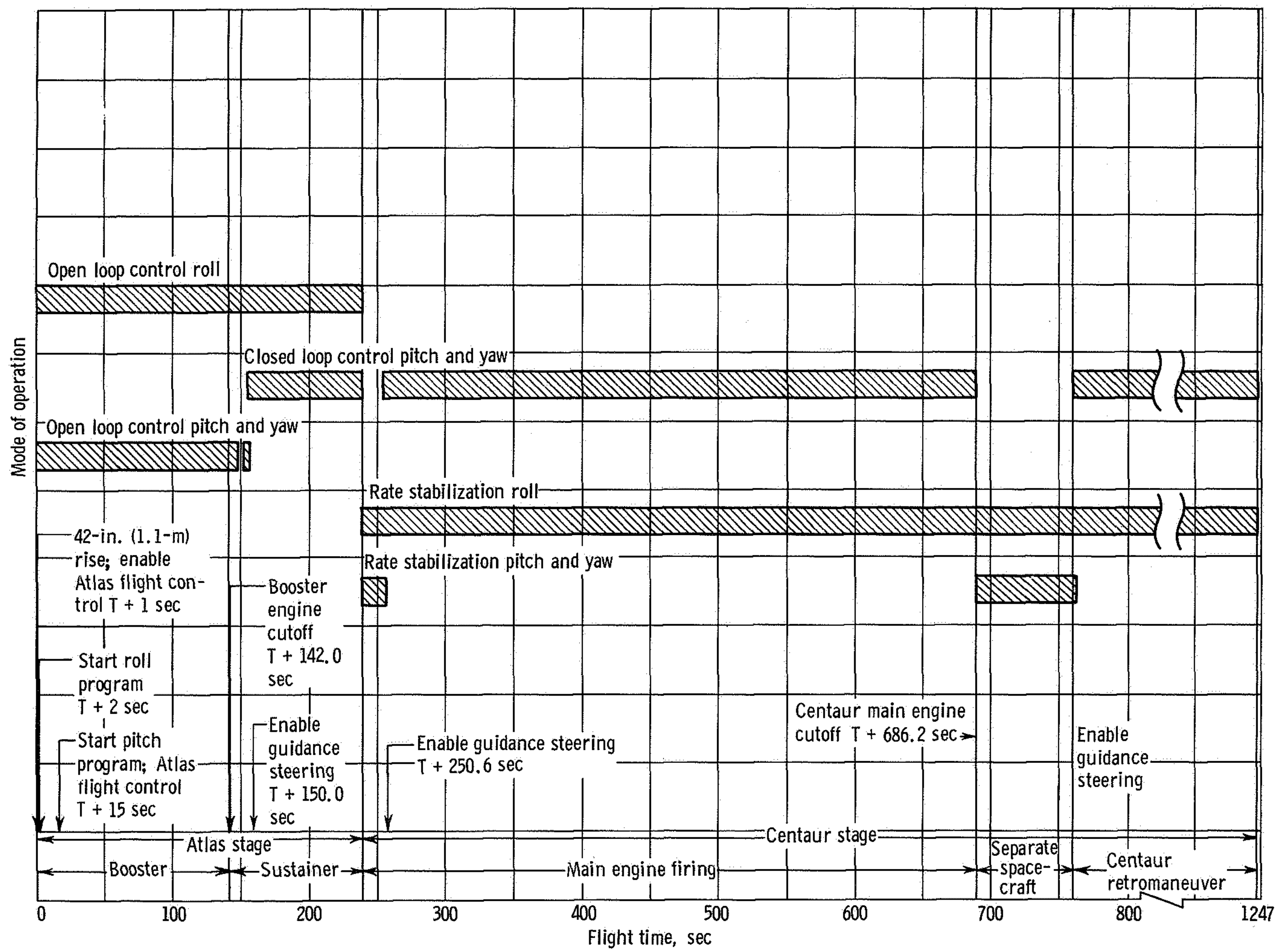

Figure V-61. - Guidance and flight control modes of operation, AC-7.

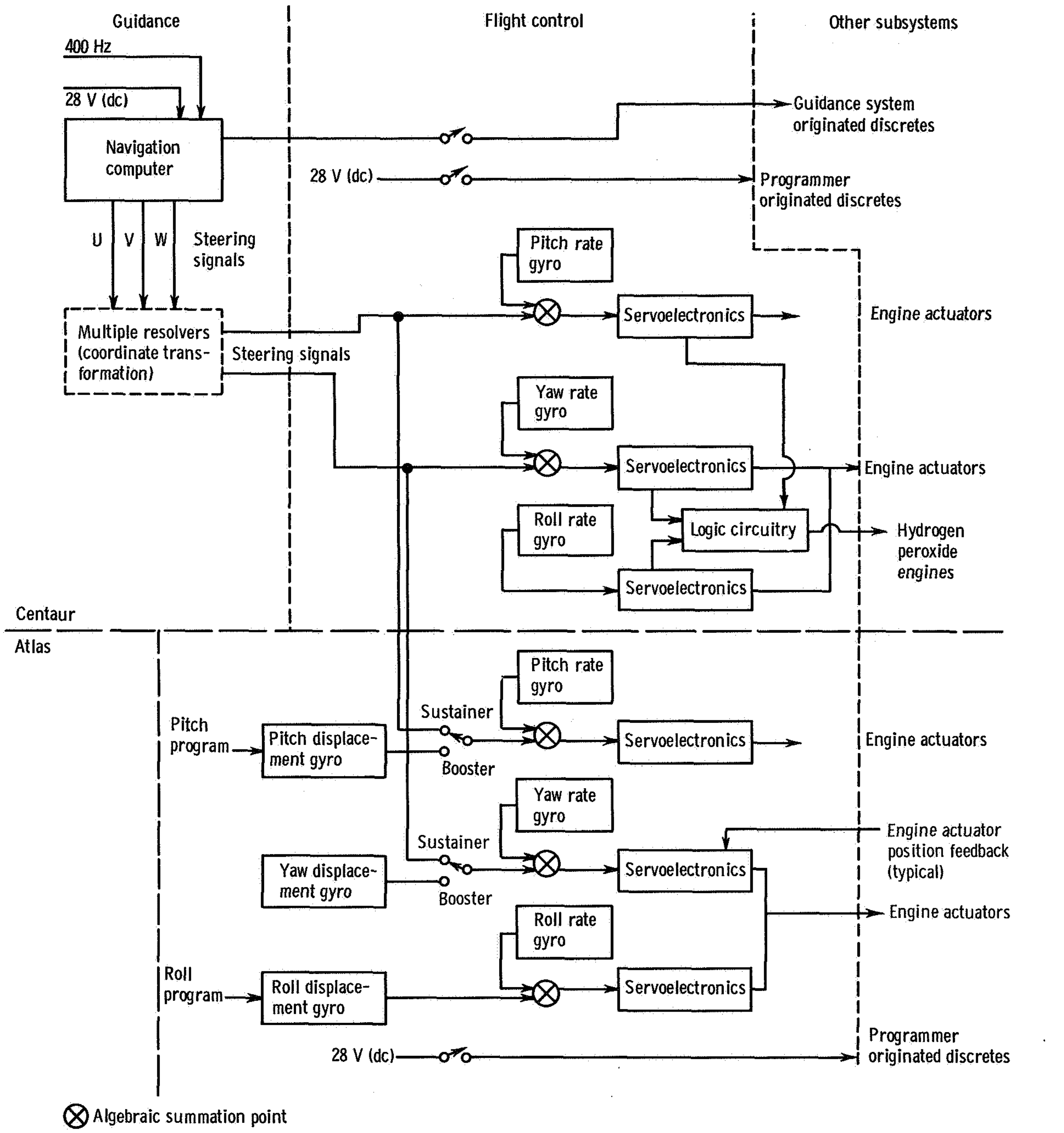

Figure V-62. - Simplified guidance and flight control systems interface, AC-7.

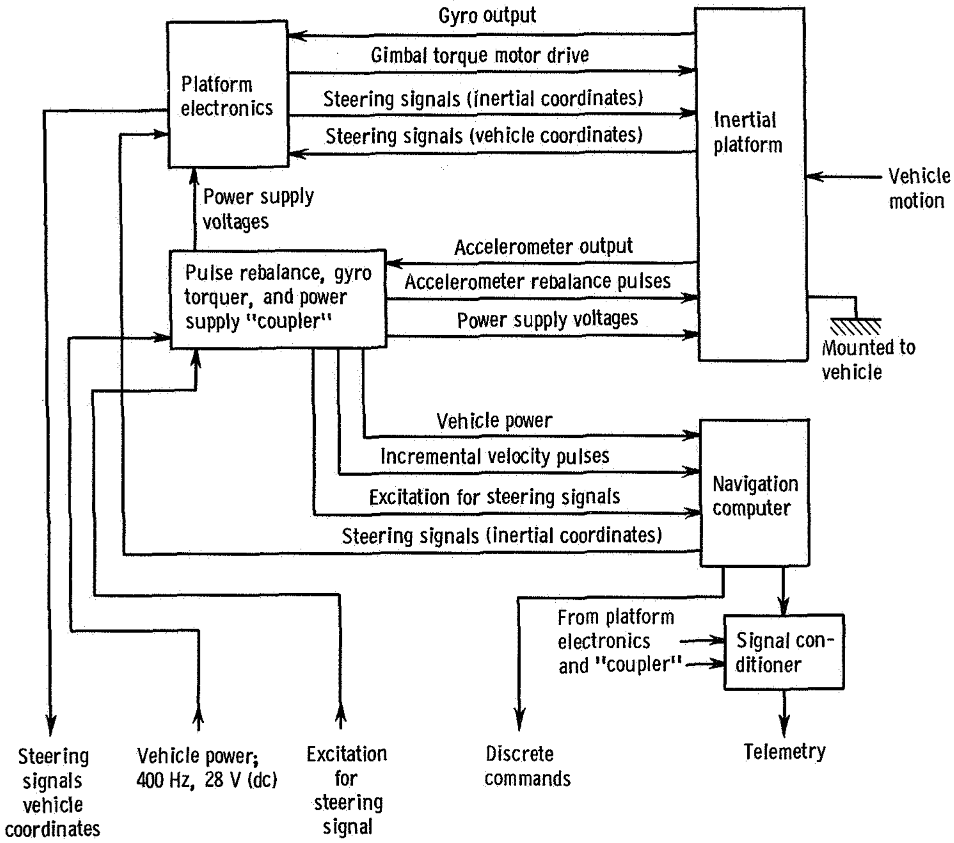

Figure V-63. - Simplified block diagram of Centaur guidance system, AC-7.

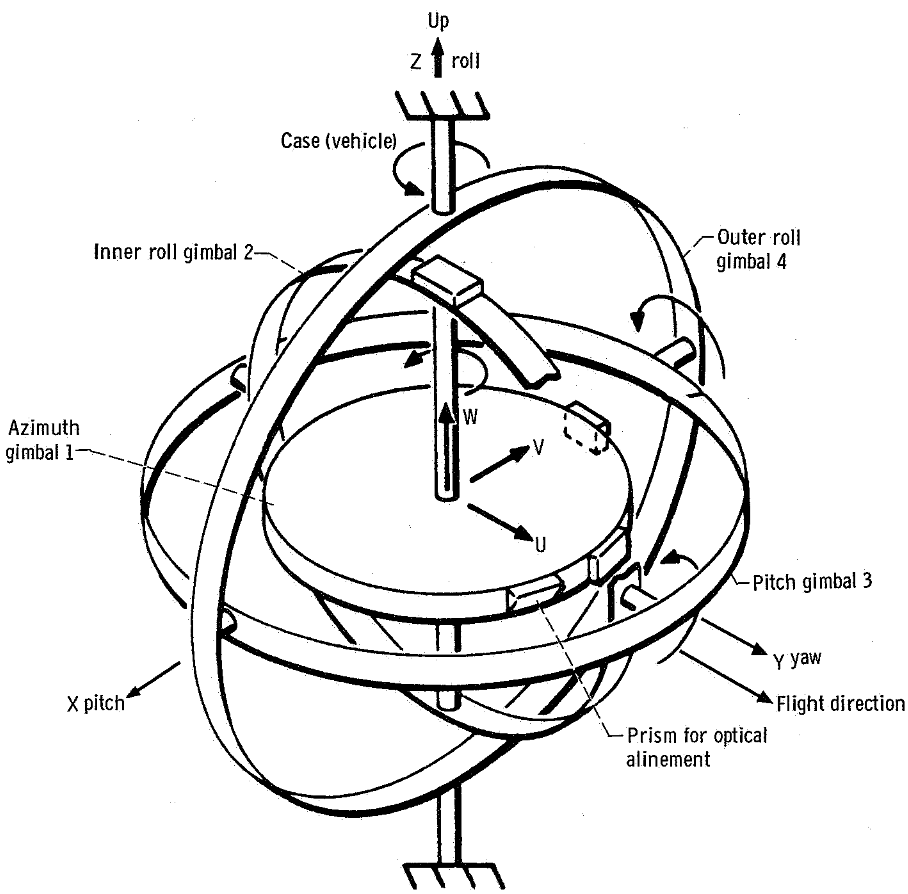

Figure V-64. - Gimbal diagram, AC-7. Launch orientation: inertial platform coordinates, U, V, and W; vehicle coordinates, X, Y, and Z.

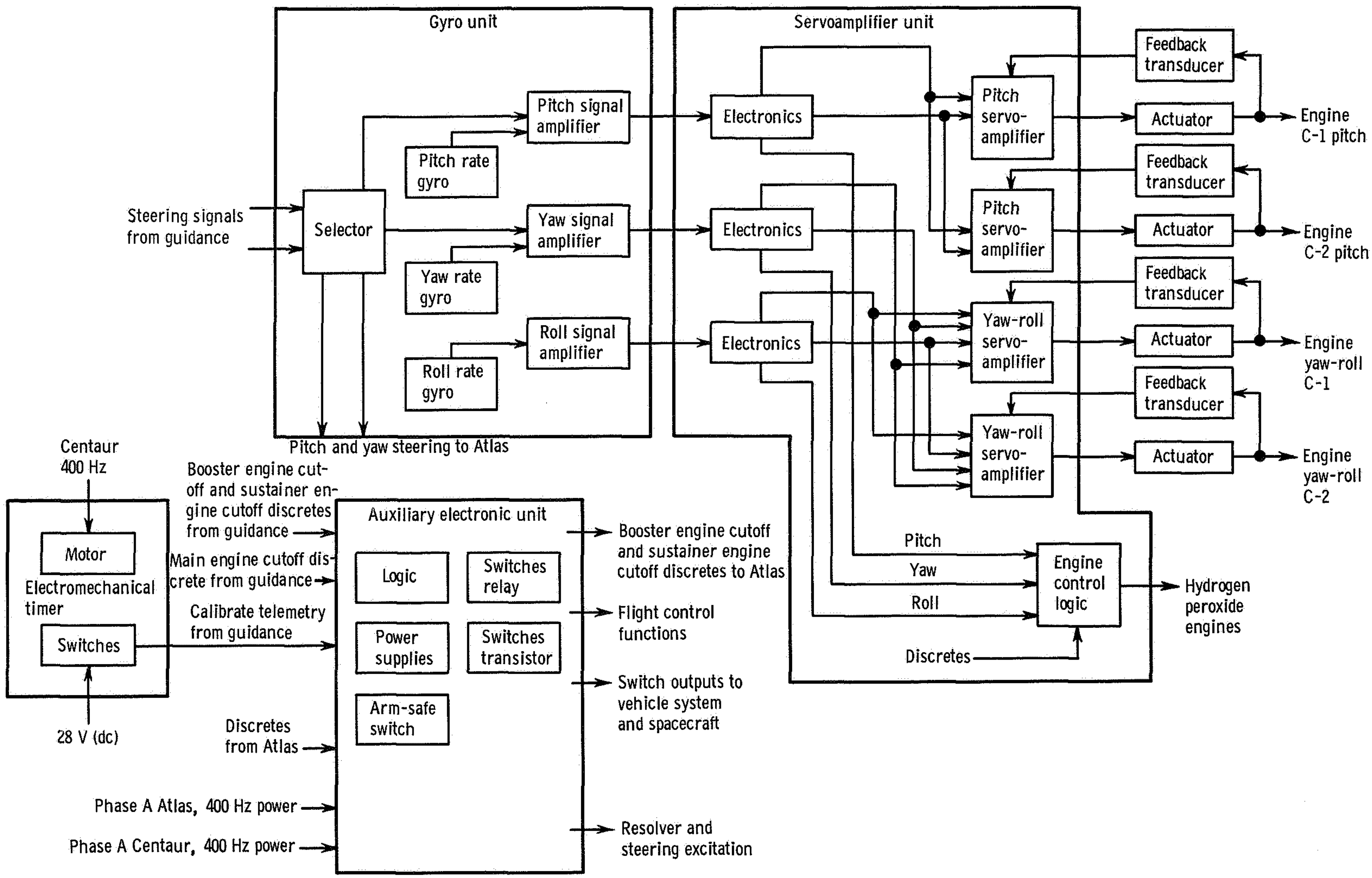

Figure V-65. - Centaur flight control system, AC-7.

VI. CONCLUDING REMARKS

The Atlas-Centaur AC-7 launch operation was completely successful in supporting the Surveyor II mission. The launch vehicle inserted the Surveyor into a highly accurate lunar transfer orbit that would have required a midcourse correction of only 3.9 feet per second (1.20 m/sec) for miss plus time of flight to impact the designed landing site on the Moon.

The launch vehicle lift-off occurred during the last minute of a 32-minute window on September 20, the first day of the September 1966 launch opportunity. All launch vehicle systems performed satisfactorily and within the specifications for a normal direct-ascent (one-burn) mission.

Lewis Research Center,
National Aeronautics and Space Administration,
Cleveland, Ohio, October 31, 1967,
491-05-00-02-22.

PRECEDING PAGE BLANK NOT FILMED.

APPENDIX A

SUPPLEMENTAL FLIGHT, TRAJECTORY, AND PERFORMANCE DATA

by John J. Nieberding

The postflight weight summary for the Atlas-Centaur vehicle AC-7 with the Surveyor spacecraft SC-2 is given in tables A-I and A-II.

TABLE A-I. - POSTFLIGHT ATLAS STAGE WEIGHT SUMMARY, AC-7

	Weight	
	lb	kg
Booster jettison:		
Booster dry	6 197	2 811
Booster residuals	1 117	507
Unburned lubrication oil	29	13
Total	7 343	3 331
Sustainer jettison:		
Sustainer dry	5 593	2 537
Sustainer residuals	1 620	735
Interstage adapter	1 036	470
Unburned lubrication oil	17	8
Total	8 266	3 750
Ground expendables:		
Fuel, RP-1	545	247
Oxidizer, liquid oxygen	1 720	780
Lubrication oil	3	1
Exterior ice	50	23
Liquid nitrogen in helium shrouds	140	63
Preignition gaseous oxygen loss	450	204
Total	2 908	1 318
Flight expendables:		
Main impulse RP-1	75 327	34 168
Main impulse oxygen	171 795	77 926
Helium panel purge	6	3
Oxidizer vent loss	15	7
Lubrication oil	173	78
Total	247 316	112 182
Total Atlas weight at lift-off:		
Booster jettison	7 343	3 331
Sustainer jettison	8 266	3 750
Flight expendables	247 316	112 182
Total	262 925	119 263

TABLE A-II. - POSTFLIGHT CENTAUR STAGE WEIGHT SUMMARY, AC-7

	Weight	
	lb	kg
Basic hardware:		
Body group	969	439
Propulsion group	1 197	543
Guidance group	313	142
Control group	140	63
Pressurization group	137	62
Electrical group	264	120
Separation equipment	81	37
Flight instrumentation	279	127
Miscellaneous equipment	135	61
Total	3 515	1 594
Centaur flight expendables:		
Main impulse hydrogen	4 992	2 264
Main impulse oxygen	24 953	11 318
In-flight chilldown hydrogen	23	10
In-flight chilldown oxygen	42	19
Booster phase vent hydrogen	40	18
Booster phase vent oxygen	80	36
Sustainer phase vent hydrogen	18	8
Sustainer phase vent oxygen	30	14
Hydrogen peroxide, boost pumps	49	22
Helium, tank pressurization	1	.5
Total	30 228	13 709
Jettisonable hardware:		
Nose fairing	1 966	892
Insulation panels	1 207	547
Ablated ice	50	23
Total	3 223	1 462

	Weight	
	lb	kg
Centaur residuals:		
Liquid hydrogen, trapped	66	30
Liquid oxygen, trapped	68	31
Liquid hydrogen, burnable	63	29
Liquid oxygen, burnable	172	78
Gaseous hydrogen	75	34
Gaseous oxygen	167	76
Hydrogen peroxide, retromaneuver	27	12
Hydrogen peroxide, trapped	5	2
Hydrogen peroxide reserve	52	24
Helium	4	2
Ice	12	5
Total	711	323
Ground expendables:		
Hydrogen gas, ground boiloff	28	13
Oxygen gas, ground boiloff	26	12
Total	54	25
Total Centaur weight at lift-off:		
Basic hardware	3 515	1 594
Centaur residuals	711	322
Centaur flight expendables	30 228	13 711
Jettisonable hardware	3 223	1 462
Total	37 677	17 089
Combined launch vehicle lift-off weight:		
Atlas	262 925	119 263
Centaur	37 677	17 089
Spacecraft	2 204	999
Total	302 806	137 351

ATMOSPHERIC SOUNDING DATA

Ambient Temperature and Pressure

The atmospheric conditions at the launch site were determined on the day of launch at approximately 0735 hours eastern standard time. Profiles of measured temperature and pressure are compared with the values predicted on the basis of seasonal September weather. Temperature data, as shown in figure A-1, were nearly normal at all altitudes with the exception of the region between approximately 7.3 and 12.5 nautical miles (13.5 and 23.2 km). Even at these altitudes the maximum temperature variation did not exceed 8° R (4.5° K). The measured pressures in figure A-2 were in relatively close agreement with the predicted values at all altitudes.

Atmospheric Winds

Wind speed and azimuth data as a function of altitude are compared with the seasonal September wind data in figures A-3 and A-4, respectively. Wind azimuth is the direction in which the wind is blowing. Although a discrepancy existed between the magnitudes of the predicted and measured wind speeds at all altitudes up to approximately 9 nautical miles (16.6 km), the basic characteristics of the two curves in this region are similar. Figure A-4 shows that predicted and actual wind azimuths agreed reasonably well in altitude intervals between 3 and 8 nautical miles (5.5 and 14.8 km) and 13 and 17 nautical miles (24.0 and 31.5 km). Below approximately 3 nautical miles (5.5 km), the actual azimuth averaged about 280° greater than expected. At other altitudes the agreement was erratic.

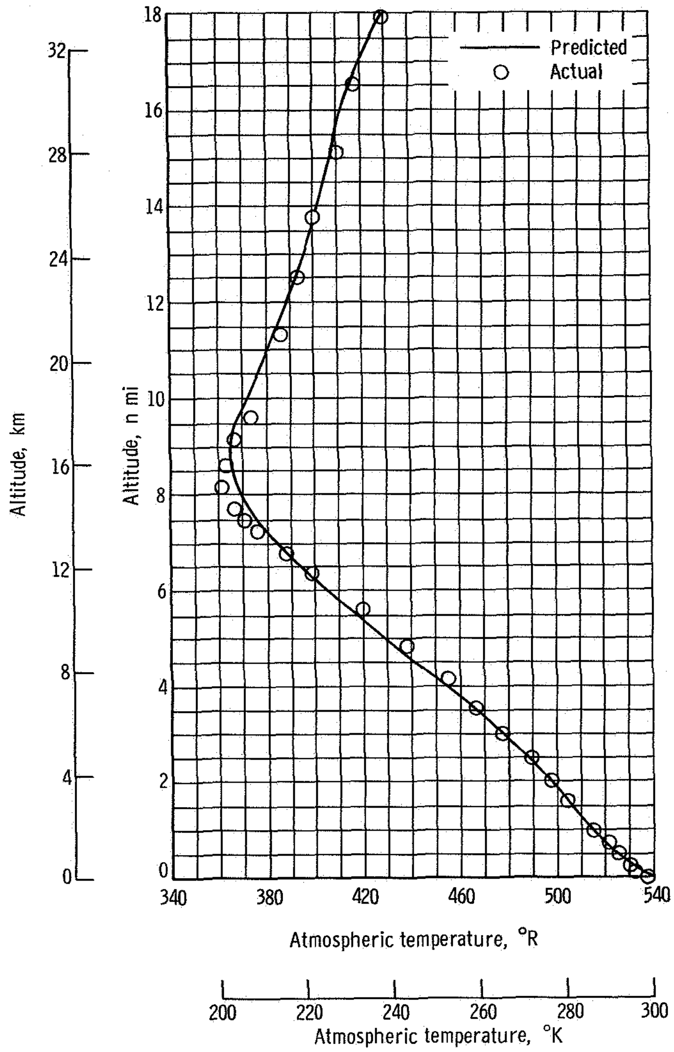

Figure A-1. - Altitude as function of temperature, AC-7.

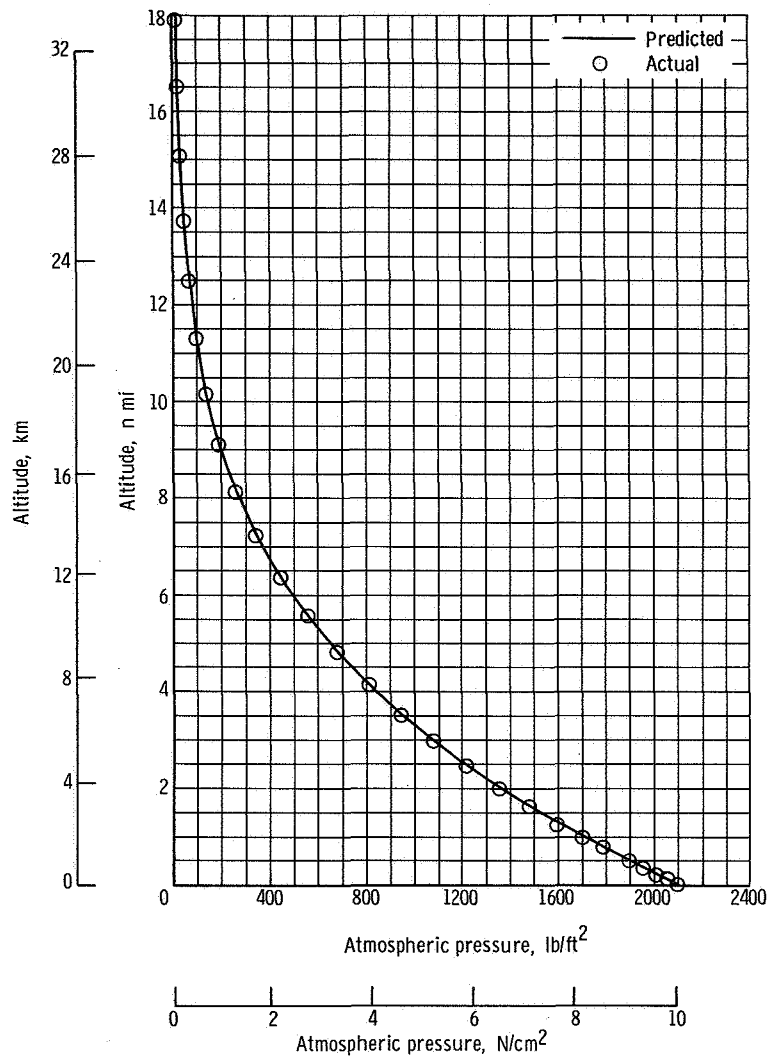

Figure A-2. - Altitude as function of pressure, AC-7.

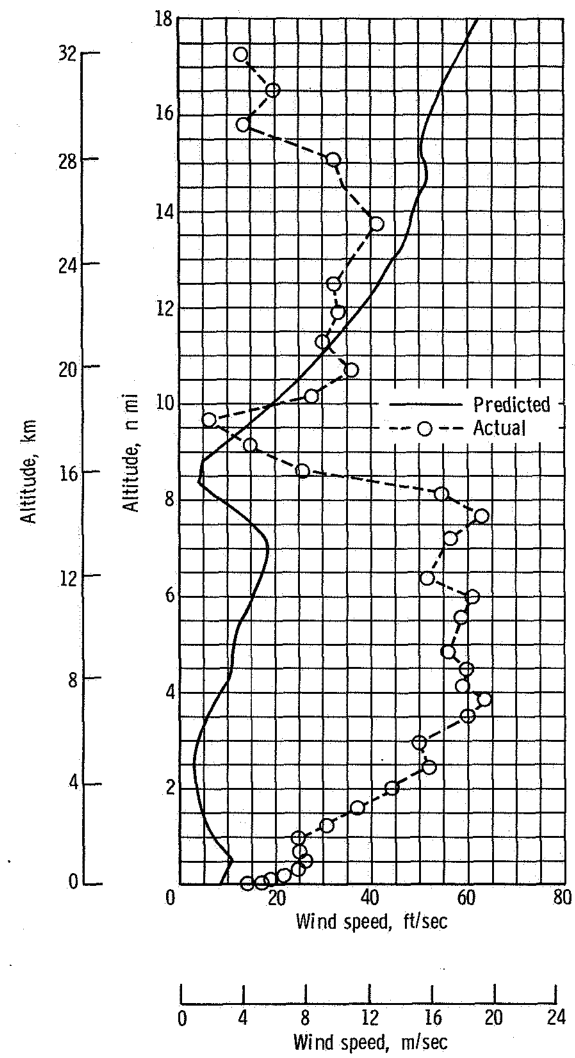

Figure A-3. - Altitude as function of wind speed, AC-7.

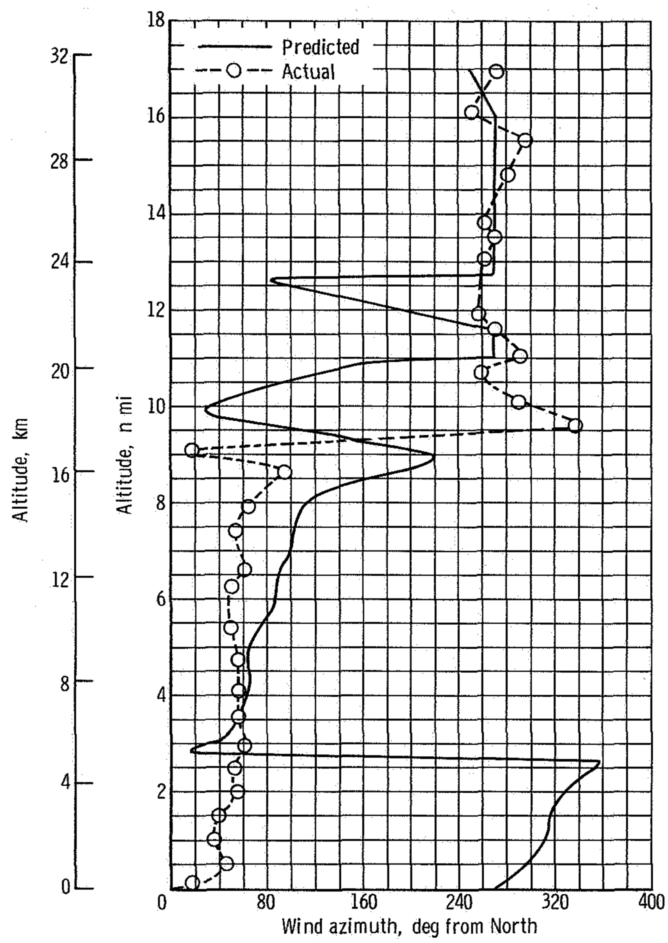

Figure A-4. - Altitude as function of wind direction, AC-7.

TRAJECTORY DATA

Dynamic Pressure and Mach Number

Dynamic pressure and Mach number data for AC-7 are presented in figures A-5 and A-6, respectively. These data were calculated from range tracking data and atmospheric sounding data taken at the time of launch. The agreement between actual and preflight values of dynamic pressure was good until approximately T + 72 seconds. From T + 72 to T + 84 seconds, the agreement was erratic. A peak value of 820 pounds per square foot (3.93 N/cm^2) was predicted at T + 76 seconds. But an actual peak of 854 pounds per square foot (4.09 N/cm^2) was measured at T + 78 seconds. Thus, the predicted and actual maximum values occurred only 2 seconds apart; they differed by approximately 34 pounds per square foot (0.163 N/cm^2).

At any one time, the maximum deviation of actual from predicted values was 50 pounds per square foot (0.239 N/cm^2) at T + 84 seconds. Even this maximum deviation represented an error of less than 1 percent. Every actual data point which disagreed with the value predicted at that time can be precisely correlated with this predicted value if known dispersions in ambient temperature and pressure and vehicle relative velocity (air speed) are considered. Deviations of actual from predicted values of these three parameters completely explain all dynamic pressure dispersions. Although no one parameter was predominantly responsible for the dispersions between T + 72 and T + 84 seconds, beyond T + 84 seconds, the consistently low dynamic pressures were caused by slightly lower than expected ambient pressures. These lower pressures resulted from a steeper than expected altitude against time profile from T - 0 to approximately T + 500 seconds (fig. A-9). Variation of the actual Mach number values from the expected values was negligible over the entire time interval shown in figure A-6. The decrease in acceleration at T + 142.6 seconds, as indicated by the decrease in slope at this time, was caused by the loss of the booster thrust at booster engine cutoff.

Axial Load Factor

The axial load factor for the Atlas and Centaur powered phases of flight is shown in figure A-7. A plot of the axial load factor is equivalent to a plot of the thrust acceleration in g's. Actual and predicted data showed good agreement. The maximum deviation occurred at T + 670 seconds when the actual value was approximately 2.5 percent lower than predicted. A flattening of the curve occurs from approximately T + 52 to T + 60 seconds. This interval of constant acceleration reflects the severe vehicle perturbations experienced when the vehicle approached and surpassed Mach 1 (see fig. A-6). An abrupt decrease in acceleration from 5.65 to 1.16 g's occurred, as expected, at booster engine cutoff. After booster jettison 3.0 seconds later, the acceleration increased steadily, except for small perturbations caused by sudden weight losses at insulation panel and nose fairing jettison, until sustainer engine cutoff at T + 235.1 seconds. After the Centaur main engines started, the uniformly decreasing Centaur weight caused the axial load factor to again increase smoothly until termination of the Centaur burn at T + 686.2 seconds.

Inertial Velocity

Inertial velocity data for the flight are presented in figure A-8. The predicted and actual results were in good agreement. As expected, abrupt changes in the vehicle total acceleration, the slope of the inertial velocity curve, coincided with the sharp changes in thrust acceleration (axial load factor, see fig. A-7). The slightly low values of axial load factor during the latter part of the Centaur burn are reflected in the lower than predicted inertial velocities during the same period. The maximum velocity deviation occurred at approximately T + 670 seconds when the actual velocity was about 311 feet per second (102 m/sec) lower than predicted. By Centaur main engine cutoff, T + 686.2 seconds, the actual velocity was only 78 feet per second (25.6 m/sec) low. Because the actual and preflight altitudes were in good agreement at this time (fig. A-9), this close velocity agreement was necessary to ensure that the vehicle attained the proper mission energy for the lunar transfer trajectory.

Altitude and Range Tracking Data

Altitude and ground range data are shown in figures A-9 and A-10, respectively. The ground trace of the vehicle subpoint, latitude against longitude, is given in figure A-11. Agreement between actual and preflight values of altitude was good until about T + 150 seconds and beyond T + 550 seconds. In the interval between, the actual altitudes were slightly greater than predicted. The maximum deviation was approximately 2 nautical miles (3.7 km) at about T + 300 seconds. Injection into the elliptical orbit occurred at T + 686.2 seconds at an altitude of approximately 144 nautical miles (266 km). This injection altitude was approximately only 1 nautical mile (1.85 km) lower than predicted. Figure A-9 shows that the vehicle was climbing at injection. This result was expected since the injection true anomaly was positive (see table A-III). The absence of significant altitude lofting before injection that is characteristic of negative injection true anomalies can also be seen. The plots of altitude against ground range and latitude against longitude show good agreement between actual and predicted flight results at all times.

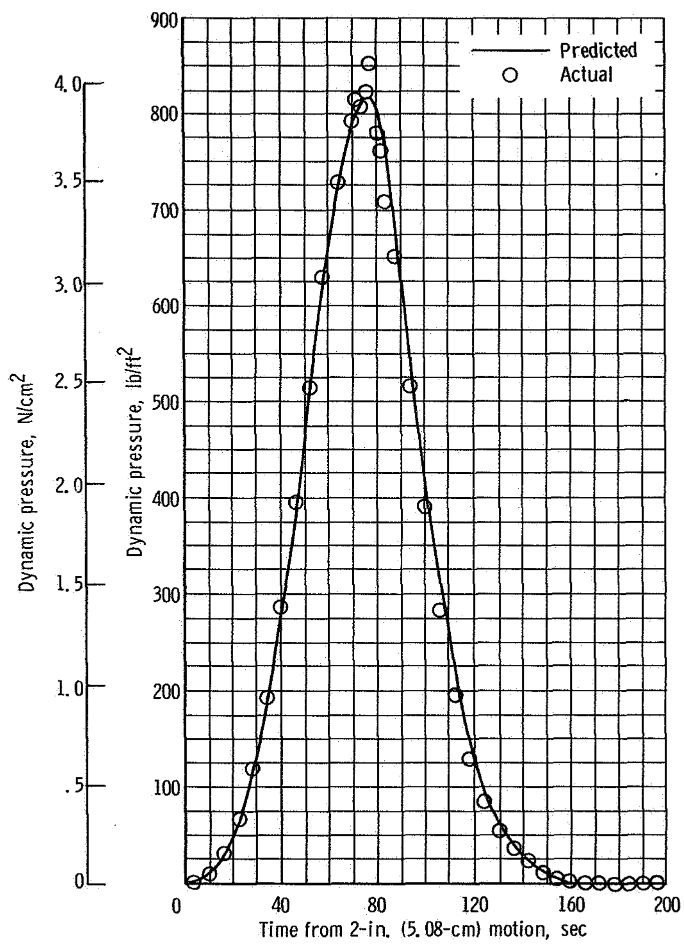

Figure A-5. - Dynamic pressure as function of time, AC-7.

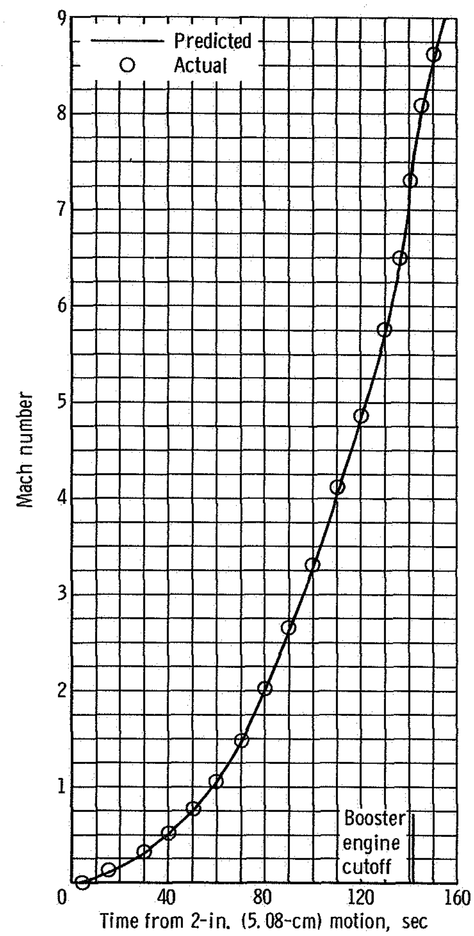

Figure A-6. - Mach number as function of time, AC-7.

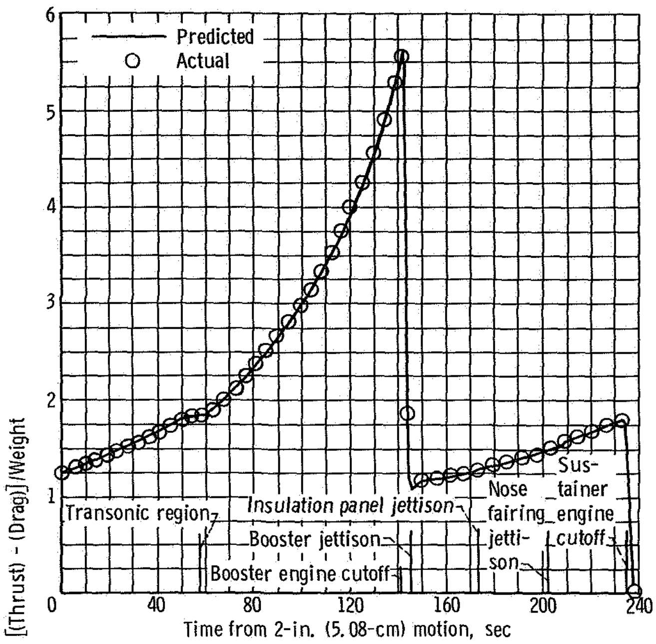

(a) Time, 0 to 240 seconds.

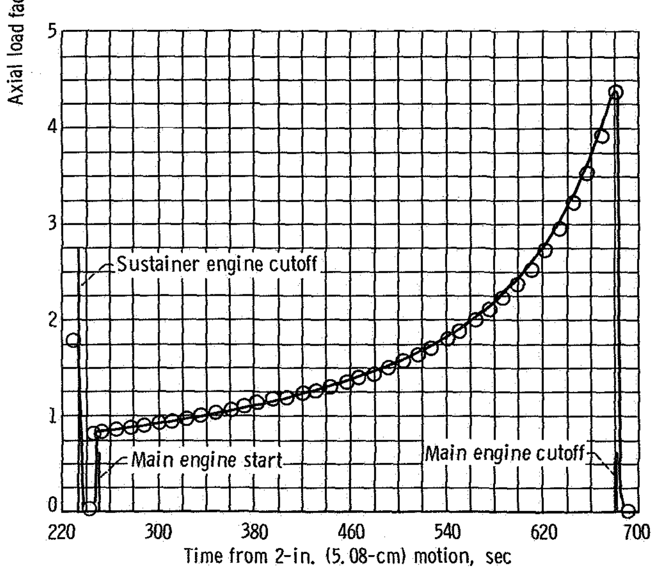

(b) Time, 220 to 700 seconds.

Figure A-7. - Axial load factor as function of time, AC-7.

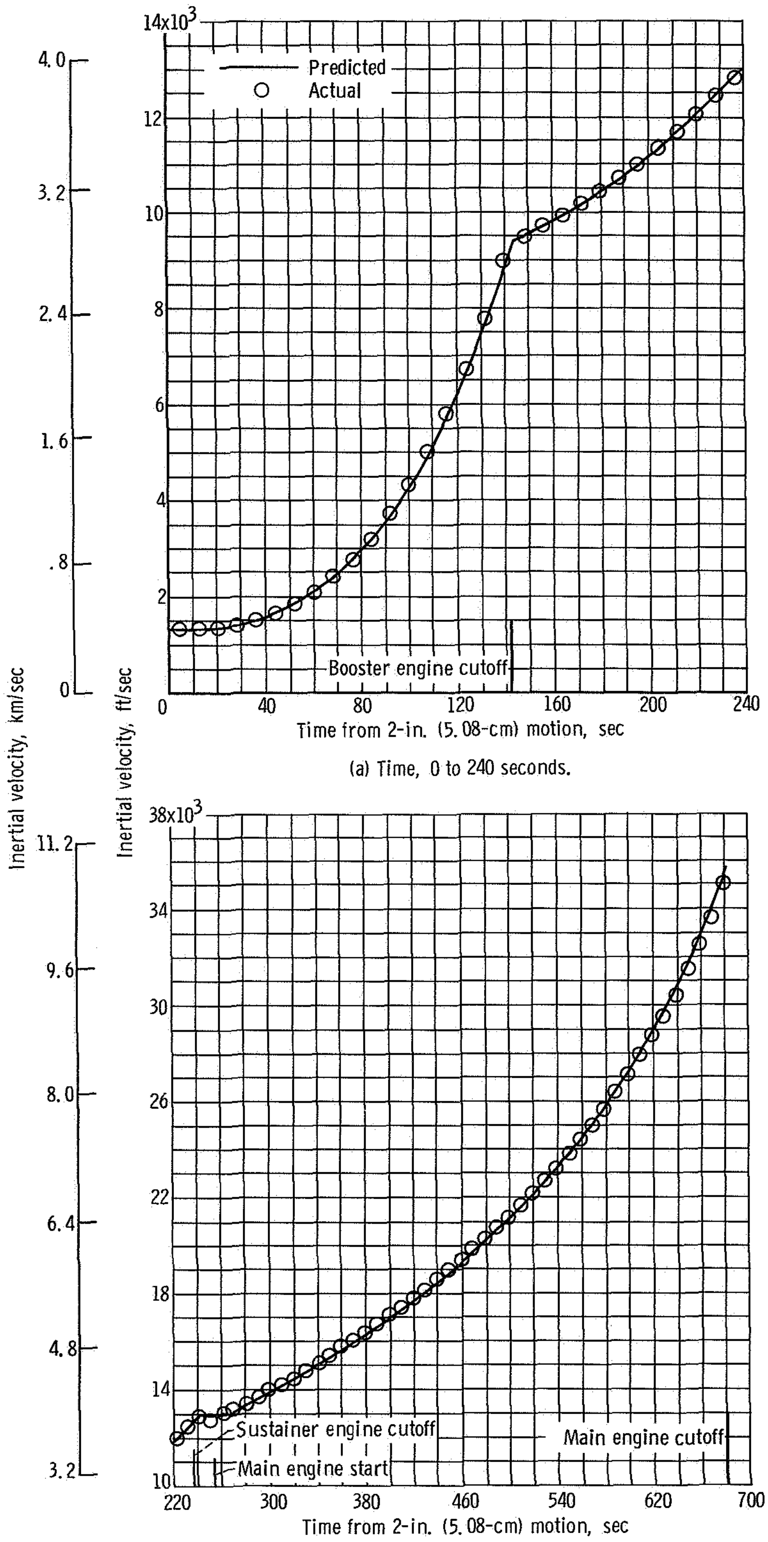

(a) Time, 0 to 240 seconds.

(b) Time, 220 to 700 seconds.

Figure A-8. - Inertial velocity as function of time, AC-7.

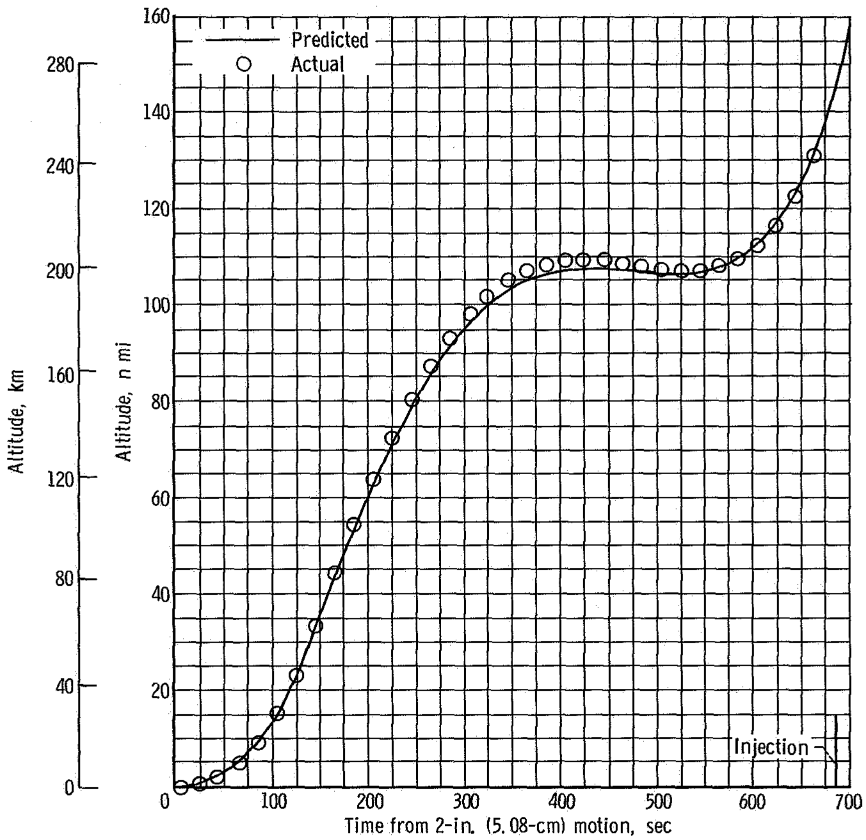

Figure A-9. - Altitude as function of time, AC-7.

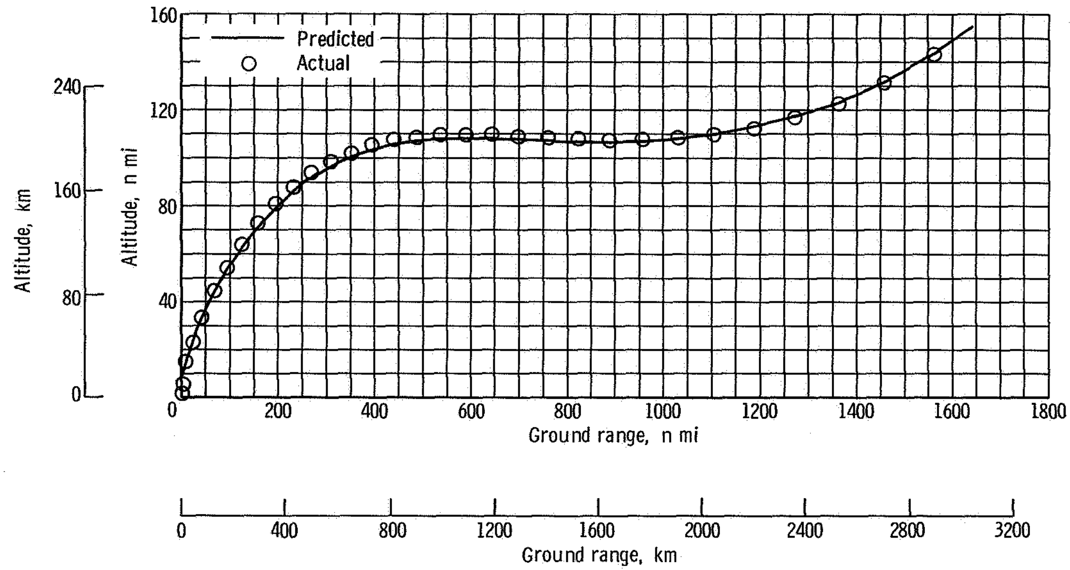

Figure A-10. - Altitude as function of ground range, AC-7.

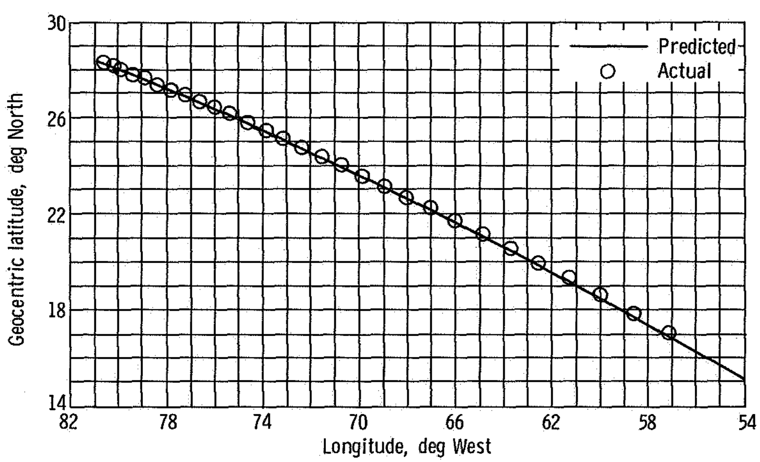

Figure A-11. - Ground trace of vehicle subpoint, AC-7.

Orbital Parameters

Centaur and Surveyor orbital parameters are given in table A-III. Centaur data are based on a reference time which occurred after the Centaur retromaneuver. Surveyor data represent a best estimate based on telemetered data at approximately 12.3 seconds before Centaur main engine cutoff. The word "injection" refers to Centaur main engine cutoff.

TABLE A-III. - ORBITAL PARAMETERS

Parameter	Centaur	Surveyor
Time from 2-in. (5.08-cm) motion, sec	1759.8	673.9
Greenwich mean time, hr	1301:2 (Sept. 20)	1243:13.7 (Sept. 20)
Apogee altitude, n mi; km	318 374; 588 992	423 324; 784 170
Perigee altitude, n mi; km	91; 168	89.2; 165.0
Injection energy, C_3, km^2/sec^2	-1.32301	-1.000138
Semimajor axis, n mi; km	162 680; 300 958	215 435; 398 546
Eccentricity	0.978250	0.983582
Orbital inclination, deg	33.45176	33.423575
Injection true anomaly, deg	13.038211	13.039233
Injection flight path angle, deg	7.36	7.36
Period, days	19.1	29.1
Longitude of ascending node, deg	340.29300	340.26840
Argument of perigee, deg	135.71733	135.66564
Inertial velocity at injection, ft/sec; m/sec	35 857; 10 936	35 857; 10 936
Earth relative velocity at injection, ft/sec; m/sec	34 549; 10 530	34 549; 10 530
Geocentric latitude at injection, deg North	16.05	16.05
Longitude at injection, deg West	55.40	55.40

SURVEYOR LAUNCH WINDOWS

September 1966 launch opportunities for the AC-7 flight are shown in table A-IV. These launch windows are based on vehicle performance and on the requirement for 60 seconds of tracking after main engine cutoff. The vehicle was launched at 1231:59.8 Greenwich mean time on September 20, 1966. The lift-off occurred during the last minute of the window. Prior to lift-off, difficulty with the liquid oxygen boiloff valve caused a 26-minute hold (see PNEUMATIC SYSTEMS, p. 53).

TABLE A-IV. - SEPTEMBER 1966 LAUNCH WINDOWS

Date	Opening time[a], hr	Opening azimuth, deg	Closing time[a], hr	Closing azimuth, deg	Window length, min
September 20	1200	96.104	1232	114.361	32
September 21	1224	98.934	1303	114.984	39
September 22	1258	105.226	1325	114.843	27
September 23	1343	113.214	1349	114.997	6

[a]Greenwich mean time.

FLIGHT EVENTS RECORD

The major flight events during the AC-7 flight are presented in table A-V. Actual times listed are the measured times of the given flight events. Programmer times, when given, are for those flight events sequenced and commanded by an in-flight timer. Timers for given sequences are enabled either at BECO or SECO:

Booster engine cutoff (BECO): guidance cutoff command when vehicle acceleration reaches 5.7±0.08 g's; start timer for sequencing Centaur insulation panel and nose fairing jettison, start Centaur boost pumps, and pressurize oxidizer tank

Sustainer engine cutoff (SECO): burnable fuel depletion cutoff command; start timer for Centaur main engine start, spacecraft separation, and Centaur retromaneuver sequences

Centaur main engine start (MES)

Centaur main engine cutoff (MECO): guidance cutoff command when vehicle attains orbital injection energy

TABLE A-V. - FLIGHT EVENTS RECORD, AC-7

Event	Programmer time, sec	Actual time, sec
Guidance flight mode acceptance	--------------	T - 8.5
Programmer start; 2-in. (5.08-cm) rise	--------------	T + 0
Initiate roll program	--------------	T + 2.0
Initiate pitch program	--------------	T + 15.2
Unlock liquid hydrogen vent valve	--------------	T + 68.8
Booster engine cutoff (BECO)	BECO	T + 142.6
Jettison booster engines	BECO + 3.1	T + 145.6
Jettison insulation panels	BECO + 34	T + 176.6
Unlatch nose fairing	BECO + 60.5	T + 202.4
Fire thrustor bottles	BECO + 61	T + 202.9
Start Centaur boost pumps	BECO + 62	T + 204.2
Sustainer engine cutoff; vernier engine cutoff; start Centaur programmer (SECO/VECO)	SECO	T + 235.1
Start hydraulic recirculating pump	SECO + 0.5	T + 235.6
Separate (first and second stage)	SECO + 1.9	T + 237.1
Prestart	SECO + 3.5	T + 238.6
Centaur main engine start (MES)	SECO + 11.5	T + 246.6
Centaur main engine cutoff (MECO)	MECO	T + 686.2
Preseparation arming signal; extend landing gear	SECO + 475.5	T + 710.3
Unlock omniantennas	SECO + 486.0	T + 720.2
High power transmitter on	SECO + 506.5	T + 736.2
Electrical disconnect	SECO + 512	T + 747.1
Spacecraft separation	SECO + 517.5	T + 752.6
Begin Centaur reorientation maneuver	SECO + 522.5	T + 757.7
Start Centaur lateral thrust	SECO + 562.5	T + 797.7
End Centaur lateral thrust	SECO + 582.5	T + 817.6
Start Centaur tank discharge	SECO + 757.5	T + 992.6
End Centaur tank discharge	SECO + 1007.5	T + 1242.6
Energize power changeover	SECO + 1007.5	T + 1242.6

PRECEDING PAGE BLANK NOT FILMED.

APPENDIX B

CENTAUR ENGINE PERFORMANCE CALCULATIONS

by William A. Groesbeck, Ronald W. Ruedele, and John J. Nieberding

SUMMARY

Flight values of engine thrust, engine specific impulse, and oxidizer to fuel mixture ratio were calculated by using the Pratt & Whitney characteristic velocity (C*) iteration and the Pratt & Whitney regression methods. In addition, vehicle specific impulse was calculated by the guidance thrust velocity method. The Pratt & Whitney techniques calculate individual engine performance at discrete times. In contrast, the guidance thrust velocity method calculates average vehicle performance over an interval of time. The engine specific impulse, calculated by the C* method, was approximately 437 seconds. The average vehicle specific impulse, calculated by the guidance thrust velocity method, was approximately 432.5 seconds over the period of time between T + 420 and T + 645 seconds. These values are considered to be in good agreement. A comparison of the specific engine data calculated by the Pratt & Whitney C* and the regression methods is shown in figure V-7. The Pratt & Whitney and guidance thrust velocity calculation techniques are discussed in the following sections.

METHODS OF CALCULATION

Pratt & Whitney C^* Technique

This technique is an iteration process for determining engine performance parameters. Flight data are used with calibration coefficicients obtained from the engine acceptance tests. Calculations are made to determine C*, individual propellant weight flow rates, and subsequently, specific impulse and engine thrust. The procedure is as follows:

(1) Calculate the hydrogen flow rate by using acceptance test calibration data and venturi measurements of pressure and temperature as obtained from telemetry.

(2) Assume a given mixture ratio and calculate corresponding oxidizer flow rate and total propellant flow rate.

(3) Obtain C* ideal from performance curve as a function of mixture ratio.

(4) Correct to C* actual by using characteristic exit velocity efficiency factor obtained from acceptance test results.

(5) Calculate total propellant flow rate, using C* actual:

$$\dot{\omega}_t = \frac{P_o A_t g}{C^*}$$

where $\dot{\omega}_t$ is the total engine propellant flow rate, P_o is the measured chamber pressure from telemetry, A_t is the thrust chamber throat area, g is the gravitational constant 32.17 feet per second per second, and C* is the characteristic (actual) exhaust velocity.

(6) Determine the mixture ratio by using the calculated total propellant flow rate and the measured hydrogen flow rate.

(7) Compare the calculated mixture ratio with that assumed in step (2).

(8) If two values of mixture ratio do not agree, assume a new value of the mixture ratio and repeat the process until agreement is obtained.

(9) When the correct mixture ratio is determined, obtain the ideal specific impulse from the performance curve as a function of actual mixture ratio.

(10) Correct to actual specific impulse by using specific impulse efficiency factor determined from acceptance test results.

(11) Calculate engine thrust as a product of propellant flow rate and specific impulse.

Pratt & Whitney Aircraft Regression Technique

This program determines engine thrust, specific impulse, and propellant mixture ratio from flight values of engine inlet pressures, engine inlet temperatures, and propellant utilization valve angle. The program is strongly dependent on engine ground testing. The method in which ground testing is correlated with the flight is as follows.

A large group of RL10A3-1 engines was ground tested. An average level of engine performance was obtained as a function of engine pump pressures, inlet temperatures, and the propellant utilization valve angle. During any specific engine acceptance test, the differences in performance from this average level are noted.

Flight performance is then determined in two steps: (1) the average engine level of performance is obtained for flight values of engine inlet conditions and propellant utilization valve angle and (2) corrections are made for the difference between the average engine level and the specific engine as noted during the engine acceptance test.

Guidance Thrust Velocity Method

The guidance thrust velocity method computes vehicle specific impulse by using guidance-computed inertial thrust velocities. Centaur vehicle specific impulse is defined as

$$\left(I_{sp}\right)_v = \frac{|\vec{F}|}{\dot{W}} \qquad \text{(B}$$

where $|\vec{F}|$ is the magnitude of the total Centaur thrust vector and $\dot{W}$ is the time rate of change of instantaneous total vehicle weight.

It should be noted that vehicle specific impulse differs from the engine specific impulse which is defined as

$$\left(I_{sp}\right)_e = \frac{|\vec{F}|}{\dot{\omega}_t} \tag{B2}$$

where $\dot{\omega}_t$ is the total engine propellant flow rate. The time rate of change of total vehicle weight in equation (B1) includes weight losses due to hydrogen peroxide used to drive the boost pumps and all other losses in addition to the total propellant flow rate through the engines. Consequently, the vehicle specific impulse would be less than the engine specific impulse. Vehicle specific impulse is a measure of total vehicle performance, whereas engine specific impulse is an index of engine performance only.

The derivation of vehicle specific impulse is based on the vehicle vector equation of motion

$$\vec{F} + M\vec{G} - \vec{X} = M\vec{A} \tag{B3}$$

where $\vec{F}$ is the magnitude of the total Centaur thrust vector, M is the instantaneous vehicle mass, $\vec{G}$ is the vehicle acceleration vector due to gravity, and $\vec{A}$ is the instantaneous vehicle total acceleration vector. It was assumed that drag and other perturbing forces are negligible over the time interval of interest, that the time rate of change of total vehicle weight is either constant or at least varies symmetrically about a mean value over this interval, and that only a negligible amount of axial thrust is lost because of engine gimbaling. Based on these assumptions, the equation of motion can be rewritten as

$$\vec{F} = M(\vec{A} - \vec{G}) \tag{B4a}$$

or

$$\frac{\vec{F}}{M} = (\vec{A} - \vec{G}) \tag{B4b}$$

The acceleration $(\vec{A} - \vec{G})$, designated as the thrust acceleration, is the acceleration imparted to the vehicle by thrust alone. It is obtained as the time rate of change of the inertial thrust velocity which is computed by the Centaur guidance system.

The thrust acceleration is used in a computer program to calculate the vehicle axial load factor, and this load factor is then used to determine the total vehicle specific impulse. Axial load factor, which is defined as the ratio of vehicle thrust minus drag over vehicle weight, is obtained by dividing the magnitude of the thrust acceleration in equations (B4) by g

$$\frac{|\vec{F}|}{Mg} = \frac{|\vec{A} - \vec{G}|}{g} \tag{B5}$$

where g is the gravitational acceleration at the Earth's surface. But

$$\frac{|\vec{F}|}{Mg} = \frac{|\vec{F}|}{W} = \alpha \tag{B6}$$

where $W = Mg$ is the instantaneous total vehicle weight, and α is defined as the axial load factor. If the instantaneous vehicle weight is written as

$$W = W_o = \dot{W}(t - t_o) = W_o - \dot{W}\,\Delta t \tag{B7}$$

where W_o is the total vehicle weight at main engine start, t_o is the time of main engine start (measured from lift-off), t is the instantaneous time from lift-off, and Δt equals $t - t_o$, and the substitution is made in equation (B6), the result is

$$\alpha = \frac{|\vec{F}|}{W} = \frac{|\vec{F}|}{W_o - \dot{W}\,\Delta t} \tag{B8}$$

The reciprocal of this equation is

$$\frac{1}{\alpha} = \frac{W_o - \dot{W}\,\Delta t}{|\vec{F}|} = \frac{W_o}{|\vec{F}|} - \frac{\dot{W}\,\Delta t}{|\vec{F}|} \tag{B9}$$

if $\dot{W}$ and $\vec{F}$ are constant, a plot of $1/\alpha$ as a function of time is a straight line with a slope equal to $-(\dot{W}/|\vec{F}|)$. Since, by definition, the vehicle specific impulse is

$$\left(I_{sp}\right)_v = \frac{|\vec{F}|}{\dot{W}}$$

the slope $-(\dot{W}/|\vec{F}|)$ is the negative reciprocal of the vehicle specific impulse. The computer program therefore determined the specific impulse by

(1) Calculating thrust acceleration based on guidance-computed thrust velocities
(2) Computing axial load factor from equation (B5)
(3) Plotting reciprocal of axial load factor against time
(4) Curve fitting $1/\alpha$ as a function of time with a straight line by the method of least squares
(5) Taking the negative reciprocal of line slope to obtain an average value of vehicle specific impulse for the time interval considered

The time interval for calculating the vehicle specific impulse on AC-7 was from T + 420 to T + 645 seconds. During this interval the propellant utilization valve motion was approximately symmetrical about a mean value; consequently, the mean values of thrust and weight flow could be assumed to be constant. Calculations were made for 151 data points, and the resultant vehicle specific impulse was 432.5 seconds.